Aus dem Neurowissenschaftlichen Forschungszentrum

der Medizinischen Fakultät Charité – Universitätsmedizin Berlin

DISSERTATION

Effects of patient-derived anti-NMDAR antibodies on synaptic function and network activity

Effekte pathogener Anti-NMDAR-Antikörper auf die Funktionalität von Synapsen und neuronalen Netzwerken

zur Erlangung des akademischen Grades

Doctor of Philosophy (PhD)

vorgelegt der Medizinischen Fakultät

Charité – Universitätsmedizin Berlin

von

Ewa Andrzejak

aus Lodz, Polen

Datum der Promotion: 30 November 2023

Contents

List of abbreviation 6

Abstract i

Zusammenfassung ii

1. Introduction 1

2. Objectives 5

3. Materials and Methods 6

3.1. Neuronal cell culture 6

3.2. Generation of monoclonal antibodies 7

3.3. Immunocytochemistry of cultured neurons 7

3.4. Confocal imaging and image analysis 8

3.5. Multi-electrode arrays 8

3.6. Patch clamp electrophysiology 9

3.7. Calcium imaging 10

3.8. Experimental design and statistical analysis 11

4. Results 12

4.1. Both germline and affinity-matured anti-NMDAR antibodies selectively decrease NMDA currents in hippocampal neurons 12

4.2. hNR1 antibody impairs function of inhibitory, but not excitatory, cortical neurons and differentially targets their NMDAR pools 14

4.3. hNR1 antibody impairs E/I balance and disinhibits cortical networks 19

4.4. hNR1 antibody affects cortical inhibitory synapses, specifically onto excitatory neurons 26

5. Discussion 30

5.1. Germline g-hNR1 antibody shows pathogenic potential 30

5.2. hNR1 antibody acts with brain regional and neuronal-subtype specificity 31

5.3. hNR1 antibody causes synaptic inhibitory dysfunction in cortex 33

5.4. Disinhibition of cortical networks 34

5.5. hNR1 antibody binds distinct NMDAR pools and affects inhibitory synapses 35

5.6. Implications for neuropsychiatry 37

References 38

Statutory Declaration 45

Detailed Declaration of Contribution 47

Excerpt from Journal Summary List (ISI Web of Knowledge) - 1 49

Publication 1 52

Excerpt from Journal Summary List (ISI Web of Knowledge) - 2 71
Publication 2 72
Curriculum vitae 79
Publication List 82
Acknowledgements 83

List of figures

Figure 1. Properties and functions of NMDARs and their targeting by pathogenic autoantibodies. 2

Figure 2. Both affinity-matured (hNR1) and germline (g-hNR1) NMDAR autoantibodies specifically decrease whole-cell and synaptic NMDA currents in hippocampal excitatory autapses 13

Figure 3. In cortical cultures, hNR1 antibody specifically decreases NMDA-mediated and synaptic currents in inhibitory, but not excitatory, autaptic neurons 15

Figure 4. hNR1 antibody does not change sensitivity of cortical neurons to ifenprodil – NR2B-specific blocker. 17

Figure 5. hNR1 antibody targets different NMDAR pool on excitatory and inhibitory neurons, in a brain region-specific manner 19

Figure 6. hNR1 antibody increases spiking and bursting activity of cortical cultures 21

Figure 7. Bicuculline does not further disinhibit cortical networks treated with hNR1 antibody..... 23

Figure 8. In cortical networks, hNR1 antibody treatment decreases inhibitory drive onto excitatory neurons, without affecting excitatory drive 25

Figure 9. hNR1 antibody decreases levels of inhibitory proteins VGAT and GAD65 at synapses formed onto excitatory, but not inhibitory, neurons. 27

Figure 10. hNR1 antibody binds within inhibitory synapses, preferentially on excitatory neurons. .. 29

List of abbreviation

AMPA - α-amino-3-hydroxy-5-methyl-4-isoxazolepropionic acid

ANOVA – analysis of variance

AP5 - (2R)-amino-5-phosphonovaleric acid

Bic – bicuculline

BSA – bovine serum albumin

CaMKII - Ca^{2+}/calmodulin-dependent protein kinase II

CNS – central nervous system

CSF – cerebrospinal fluid

Ctrl – control antibody

DIV – days in vitro

EEG - electroencephalography

ELISA – enzyme-linked immunosorbent assay

EPSCs- excitatory post-synaptic currents

E/I balance – excitation and inhibition balance

GABA – gamma aminobutyric acid

GABAAR – $GABA_A$ receptor

GAD65 – glutamate decarboxylase 65

GAD67 – glutamate decarboxylase 67

GFP – green fluorescent protein

g-hNR1 – germline configured, patient-derived autoantibody against NR1 subunit of NMDAR

HEK297T cells – human embryonic kidney 293 cells

ICC – immunocytochemistry

IgG – immunoglobulin G

IPSCs – inhibitory post-synaptic currents

h-NR1 – matured patient-derived autoantibody against NR1 subunit of NMDAR

MAP2 – microtubule-associated protein 2

MEA – multi-electrode array

mEPSCs – miniature excitatory post-synaptic currents

mIPSCs – miniature inhibitory post-synaptic currents

mRNA – messenger ribonucleic acid

NA – numerical aperture

NBA – neurobasal medium

NBQX - 2,3-dioxo-6-nitro-7-sulfamoyl-benzo[f]quinoxaline

NR1 – NR1 subunit of NMDAR

NR2A – NR2A subunit of NMDAR

NR2B – NR2B subunit of NMDAR

NMDA – N-methyl-D-aspartic acid

NMDAR – N-methyl-D-aspartic acid receptor

norm. - normalized

PBS – phosphate buffered saline

PCP – phencyclidine

PFA – paraformaldehyde

pre-NMDAR – presynaptic NMDAR

RNA- ribonucleic acid

ROI – region of interest

SEM – standard error of the mean

TTX – tetrodotoxin

UT - untreated

VGAT – vesicular GABA transporter

VGLUT1 – vesicular glutamate transporter 1

WT – wild type

Abstract

N-methyl-D-aspartate (NMDA) receptors lay at the core of excitatory glutamatergic transmission and their dysfunction has been implicated in a number of neurological and psychiatric disorders. One such recently described disease is anti-NMDAR encephalitis, characterized by prominent psychiatric, cognitive and autonomic symptoms, which are linked to presence of autoantibodies targeting the NMDARs. To date, the majority of mechanistic studies have focused on antibodies' action in the hippocampus, where they cause receptor cross-linking and internalization. However, little is known what is the specific contribution of individual antibodies and what are their effects in other brain regions such as cortex, which could help explain dysfunction on higher cognitive level. Here, we employed recently developed monoclonal anti-NMDAR autoantibodies and studied their effects on *in vitro* rodent neuronal cultures, using electrophysiological and imaging techniques. We report that both affinity-matured and germline, "naïve" NMDAR autoantibodies can pose pathogenic effects and impair NMDAR transmission. Moreover, these autoantibodies show brain regional specificity, exerting different effects in hippocampal versus cortical neurons. While in hippocampus they impair NMDAR currents of excitatory neurons, in cultures from cortex they selectively decrease NMDA currents and synaptic output of inhibitory, but not excitatory, neurons. Consequently, decreased inhibitory drive leads to disinhibition of networks from cortical neurons, bringing them into a hyper-excitable state. This is further associated with lowered levels of crucial pre-synaptic inhibitory proteins, specifically in inhibitory-to-excitatory neuron synapses. Together, these findings deepen our understanding of the pathology of autoimmune encephalitis by showing pathogenic potential of both matured and naïve autoantibodies and providing a novel, cortex specific mechanism of antibody-induced network hyper-excitability. Of note, similar mechanisms of NMDA-mediated cortical disinhibition have been suggested to underlie the etiology of schizophrenia, therefore there is an emerging framework for common mechanisms across neuropsychiatric disorders.

Zusammenfassung

N-Methyl-D-Aspartat-Rezeptoren (NMDA-Rezeptoren) sind das Herzstück der exzitatorischen glutamatergen Signalübertragung, und ihre Fehlfunktion wird mit einer Reihe von neurologischen und psychiatrischen Erkrankungen in Verbindung gebracht. Eine solche kürzlich beschriebene Krankheit ist die Anti-NMDAR-Enzephalitis, die durch auffällige psychiatrische, kognitive und andere autonome Symptome gekennzeichnet ist, alle werden mit dem Vorhandensein von Autoantikörpern gegen NMDARs in Verbindung gebracht. Bisher haben sich die meisten mechanistischen Studien auf die Wirkung der Antikörper im Hippocampus konzentriert, wo sie eine Vernetzung und Internalisierung der Rezeptoren verursachen. Es ist jedoch nur wenig darüber bekannt, welchen spezifischen Beitrag einzelne Antikörper leisten und welche Auswirkungen sie in anderen Hirnregionen wie zum Beispiel dem Kortex haben. Effekte der Autoantikörper im Kortex könnten eine Erklärung für die beobachtete Dysfunktion auf höherer kognitiver Ebene liefern. In dieser Studie haben wir kürzlich entwickelte monoklonale Anti-NMDAR-Autoantikörper eingesetzt und ihre Auswirkungen auf neuronale In-vitro-Kulturen von Nagetieren mit Hilfe bildgebender und elektrophysiologischer Verfahren untersucht. Wir berichten, dass sowohl affinitätsgereifte als auch keimbahnspezifische, "naive" NMDAR-Autoantikörper pathogen wirken und die NMDAR-Signalübertragung beeinträchtigen können. Darüber hinaus weisen diese Autoantikörper eine hirnregionale Spezifität auf, indem sie in hippocampalen und kortikalen Neuronen unterschiedliche Wirkungen entfalten. Während sie im Hippocampus die NMDAR-Ströme exzitatorischer Neuronen beeinträchtigen, vermindern sie in kortikalen Kulturen selektiv die NMDA-Ströme und die synaptische Übertragung inhibitorischer, aber nicht exzitatorischer Neuronen. Infolgedessen führt die verringerte hemmende Wirkung zu einer generellen Enthemmung kortikaler neuronaler Netzwerke und was diese in einen übererregbaren Zustand versetzt. Dies geht zusätzlich einher mit einer Abnahme wichtiger präsynaptischer inhibitorischer Proteine, insbesondere in Synapsen zwischen inhibitorischen und erregenden Neuronen. Zusammengenommen vertiefen diese Ergebnisse unser Verständnis der Pathologie der Autoimmunenzephalitis, indem sie das pathogene Potenzial sowohl gereifter als auch naiver Autoantikörper aufzeigen und einen neuen, Kortex-spezifischen Mechanismus der antikörperinduzierten Hypererregbarkeit von neuronalen Netzwerken liefern. Es ist bemerkenswert, dass ähnliche Mechanismen der NMDA-

vermittelten kortikalen Enthemmung auch für die Pathologie der Schizophrenie verantwortlich gemacht werden, so dass sich gemeinsame, grundlegende Mechanismen bei neuropsychiatrischen Störungen abzeichnen.

1. Introduction

N-methyl-D-aspartate (NMDA) receptors are ligand-gated ion channels of the CNS's most abundant excitatory neurotransmitter glutamate and are therefore critically involved in a plethora of brain functions and neuropathological conditions (Fig. 1). Under physiological conditions, activation of these tetrameric channels requires concurrent binding of glutamate and its co-agonist glycine, as well as relief of magnesium block at the ion channel pore through membrane depolarization. Because of these special activation properties, NMDARs are capable of converting specific patterns of neuronal activity into long-term changes in synapse structure and function (synaptic plasticity) and are therefore thought to underlie such mechanisms as learning and memory, in particular within hippocampal structures (Bliss & Collingridge, 1993; Nicoll, 2017). Moreover, NMDARs are crucial for higher mental functions as their dysregulation has been implicated in a number of psychiatric disorders such as schizophrenia (Howes et al., 2015) and autism (Lee et al., 2015). Further yet, their function seems to be crucial for conscious experience as NMDAR blockers serve as potent anesthetics (Petrenko et al., 2014). Because of these central roles in CNS function and their associated modulatory therapeutic potential, NMDARs have kept fascinating neuroscientists since their discovery nearly six decades ago.

Interestingly, it is often through dysfunction of NMDAR signaling that we learn about the ever-emerging functions of these receptors. One such recently described disease, which provides new insights into the function of NMDARs and perhaps a glimpse into the nature of consciousness, is anti-NMDAR encephalitis. Here, patients present with a wide range of symptoms, from prominent psychiatric and cognitive manifestations such as psychosis, delusions, memory loss and personality change, to severe seizures, autonomic instability and fluctuating levels of consciousness often resulting in coma (Dalmau et al., 2007; Irani et al., 2010). Interestingly, patients show marked recovery in response to sufficient immunotherapy, which typically consists of plasmapheresis, infusion of intravenous IgG or B-cell depletion (Lancaster et al., 2011; Titulaer et al., 2013). Indeed, the hallmark of the disease is the presence of pathogenic autoantibodies against NMDA receptors (Fig. 1), and ever since their first discovery (Dalmau et al., 2007), there has been a search for underlying disease mechanisms to understand how specific antibodies give rise to a broad symptomatology observed in patients.

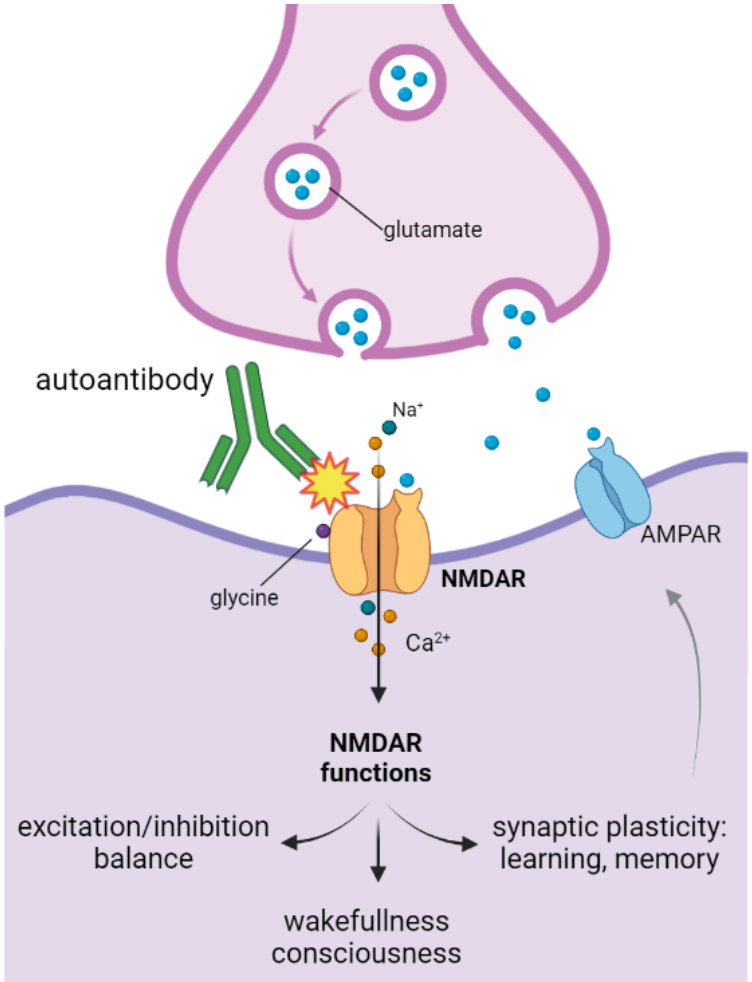

Figure 1. Properties and functions of NMDARs and their targeting by pathogenic autoantibodies. Pre-synaptic release of glutamate activates post-synaptic glutamate receptors: AMPARs (blue) and NMDARs (orange). Activation of NMDARs requires additional binding of the co-agonist glycine and a relief of a Mg^{2+} block. Activated NMDARs allow intracellular influx of Ca^{2+} and, to a smaller extent, Na^{+} ions which trigger downstream signaling cascades. NMDARs are involved in a plethora of brain functions, from synaptic plasticity underlying learning and memory (by regulating levels of AMPARs), through maintaining proper levels of excitation/inhibition to controlling levels of consciousness. Patient-derived autoantibodies (green) target the extracellular amino-terminal domain of NMDARs (yellow star – antibody binding) and disrupt their proper function leading to distinct clinical symptoms. Image created with BioRender.com.

Regarding molecular mechanisms of the disease, most studies to date have focused on the effects of NMDAR autoantibodies on neurons in the hippocampus, where there likely contribute to deficits in a patient's memory. Studies of patient CSF revealed that most antibodies target epitopes situated within the N-terminal domain of NR1 subunits (Gleichman et al., 2012). Elevated levels of these antibodies in CSF appear to trigger receptor

internalization, decreasing the levels of surface NMDAR pools in cultured hippocampal neurons (Moscato et al., 2014; Hughes et al., 2010) and hippocampi of animal models (Planagumà et al., 2015). Surface receptor loss in turn leads to decreased synaptic NMDAR–mediated currents (Hughes et al., 2010; Kreye et al., 2016) and impaired synaptic plasticity (Würdemann et al., 2016; Q. Zhang et al., 2012; Mikasova et al., 2012). These effects likely contribute to memory deficits observed in animal models and patients with NMDAR encephalitis (Malviya et al., 2017; Planagumà et al., 2016).

However, prominent psychiatric symptoms and epileptic seizures point towards additional dysfunctions on a higher network level, especially within cortical circuits. At present, it is unclear how these autoantibodies cause such symptoms. Intriguingly, involvement of NMDARs in the pathology of psychosis has long been suggested in the so-called "glutamatergic hypothesis of schizophrenia". This theory was originally based on clinical observations that NMDAR antagonists such as phencyclidine (PCP) and ketamine induce psychotic symptoms and dissociative states similar to those observed in schizophrenia (Jentsch & Roth, 1999; Krystal et al., 1994). Furthermore, it was later substantiated by post-mortem histological analyses showing reduction of mRNA and/or protein levels of NMDARs in cortices of schizophrenic patients (Catts et al., 2016). Therefore, the emerging hypothesis postulates that hypofunction of NMDARs on inhibitory interneurons (Belforte et al., 2010), leads to excitation/inhibition imbalances and disinhibition of prefrontal cortical circuits (Homayoun & Moghaddam, 2007), as well as alterations in gamma oscillations (Carlén et al., 2012) similar to these seen in schizophrenic patients (Uhlhaas & Singer, 2010). Whether these cortical interneurons play a similar role in the pathophysiology of NMDAR encephalitis and how the autoantibodies affect cortical networks properties at large has not yet been described.

The diverse symptomatology of the disease also suggests a possibility of receptor- or cell-type specificity of antibody action. Apart from the above-mentioned cortical interneuron hypothesis, another/concomitant possibility is that the antibodies affect preferentially a subpopulation of receptors with specific subunits composition or a distinct subcellular localization. Although previous studies indicate that the antibodies bind predominantly the obligatory NR1 subunit of NMDARs, conformational changes, synaptic localization and protein-protein interactions depending on receptor subunit composition may further affect

their binding. Recent studies report seemingly opposing results: Ladépêche et al. (2018) showed that antibody-induced receptor clustering affects predominantly NR2B-contraining receptors, whereas others report that antibodies action is partially blocked by stabilization of NR2A-containing receptors through activation of Ephyrin-B2 receptor (Mikasova et al., 2012; Planagumà et al., 2016). Again, how specific NMDAR subunits are affected in cortical neurons has not yet been explored.

Finally, despite the growing body of data linking auto-antibodies to neuronal dysfunction, nearly all previous *in vitro* research suffered from a technical limitation, namely, that the CSF from patients contains numerous autoantibodies, often targeting additional epitopes apart from NMDARs (Kreye et al., 2016). Consequently, if used without further purification, this approach makes it difficult to assign casual-links to a specific antibody. To address this limitation, the group of Prof. Harald Prüss has developed recombinant technologies to isolate and clone panels of monoclonal antibodies derived from the CSF of individual patients (Kreye et al., 2016). Interestingly, this analysis revealed a broad repertoire of antibody-secreting cells and associated antibodies present in patient CSF, including also germline, unmutated antibodies produced by naive B lymphocytes (Kreye et al., 2016; Wenke et al., 2019). This ground-breaking work has now set the stage for the in-depth mechanistic characterization of individual antibodies and their specific contribution to disease pathology.

2. Objectives

This dissertation aimed to deepen our understanding of the molecular and physiological mechanisms of action of patient-derived monoclonal antibodies against NMDARs, and their specific contribution to the pathology of anti-NMDAR encephalitis, especially within cortical circuits. To this end, we used molecular imagining techniques and extensive electrophysiological investigations on rodent *in vitro* neuronal cultures to assess how these antibodies affect the physiological function of the NMDA receptor, the synapse, as well as higher-level network properties.

The specific objectives of this work were as follows:

- to verify the pathogenic character of both **germline and matured** patient-derived NMDAR autoantibodies
- to investigate the previously un-explored brain region- and neuronal type-specificity of NMDAR antibodies to **cortical excitatory and inhibitory neurons**
- to investigate the effects of NMDAR autoantibodies on neuronal **signal transduction** and cortical **network activity**
- to explore further potential antibody specific binding to certain **NMDAR subunit compositions** and/or **synaptic/extra-synaptic** receptor pools.

3. Materials and Methods

The following chapter describes the crucial chemical reagents, methodological approaches and experimental designs used in this dissertation.

3.1. Neuronal cell culture

All experiments were performed on rodent neuronal cultures with approval of the animal welfare committee of Charité Medical University and the Berlin state government. Part of the experiments were performed on neurons from WT mice (C57BL/6J) (RRID:IMSR_JAX:000664)(license: T-CH 0008/22). In some experiments (Fig. 3, 4, 5, 8, 9, 10) we employed GAD67-GFP (Δneo)/+ (GAD67-GFP) (license: T0220/09) mice for easier distinction between inhibitory and excitatory neurons. In these animals, electrophysiological properties of inhibitory neurons which express GFP under the GAD67 promoter (Tamamaki et al., 2003) are not changed when compared to WT neurons (Chang et al., 2014). For immunocytochemistry (ICC) and patch clamp electrophysiological experiments on mass cultures, primary neuronal cultures were prepared and grown on coverslips according to a "Banker Protocol" described previously (Meberg & Miller, 2003; Banker & Goslin, 1988). The exact protocol and seeding density can be found in Andrzejak et al., 2022.

Single-cell electrophysiological recordings were performed in autaptic cultures. Here, hippocampal or cortical neurons were plated on 1-week old astrocyte micro-islands feeder layers (Arancillo et al., 2013). Neurons were plated at a low density to obtain a single neuron per island.

In calcium imaging experiments, cortical neurons from WT mice at a density of 250,000 cells per dish were plated directly on top of feeder layer of 1-week old astrocytes to obtain dense networks. Here, we used round dishes with a cell location grid at the bottom (µ-Dish 35 mm, high Grid-500, Ibidi).

Multi-electrode array experiments were performed on primary cultures of rat cortical neurons with approval of the Technion committee for the supervision of animal experiments (IL-116-08-71). Cortical neuronal cultures were prepared according to a protocol described previously (Minerbi et al., 2009) and the exact culturing conditions, seeding and feeding regimes for both calcium imaging and MEA cultures can be found in Andrzejak et al., 2022.

3.2. Generation of monoclonal antibodies

Both human monoclonal antibodies the hNR1 (#003-102, Kreye et al., 2016) and the germline configured g-hNR1 (#003-109, Wenke et al., 2019) were isolated from cerebrospinal fluid of a patient with acute NMDAR encephalitis at the Charité clinic (Kreye et al., 2016). An isotope-matched control antibody (ctrl) was isolated and cloned from the blood of a healthy donor (mGO53, Wardemann et al., 2003). Recombinant heavy and light chains of antibodies were expressed by transiently transfecting HEK293T cells with two plasmid vectors encoding each antibody chain. Antibodies were then purified from supernatants of HEK cell cultures and ELISA kit (3850-1AD-6, Mabtech) was used to determine their concentration.

3.3. Immunocytochemistry of cultured neurons

Synaptic/extrasynaptic hNR1 binding. To study the binding pattern of hNR1 antibodies and their degree of co-localization to excitatory and inhibitory synaptic markers, GAD67-GFP cortical neurons were live stained with hNR1 antibody and anti-human secondary antibody. Here, neurons were incubated for 20 min at 10°C with 1µg/ml of the hNR1 antibody in the original culture medium (NBA). Neurons were then washed once in NBA medium and then incubated for 20 min at 10°C with Alexa-568 conjugated anti-human secondary antibody (1:1000, Thermo Fisher Scientific). Next, the cells were washed once with NBA medium, before being fixed with 4% PFA for 10 min and blocked with blocking solution (2% BSA, 0.1% Triton and 5% normal goat serum in PBS) for 1h. Cultures were then labeled with antibodies against VGLUT1 (1:4000, SySy 135 304, Synaptic Systems) an excitatory presynaptic marker, or gephyrin (1:500, SySy 147 011, Synaptic Systems) an inhibitory post-synaptic marker for 2h. These were then washed (3x 5 min in PBS) and stained with corresponding secondary antibodies (1:1000, Invitrogen, Thermo Fisher Scientific), before mounting in Pro-Long Diamond Antifade Mountant (Thermo Fisher Scientific).

Levels of inhibitory pre-synaptic proteins. To determine the levels of inhibitory pre-synaptic proteins after hNR1 antibody treatment, 1 µg/ml of hNR1 antibody was added to GAD67-GFP cortical neurons in original medium for 0h, 6h or 24h at 37°C. Neurons were then fixed for 10 min with 4% PFA, blocked, labeled with antibodies against GAD65 (1:750, MAB5406, Millipore), MAP2 (1:2000, AB5543, Millipore) or VGAT (1:4000, SySy 131 003, Synaptic

Systems). Neurons were then stained with secondary antibodies and mounted as described above.

3.4. Confocal imaging and image analysis

Images of acute hNR1 staining and labeling of inhibitory pre-synaptic markers were acquired on a spinning disc confocal microscope (Carl Zeiss Axio Oberserver.Z1 with Andor spinning disc and cobalt, omricron, i-beam laser) with a 63x (1.4 NA) or a 100x (1.4 NA) Plan-Apochromat oil objective and an iXon ultra (Andor) camera controlled by iQ software (RRID: SCR_014461) (Andor). Dendrites from excitatory and inhibitory neurons were distinguished using the GFP signal of GAD67-eGFP animals and imaged only in proximity to neuronal somas. ImageJ and OpenView software (written by Prof. N. Ziv, Technion, Israel) were used to process confocal images. To measure levels of inhibitory pre-synaptic proteins, individual VGAT and GAD65 puncta were detected along dendrites by OpenView software, which placed 6x6 pixels boxes over puncta and mean fluorescence intensity within the boxes was measured. To determine synaptic/extrasynaptic distribution of the hNR1 antibody, hNR1 antibody puncta were detected in a similar way and we measured intensities of VGLUT1 within hNR1-positive puncta. hNR1 antibody puncta were considered synaptic if VGLUT1 intensity values were higher than 5x background intensity. Similarly, the presence of hNR1 antibody at inhibitory synapses was determined by measuring puncta intensity within boxed gephyrin puncta. Here, the Volume Viewer plugin in ImageJ was used to analyze Z-plane images. For each region of interest (individual dendrites), values of all puncta were averaged and considered one data point.

3.5. Multi-electrode arrays

Spiking activity of cortical neuronal networks was recorded continuously from MEA dishes (59 electrodes of 30 µm diameter in 8 × 8 array) supplied with constant ultra-slow perfusion and maintained at 37°C and 5% CO_2 (L. Hazan & Ziv, 2020). Following setting up the perfusion system and an equilibration period (1h), we recorded 15 h of baseline network activity. Then, 1 µg/ml of hNR1 or ctrl antibody was added and cell spiking was recorded for another 24h. Finally, 50 µM of AP5 was added to each culture to block remaining NMDA receptors, and activity traced for another 6h. Recording apparatus, data acquisition and data analysis was performed using commercial equipment and custom-written MATLAB scripts

[Closed Loop Experiment Manager (CLEM)] as described previously (H. Hazan & Ziv, 2017). In each MEA dish, data was normalized to the mean of the last 3 hours of baseline activity. To test the within-dish effects of antibody treatment, the mean activity of the last 1h of baseline recording was compared to the mean activity of 1h at the end of the 24h treatment and evaluated by paired t-test. To evaluate effects of different phases of the experimental protocol between groups, mean activities of 10 min intervals at the beginning or end of the respective treatments (24h with antibodies, addition of 50 µM AP5 or recovery at the end of the experiment) were compared by unpaired t-test.

3.6. Patch clamp electrophysiology

Mass cultures or autaptic cultures of cortical or hippocampal neurons at 14–18 DIV were used to perform whole-cell patch-clamp recordings after 24h incubation with 1µg/ml of hNR1 or control antibodies. In some experiments, excitatory and inhibitory neurons were distinguished by using cortical neurons from GAD67-eGFP animals. Experiments were performed at ~25°C from neurons clamped at -70 mV with a Multiclamp 700B amplifier (Molecular Devices) using Clampex 10.4 software (Molecular Devices). Data were sampled at 10 kHz and low-pass Bessel filtered at 3 kHz. Typical series resistance was under 15 MΩ and compensated at 70%.

Except for NMDA currents, all recordings were performed in standard extracellular and pipette internal solutions adjusted to pH 7.4 and osmolarity of ~300 mOsm (Andrzejak et al., 2022). Whole-cell NMDA responses were induced chemically while recording in the following extracellular solution: 0 mM Mg^{2+}, 0.2 mM $CaCl_2$, and 10 µM glycine. Evoked synaptic NMDAR currents were recorded in extracellular solution containing 0 mM Mg^{2+}, 2mM $CaCl_2$, 10 µM glycine and 10 µM NBQX.

To selectively measure whole-cell GABA, kainate and NMDA currents, GABA (5 µM, Tocris), kainic acid (20 µM, Tocris) or NMDA (10 µM, Tocris) were acutely added using a fast-flow system to the neurons in 1 second pulses. Synaptic responses in autaptic neurons were elicited by brief somatic depolarization of autaptic neurons from −70 mV to 0 mV for 2 ms. To measure the sensitivity of whole-cell NMDA currents to ifenprodil, NMDA (10 µM) was acutely applied to a neuron by a fast-flow system for 3s, after which it was co-applied with 3 µM ifenprodil for another 5s.

Extracellular solutions for all recordings in mass neuronal cultures contained TTX (0.5 µM, Tocris). To identify spontaneous mEPSCs, neurons were additionally immersed in and bicuculline (20 µM, Tocris) and AP5 (50 µM), while spontaneous mIPSCs were detected in presence of NBQX (10 µM) and AP5 (50 µM). mEPSCs/mIPSCs signals were recorded, filtered and detected and the false-positive events were excluded as described previously (Andrzejak et al., 2022). For detection of mIPSCs in mass cultures, excitatory neurons were identified by infecting WT mouse neurons with a lentivirus expressing mKate2 under a CamKII promoter, at 3-4 DIV. GAD67-GFP neurons were used for experiments detecting mEPSCs. Axograph X (RRID:SCR_014284) (Axograph Scientific), Excel (Microsoft), and Prism (GraphPad) were used to analyze electrophysiological data offline.

3.7. Calcium imaging

Cortical cultures were infected at 4 DIV with f(syn)-NES-jRCamP1b-WPRE-w. This is a lentivirus expressing a genetically encoded calcium indicator jRCamP1b under the control of synapsin promoter (Viral Core Facility, Charité – Universitätsmedizin). Activity of neuronal networks was imaged at 37°C and 5% CO_2, using a Nikon Spinning Disk Confocal CSU-X microscope controlled by the NIS-Elements software (Nikon). This was equipped with a 20× Plan Apo objective lens (NA = 0.8) and an iXon3 DU-888 Ultra camera (Andor). This was used to collect time-lapse images at 5 Hz using a 561 nm excitation laser. In each dish/neuronal network, 3 fields of view were selected with approximately 10-20 neuronal somas. Two minutes of spontaneous activity was then measured twice, separated by a 5 min waiting interval. Bicuculline-induced changes in network activity were then studied following the manual addition of bicuculline (30 µM) immediately after the end of the second imaging run. Bicuculline was allowed to diffuse within the dish for 30 seconds, and again network activity was imaged for 2-minutes twice, with a 5 min waiting interval in between.

To detect somatic calcium transients, time-lapse images were analyzed with OpenView software for automatic time-series event detection. Here, neuronal somas (ROIs) were visually identified before placing boxes of 27 x 27 pixels over them. Silent neurons were excluded from the analysis. After time series fluorescence values were converted into ΔF/F, we used a custom-written script to identify timestamps of onsets of calcium transient. These were then averaged per min to obtain the frequency of events.

3.8. Experimental design and statistical analysis

GraphPad Prism was used to analyze data, perform statistical tests and create graphs. Statistical design, sample sizes, statistical tests and exact p-values for each experiment can be found in the figure legends or in the detailed report in Andrzejak et al., 2022. All graphs, except for synaptic labeling of hNR1 antibody (Fig. 5), represent data from at least 3 independent experiments (independent cultures). Figure 5 shows results from 2 independent cultures. To avoid over-sampling in immunocytochemical analyses of individual synaptic puncta, mean values of all puncta per ROI (dendrite) were averaged and considered a single data point. For within-dish (MEAs, Fig. 6; calcium imaging, Fig. 7) or within-cell (ifenprodil experiment, Fig. 4) comparisons, paired t-test was used to evaluate statistical significance. For comparisons between treatments, we used an unpaired t-test or ANOVA Tukey's multiple-comparison test. Statistical significance of $p<0.05$ was as a cut-off. BioRender.com was used to create schematic figures.

4. Results

4.1. Both germline and affinity-matured anti-NMDAR antibodies selectively decrease NMDA currents in hippocampal neurons

To study the effects of patient-derived antibodies against NMDAR on synaptic and neuronal network function, we have recently generated a panel of human monoclonal NMDAR autoantibodies derived from antibody-secreting cells in CSF of patients with NMDAR encephalitis (Kreye et al., 2016). As encephalitis patients often suffer from severe memory and cognitive impairments, and patient-derived IgG/CSF tend to accumulate within hippocampal structures when applied onto murine brain slices (Dalmau, 2016; Dalmau et al., 2007; Moscato et al., 2014), most studies to date have focused on disease mechanisms in this brain region. We therefore began to test the effects of isolated monoclonal antibodies on the function of hippocampal excitatory neurons by autaptic electrophysiological recordings. Here, single neurons are grown on astrocytic micro-islands, allowing the study of neuronal function and synaptic transmission at a single-cell level. Here, we observed that a 24h treatment with 1 μg/ml of a high-affinity, matured antibody (hNR1) (#003-102, Kreye et al., 2016) reduced whole-cell NMDA-currents by ~35%, when compared to the treatment with a control antibody (ctrl) (mGO53) (Wardemann et al., 2003) (Fig. 2A). This effect was specific to NMDARs, as the treatment did not affect GABA- or kainate-specific currents (Fig. 2B-C). Furthermore, we measured evoked synaptic responses and observed a ~45% reduction in synaptic NMDA-currents due to hNR1 antibody treatment (Fig. 2E) and no change in AMPA-mediated synaptic currents (EPSCs, Fig. 2D).

Interestingly, among the B cells isolated from patient CSF, we also isolated antibodies with a germline-like configuration, suggestive of originating from naturally occurring B cells. We thus also explored whether such germline unmutated antibody (g-hNR1) (003-109, Wenke et al., 2019), derived from naïve B cell, could also have pathogenic potential and affect neuronal function. We therefore recorded NMDA-, GABA-, kainate-currents and evoked synaptic responses after 24h treatment with 1 μg/ml of g-hNR1 and did not observe changes when compared to control antibody treatment (Fig. 2F-J). However, as g-hNR1 antibody showed much lower binding affinity than matured hNR1 when tested on murine brain tissue (Wenke et al., 2019), we repeated the experiment in the presence of a higher

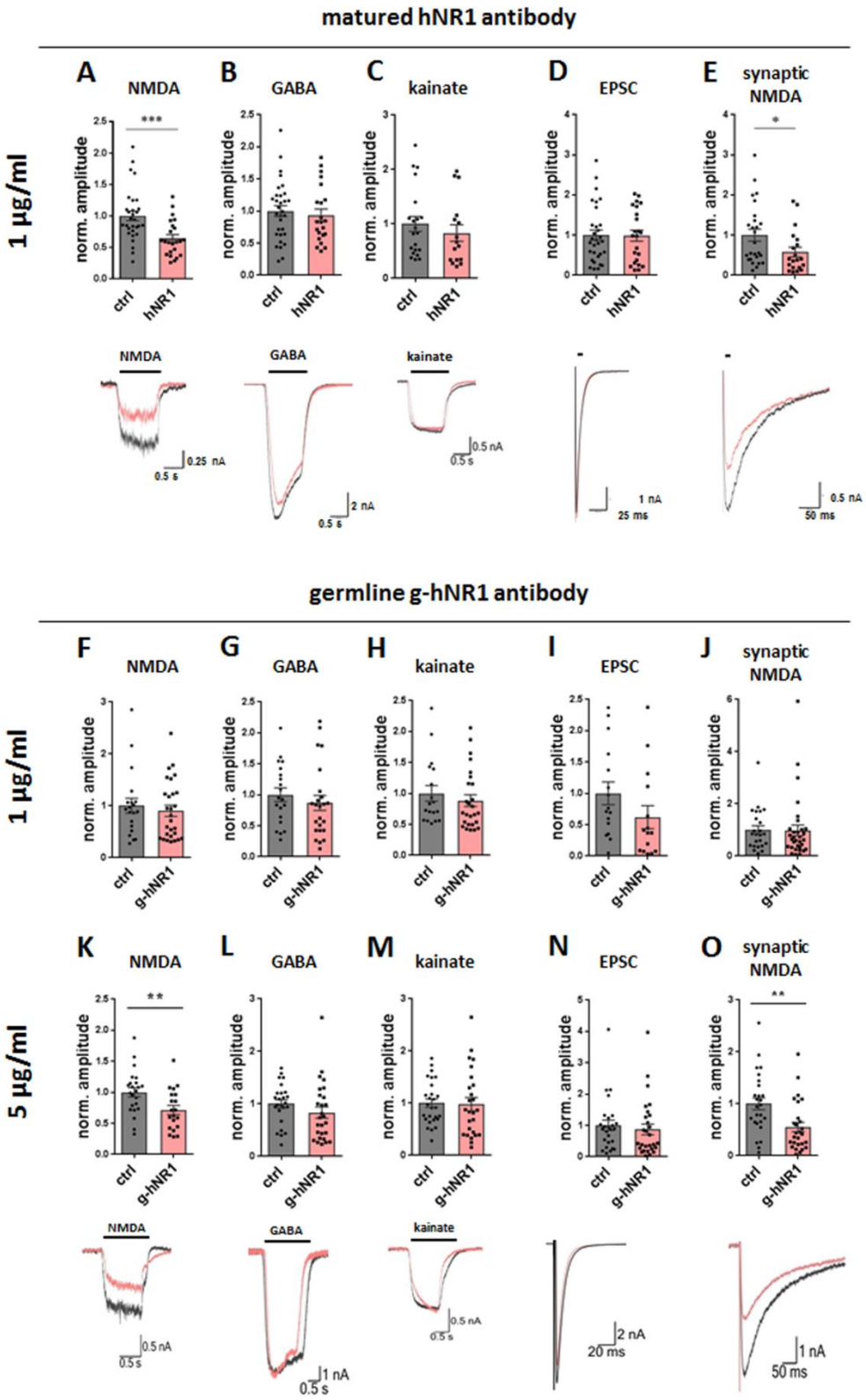

Figure 2. Both affinity-matured (hNR1) and germline (g-hNR1) NMDAR autoantibodies specifically decrease synaptic and whole-cell NMDA currents in hippocampal excitatory autapses. Recordings in whole-cell patch clamp mode were conducted on hippocampal autaptic neurons. 24h treatment with 1ug/ml of the matured hNR1 antibody caused a 35% reduction of whole-cell NMDA currents (**A**, p=0.008), without changing **(B)** GABA- or **(C)** kainate-specific currents. Each was elicited by 1s bath

application of either NMDA (10 μM), GABA (5 μM) or kainate (20 μM). Treatment with hNR1 also caused a 45% reduction in the amplitude of synaptic NMDAR currents (**E**, p=0.039), while AMPA-mediated EPSCs remained unchanged **(D)** when compared to control. Note that the g-hNR1 antibody affects currents in a concentration-dependent manner: 1 μg/ml of g-hNR1 did not change NMDA **(F)**, GABA **(G)**, kainate **(H)** or synaptic **(I-J)** currents. However, a higher concentration (5 μg/ml) of g-hNR1 antibody selectively reduced whole cell (30% decrease, **K**, p=0.009) and synaptic (45% decrease, **O**, p=0.003) NMDA currents, without affect GABA **(L)**, kainate **(M)** or EPSCs **(N)**. Error bars indicate SEM. Unpaired t-test was used to evaluate statistical significance. *p<0.05, **p<0.01, ***p<0.001. Modified from Fig. 3 in Wenke et al., 2019 and Fig. 6 in Andrzejak et al., 2022.

concentration of g-hNR1, 5 μg/ml. Here, the g-hNR1 antibody showed similar effect to matured hNR1: it selectively decreased whole-cell (~30%, Fig. 2K) and synaptic (~45%, Fig. 2O) NMDA currents, without affecting GABA- and kainate-specific currents (Fig. 2L-N).

Together, these data indicate that patient-derived anti-NMDAR antibodies can indeed functionally decrease whole-cell and synaptic NMDAR transmission. Moreover, this pathogenic character is exhibited by both matured and naturally occurring, germline autoantibodies present in patient CSF, in an affinity/concentration-dependent manner.

4.2. hNR1 antibody impairs function of inhibitory, but not excitatory, cortical neurons and differentially targets their NMDAR pools

Until now most studies on NMDAR autoantibodies have been conducted on the hippocampus, however the broad symptomatology of NMDAR encephalitis patients suggests that the pathogenic effects of autoantibodies are not confined exclusively to hippocampal regions. Prominent psychiatric symptoms, behavioral and personality changes as well as seizures suggest additional dysfunction at the cortical level. We therefore next aimed to explore if NMDAR autoantibodies affect cortical neuronal function. Here, we focused on the high-affinity matured hNR1 antibody (hNR1) and tested its effects on cortical autaptic neurons. Similarly to experiments in hippocampal cultures, we incubated cortical excitatory neurons for 24h with 1 μg/ml of hNR1 antibody and recorded whole cell and synaptic currents. Surprisingly, in contrast to our hippocampal results (Fig. 2), we observed no changes in NMDA transmission due to the antibody treatment in cortical excitatory neurons (Fig. 3A, 3E). GABA- and kainate-specific currents, as well as synaptic AMPA transmission, also remained unchanged (Fig. 3B-D).

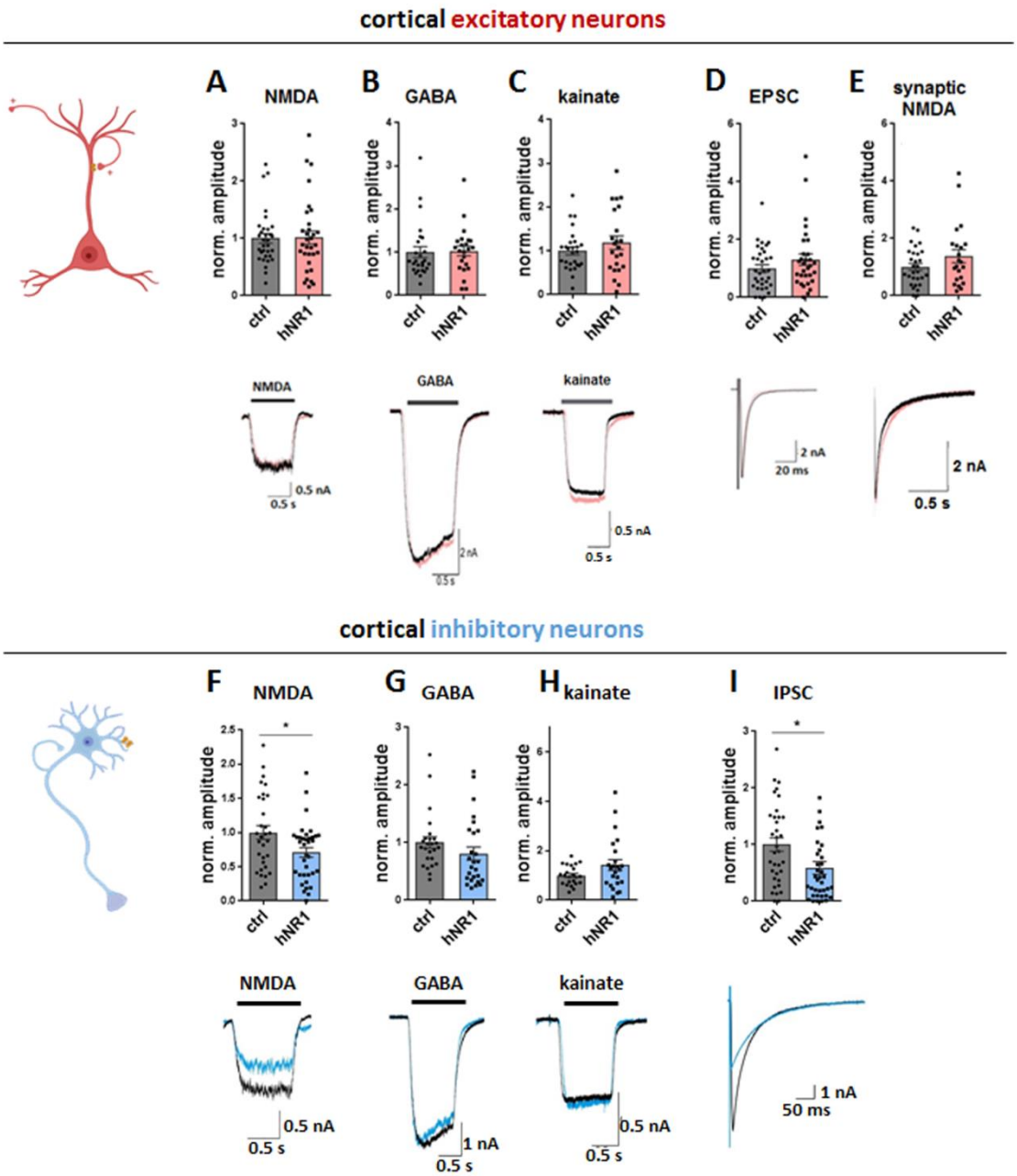

Figure 3. In cortical cultures, hNR1 antibody specifically decreases NMDA-mediated and synaptic currents in inhibitory, but not excitatory, autaptic neurons. For excitatory cortical neurons, 24h treatment with 1 μg/ml of hNR1 did not affect the amplitudes of NMDA **(A)**, GABA **(B)**, kainate **(C)**, EPSCs **(D)** or synaptic NMDA **(E)** currents. On the other hand, in inhibitory neurons hNR1 treatment reduced whole-cell NMDA currents (30% decrease, **F**, p=0.018) as well as the amplitude of evoked inhibitory post-synaptic currents (IPSCs) (41% decrease, **I**, p=0.014). GABA- **(G)** and kainate **(H)** specific currents remained unchanged when compared to control antibody treated neurons. Error bars indicate SEM. Statistical significance was evaluated with unpaired t-test. *p<0.05. Modified from Fig. 5 in Andrzejak et al., 2022.

As NMDARs are densely expressed on and contribute to the proper function of both inhibitory and excitatory neurons, we repeated the experiment with cortical inhibitory

autapses treated with the hNR1 antibody (Fig. 3F-I). To easily distinguish excitatory and inhibitory neurons, we employed GAD67-eGFP animals, in which Green Fluorescent Protein (GFP) was used to label inhibitory neurons (Tamamaki et al., 2003). Here, we observed that a 24h treatment with the hNR1 antibody significantly decreased whole-cell NMDA currents of these cells (~30% decrease, Fig. 3F), without affecting GABA- or kainate-specific currents (Fig. 3G-H). Moreover, GABAergic synaptic transmission (amplitude of IPSC) was also decreased by ~41% by the treatment with the hNR1 antibody (Fig. 3I). Together, these data suggest that in cortical cultures the hNR1 antibody does not affect NMDA currents on excitatory neurons, yet it selectively reduces NMDA currents on inhibitory neurons, in a cell-autonomous manner. This latter effect could potentially lead to impaired GABAergic synaptic transmission.

Having observed hNR1 antibody's selective effects on NMDARs of cortical inhibitory but not excitatory neurons, we next asked how this specificity arises. One possibility is that hNR1 affects NMDARs with a specific subunit composition. Remarkably, cortical inhibitory neurons express a different ratio of NR2A/NR2B subunits than their excitatory counterparts (Kinney et al., 2006). Conceptually, if hNR1 antibody preferentially affects a specific NMDAR subunit, one would expect that it could be eliminated and replaced by a different subunit leading to a change in the overall NMDAR composition. To examine if NMDAR subunit composition changed due to the antibody treatment on either cell type, we measured the sensitivity of whole-cell and synaptic NMDA currents to ifenprodil – a NR2B-selective blocker (Fig. 4) after 24h treatment with hNR1 or control antibodies. Although NMDA currents were sensitive to ifenprodil-induced blockage on both excitatory (Fig. 4A-B, 4G-H) and inhibitory (Fig. 4D-E) cells, the percentage of NMDAR current blocked was not altered due to hNR1 antibody treatment when compared to control on neither cell type (Fig. 4C, 4F, 4I). These data suggest that the hNR1 antibody does not induce dramatic changes in at least the NR2A/NR2B subunit composition of NMDARs.

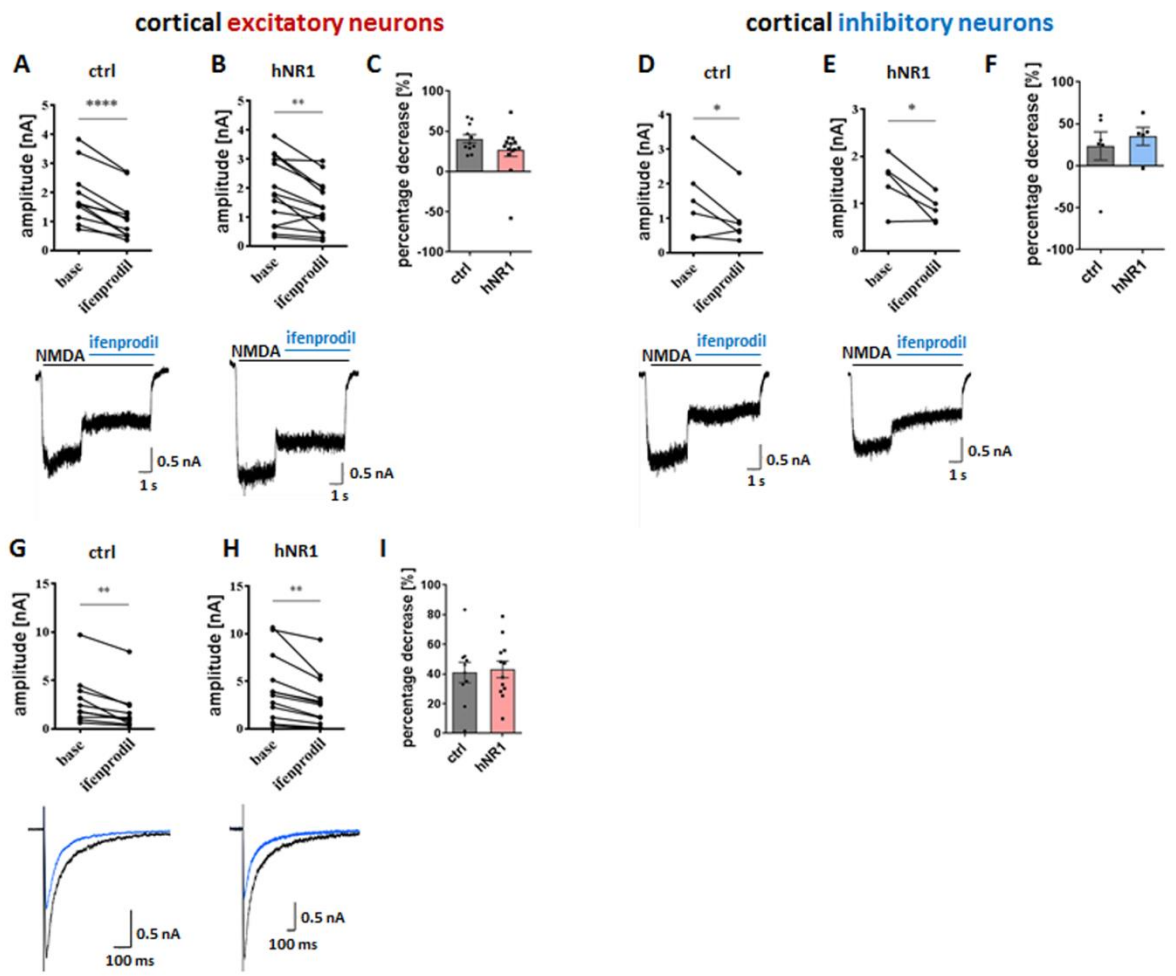

Figure 4. hNR1 antibody does not change sensitivity of cortical neurons to ifenprodil – NR2B-specific blocker. (A-C) In excitatory neurons, NMDA-elicited currents were significantly reduced by the co-application of ifenprodil (3 μM) after treatments with both control (**A,** paired t-test, p<0.0001) and hNR1 antibody (**B,** paired t-test, p=0.0017). However, the percentage of ifenprodil-mediated block was similar between treatments (**C**). (**D-E**) Similarly, in inhibitory neurons ifenprodil reduced NMDA-elicited currents after control (**D,** paired t-test, p=0.062) and hNR1 antibody treatment (**E**, paired t-test, p=0.028), yet to a similar degree in both conditions (**F**). Additionally, evoked synaptic NMDA currents in excitatory autapses were reduced by ifenprodil (**G,** paired t-test, p=0.002, **H**, paired t-test, p=0.0024), again to a same degree in hNR1 antibody and control treated conditions (**I**). Error bars indicate SEM. Paired t-test (C, F, I) and unpaired t-test (A-B, D-E, G-H) was used to evaluate statistical significance. *p<0.05, **p<0.01, ****p<0.0001.

Another possibility is that hNR1 antibody targets NMDAR pools with different subcellular localization on cortical inhibitory and excitatory neurons. Synaptic and extra-synaptic NMDARs are known to elicit distinct downstream signaling pathways (Hardingham & Bading, 2010) and their differential recognition by hNR1 antibody could contribute to cell type specific effects. To study the subcellular localization of acute hNR1 antibody binding, we

subjected cortical neuronal mass cultures to immunocytochemistry experiments (Fig. 5). Here, live neurons were incubated with the hNR1 antibody for 20 min at 10°C, before being washed and incubated with an anti-human secondary antibody for another 20 min at 10°C. After fixation, neurons were co-stained for VGLUT1, an excitatory pre-synaptic marker. The degree of co-localization with VGLUT1 served as a measure of synaptic versus extra-synaptic antibody binding. Interestingly, while all cortical neurons in culture were decorated with hNR1 antibody, it accumulated in distinct compartments on excitatory and inhibitory cells. Namely, on excitatory neurons most of the hNR1 antibody puncta were synaptic (70%), whereas on inhibitory cells only half of the antibody puncta co-localized with VGLUT1 (Fig. 5A-B). This suggests that the hNR1 antibody targets different receptor pools on cortical inhibitory and excitatory neurons, which could contribute to its differential effect on these two neuronal populations.

Since hNR1 antibody binds different NMDAR pools on inhibitory and excitatory neurons in cortex (Fig. 5A-B), we were eager to evaluate whether it also has analogous/opposite specificity in hippocampal neurons and could potentially explain antibody's contrasting effects on hippocampal vs cortical excitatory cells observed in our autaptic recordings (Fig. 2-3). We therefore repeated the immunocytochemistry experiments in hippocampal neuronal cultures. Here, we observed that on hippocampal excitatory neurons the hNR1 antibody accumulated at VGLUT1-positive puncta to a similar extent as in cortical cultures (~40%, Fig. 5C-D), suggesting that synaptic/extra-synaptic binding does not underlie antibody's differential effects on cortical vs hippocampal excitatory neurons. On the other hand, the distribution of hNR1 antibody puncta on hippocampal inhibitory neurons was strikingly different from cortical cultures. Here, only 20% of the antibody puncta co-localized with VGLUT1, implying that in hippocampal inhibitory neurons hNR1 antibody binds mostly extra-synaptic receptors.

Together, this set of experiments demonstrates that in cortical cultures the hNR1 antibody has little if any effect on excitatory neurons, but it specifically impairs the function of inhibitory neurons by decreasing their surface NMDAR function and in turn impairs synaptic GABAergic transmission (Fig. 3). Of note, this specificity does not originate from antibody's preference for a specific subunit composition (Fig. 4), but rather the hNR1 antibody appears

to target different synaptic/extra-synaptic NMDAR pools on cortical excitatory and inhibitory neurons, via an unknown mechanism (Fig. 5).

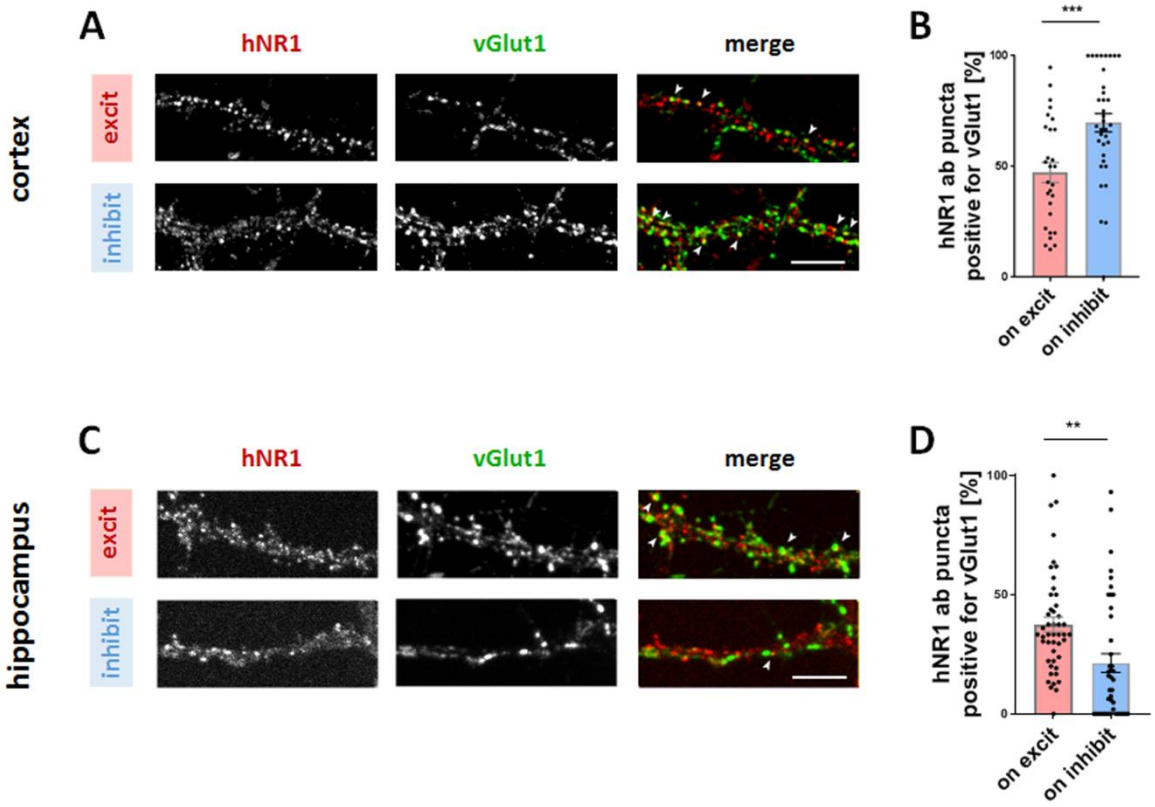

Figure 5. hNR1 antibody targets different NMDAR pools on excitatory and inhibitory neurons, in a brain region-specific manner. Live staining of cortical neuronal cultures was used to detect acute hNR1 antibody binding patterns. Neurons were live stained with the hNR1 antibody, before being fixed and co-stained with VGLUT1 synaptic marker. The degree of hNR1 and VGLUT1 co-localization served as a measure of excitatory synaptic or extra-synaptic localization of hNR1 puncta. **(A)** Representative images of stained cortical cultures. **(B)** In cortex, on excitatory dendrites ~50% of hNR1 antibody puncta co-localized with VGLUT1, whereas on inhibitory dendrites 70% of antibody puncta were synaptic (paired t-test, p=0.006). **(C)** Representative images of stained hippocampal neurons. **(D)** This trend was opposite in hippocampal cultures, where hNR1 antibody puncta co-localized with VGLUT1 to a smaller degree on inhibitory dendrites than on excitatory dendrites (~20% vs ~40%, respectively, unpaired t-test, p=0.0016). In (B, D) each data-point represents mean values per ROI (dendrite), error bars indicate SEM, scale bar = 10 µm, **p<0.01, ***p<0.001. Modified from Fig. 8 in Andrzejak et al., 2022.

4.3. hNR1 antibody impairs E/I balance and disinhibits cortical networks

The precise functioning of cortical neuronal networks relies on a finely tuned balance between excitation and inhibition (E/I), which results from a highly controlled interplay of

excitatory and inhibitory neurons. Having observed a selective impairment of cortical inhibitory neurons due to hNR1 antibody treatment in autaptic cortical cultures (Fig. 3), we next explored whether this translates into changes of neuronal activity on a network level. To continuously monitor neuronal activity of cortical networks over hours, we initially grew cortical cultures on multi-electrode array (MEA) dishes for ~11-14 days. Firstly, we recorded baseline network activity for 15h. Thereafter 1 μg/ml of hNR1 or ctrl antibody was added and the network activity was recorded for another 24h (Fig. 6A, H). Notably, the spiking activity of cortical networks gradually increased in the presence of hNR1 antibody over the period of 24h, reaching a highly active state (Fig. 6B, D). The control antibody had more modest effects, eliciting a small yet non-significant change in network spiking during this time interval (Fig. 6B-C). Consequently, to test whether cortical networks retain or lose their responsiveness to NMDAR blockage after antibody treatment, we added a saturating concentration (50 μM) of AP5, an NMDAR antagonist, at the end of the 24h antibody treatment. As expected, in control condition AP5 rapidly reduced neuronal spiking (95% reduction), which only partially recovered 6h later (61% recovery, Fig. 6F-G). In contrast, spiking only partially dropped due to AP5 (42% reduction) in networks pre-treated with hNR1 antibody. These rapidly recovered to 93% of activity levels prior to the addition of AP5 (Fig. 6F-G). These remained nearly fourfold higher than seen under control condition. These latter data indicate that the treatment with hNR1 antibody makes these networks mostly insensitive to NMDAR blockage with AP5, while increasing network excitability.

Furthermore, we analyzed the effects of hNR1 antibody on the bursting activity in these cultures and observed a dramatic increase in the burst rate due to hNR1 antibody treatment (Fig. 6I, K). At the same time, the burst rate in control antibody treated networks remained unchanged (Fig. 6I-J). Such elevated burst rates are typical for removal of inhibition from neuronal networks (Chen et al., 2012). Notably, AP5 had a smaller impact on bursting than spiking activity and its immediate impact (Fig. 6M) or degree of recovery of burst rate 6h later (Fig. 6N) were similar among treatment groups. Together, these MEAs experiments suggest that hNR1 antibody increases the overall spiking and bursting activity of cortical networks, a situation that drives them into a hyper-active state. This hyperactivity, at least in part, relies on decreased function of NMDARs, as the networks partially lose their responsiveness to NMDA receptor blockage by AP5.

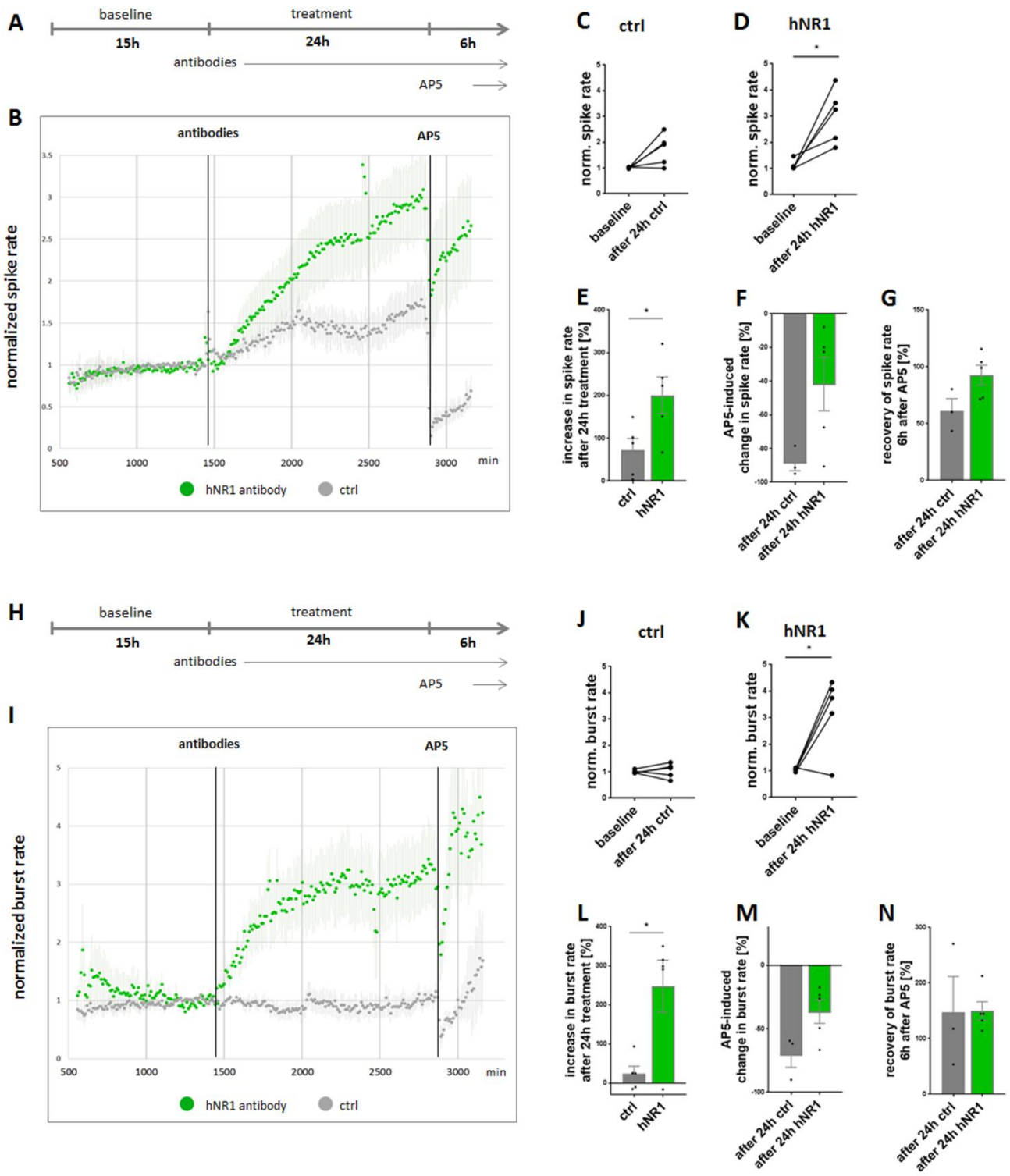

Figure 6. hNR1 antibody increases spiking and bursting activity of cortical cultures. (A, H) Cortical cultures were grown on multi-electrode arrays and their spiking was recorded continuously for ~45h: 15h of baseline recording, followed by 24h in the presence of 1 µg/ml of hNR1 or control antibodies and final 6h in presence of antibodies and 50 µM AP5. **(B, I)** Normalized spike (B) or burst (I) rate of cortical neuronal networks. Each data point represents the number of spikes/bursts recorded from all 59 electrodes within a 10 min interval, which were then normalized to the last 3h of baseline activity. Error bars indicate SEM. **(B)** Treatment with hNR1 antibody gradually increases neuronal spiking to a 3-fold higher state. **(C-D)** Within dish comparison of spiking at the end of baseline (1h)

and at the end of 24h antibody treatment (1h). **(C)** Control antibody slightly increases neuronal spiking yet without reaching significance levels (paired t-test, p=0.07), **(D)** hNR1 antibody significantly increases neuronal spiking (paired t-test, p=0.02). **(E-G)** Percentage change in normalized spike rate at the beginning (10 min) or end (10 min) of the respective treatment. Each data point represents an individual network. hNR1 antibody treatment increases neuronal spike rate significantly more than treatment with control antibody (**E**, unpaired t-test, p=0.045). **(J-K)** Within dish comparison of bursting at the end of baseline (1h) and at the end of 24h antibody treatment (1h). hNR1 antibody increases the normalized burst rate of cortical networks (**K**, paired t-test, p=0.037), whereas control antibody does not (**J**). **(L-M)** Percentage change in normalized burst rate at the beginning (10 min) or end (10 min) of a corresponding treatment. hNR1 antibody treatment increases neuronal burst rate significantly more than control antibody (**L**, unpaired t-test, p=0.01). Error bars indicate SEM. Modified from Fig. 1 in Andrzejak et al., 2022.

The observed elevation in network activity due to the hNR1 antibody (Fig. 6) was surprising as it is in contrast to previous studies reporting that active networks respond to NMDAR ketamine or AP5 by a rapid shutdown of network spiking (Teppola et al., 2018, 2019; Emnett et al., 2013). However, it has previously been suggested that disinhibition of cortical networks can be caused by NMDAR hypofunction (Y. Zhang et al., 2008; Homayoun & Moghaddam, 2007). Consequently, as we observed that on a single-cell level the hNR1 antibody impairs function of inhibitory, but not excitatory, cortical neurons (Fig. 3), we asked if the observed increase in network activity (Fig. 6) could be due to network disinhibition. This was accomplished by designing a set of electrophysiological and calcium imaging experiments. For the latter, cortical cultures were infected with RCaMP at 4DIV, a genetically encoded calcium indicator (Dana et al., 2016). After 14-17 DIV, neurons were treated for 24h with hNR1 or control antibodies, or left untreated, and then live-imaged to detect somatic calcium transients of individual cells. Here, we observed that a 24h treatment with the hNR1 increased the frequency of calcium transients when compared with control and untreated conditions (Fig. 7A-D). These data nicely support the hyperactivity observed in our MEAs experiments (Fig. 6). Of note, in this experimental design, the frequency of calcium transients was also increased by the control antibody when compared to untreated condition (Fig 7D). This was however to a smaller extent than in cultures treated with the hNR1 antibody. These data indicate that this control antibody is not without its effects, however the mechanism is unknown.

In the next set of experiments, we tested whether the antibody-treated hyper-excitable networks can be further disinhibited. This was accomplished by adding the $GABA_AR$

antagonist bicuculline (30 μM) after the 24h antibody treatment and re-imaged the activity of the same neurons, which allowed for a within-cell comparison (Fig. 7A-C, upper vs lower panels). As expected, in control conditions bicuculline increased the frequency of calcium transients, disinhibiting the networks (Fig. 7E-F). Conversely, in networks treated with hNR1 antibody bicuculline failed to increase the frequency of calcium transients (Fig. 7G). These data suggest that critical features of the GABAergic system contribute to antibody-mediated hyper-excitability, though it is important to note that bicuculline can also block Ca^{2+}-activated potassium channels (Johnston, 2013; Khawaled et al., 1999), possibly further contributing to its effects.

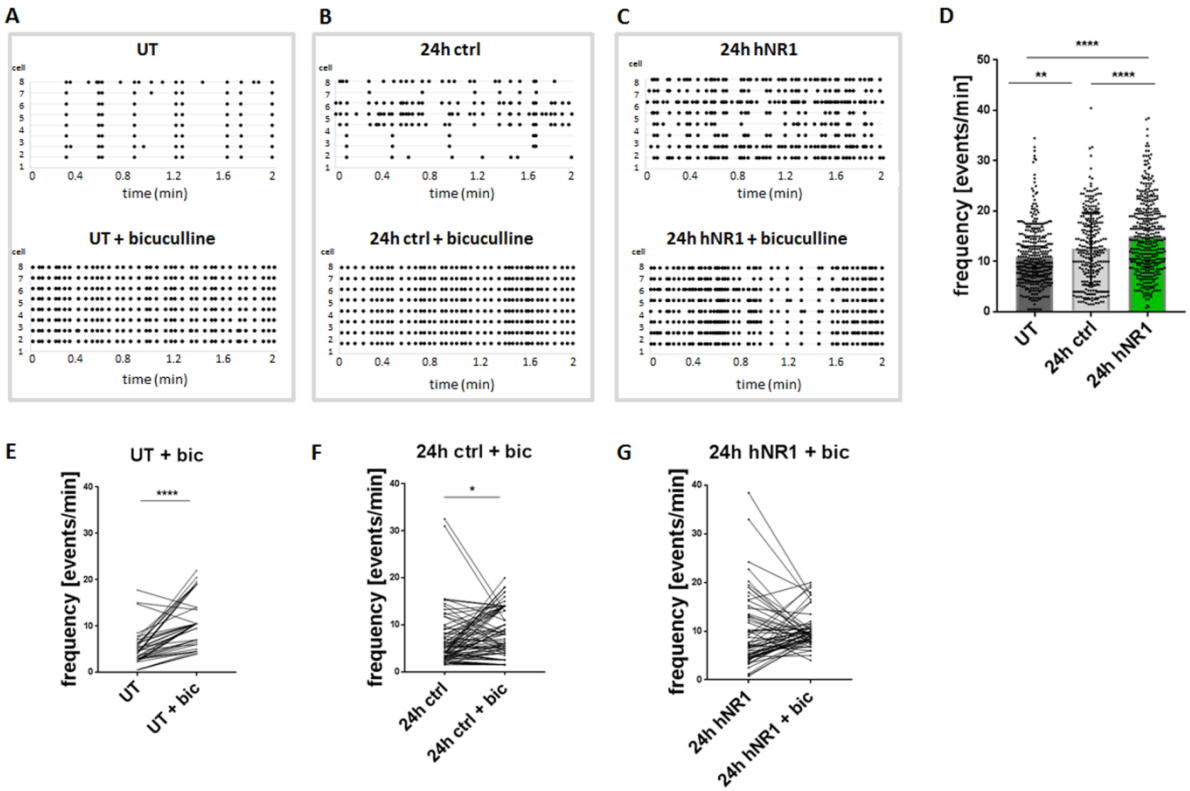

Figure 7. Bicuculline does not further disinhibit cortical networks treated with hNR1 antibody. Cortical network activity was assessed by infecting neurons with RCaMP and live-imaging to detect somatic calcium transients. **(A-C)** Upper panels: representative raster plots of detected calcium events at the end of 24h treatment. Lower panels show raster plots of the same networks following addition of bicuculline (30 μM) directly at the end of 24h treatment. Each data point represents a calcium event detected from individual cells (y axis) at a given time point (x axis). **(D)** Frequency of calcium events at the end of 24h treatment. Each data point represents an average of calcium events detected from an individual neuron. Treatment with hNR1 antibody, and to a lesser extent control antibody, increases overall frequency of calcium events (ANOVA Tukey's multiple-comparison test, **p=0.007, ****p<0.0001). **(E-G)** Within-cell comparison of frequency of calcium events at the end of respective 24h treatment and after bicuculline application. In both untreated and control

antibody condition bicuculline increases calcium events (paired t-test: **E**, ****p < 0.0001; **F**, *p=0.035), but not after hNR1 antibody treatment (**G**). Error bars indicate SEM. From Fig. 3 in Andrzejak et al., 2022.

Finally, since hNR1 antibody reduced the synaptic output of inhibitory cortical neurons in autaptic recordings (Fig. 3), we were curious to explore if similar changes in inhibitory synaptic transmission underlie hNR1 antibody-induced disinhibition of neuronal network activity. Of note, studies on the "glutamatergic hypothesis of schizophrenia" imply that NMDAR hypofunction is associated with reduced inhibitory drive onto excitatory neurons which leads to cortical disinhibition (Homayoun and Moghaddam 2007), resulting in psychiatric symptoms resembling those seen in encephalitis patients. To measure if the hNR1 antibody also affects the synaptic inhibitory drive onto excitatory neurons in our cortical neurons, we measured mIPSCs recorded from excitatory neurons after a 24h treatment with either the hNR1 or control antibody. Lentivirus expressing mKate2 under CamKII promoter was used to identify cultured excitatory neurons (Fig. 8A-B). Here, the hNR1 antibody treatment indeed reduced the frequency of these mIPSCs (Fig. 8D) and had a tendency to reduced their amplitude, yet without reaching significance levels (Fig. 8E). To verify if the reduction in mIPSCs is due to an overall hypofunction of surface GABAR on the post-synaptic excitatory neurons, whole-cell GABA currents were recorded following a 1s bath application of GABA (5 μM) (Fig. 8G-H). However, these currents remained unchanged, indicating that the antibody treatment did not alter the total pools of GABARs on excitatory neurons.

As balanced network activity relies on both excitation and inhibition, we then examined if synaptic excitatory drive in cortical cultures is also affected by hNR1 antibody. To this end, we recorded mEPSCs from both inhibitory and excitatory neurons 24h after being treated with either the control or hNR1 antibody (Fig. 8I-P). Interestingly, neither amplitude, frequency nor charge of the mEPSCs on neither cell type was altered due to hNR1 antibody treatment (Fig. 8I-P).

Together, this set of experiments illustrates that hNR1 antibody gradually drives cortical networks into a hyper-excitable state (Fig. 6), such that they cannot be further disinhibited by bicuculline (Fig. 7), possibly by selectively reducing synaptic inhibitory drive onto excitatory neurons in these cultures (Fig. 8).

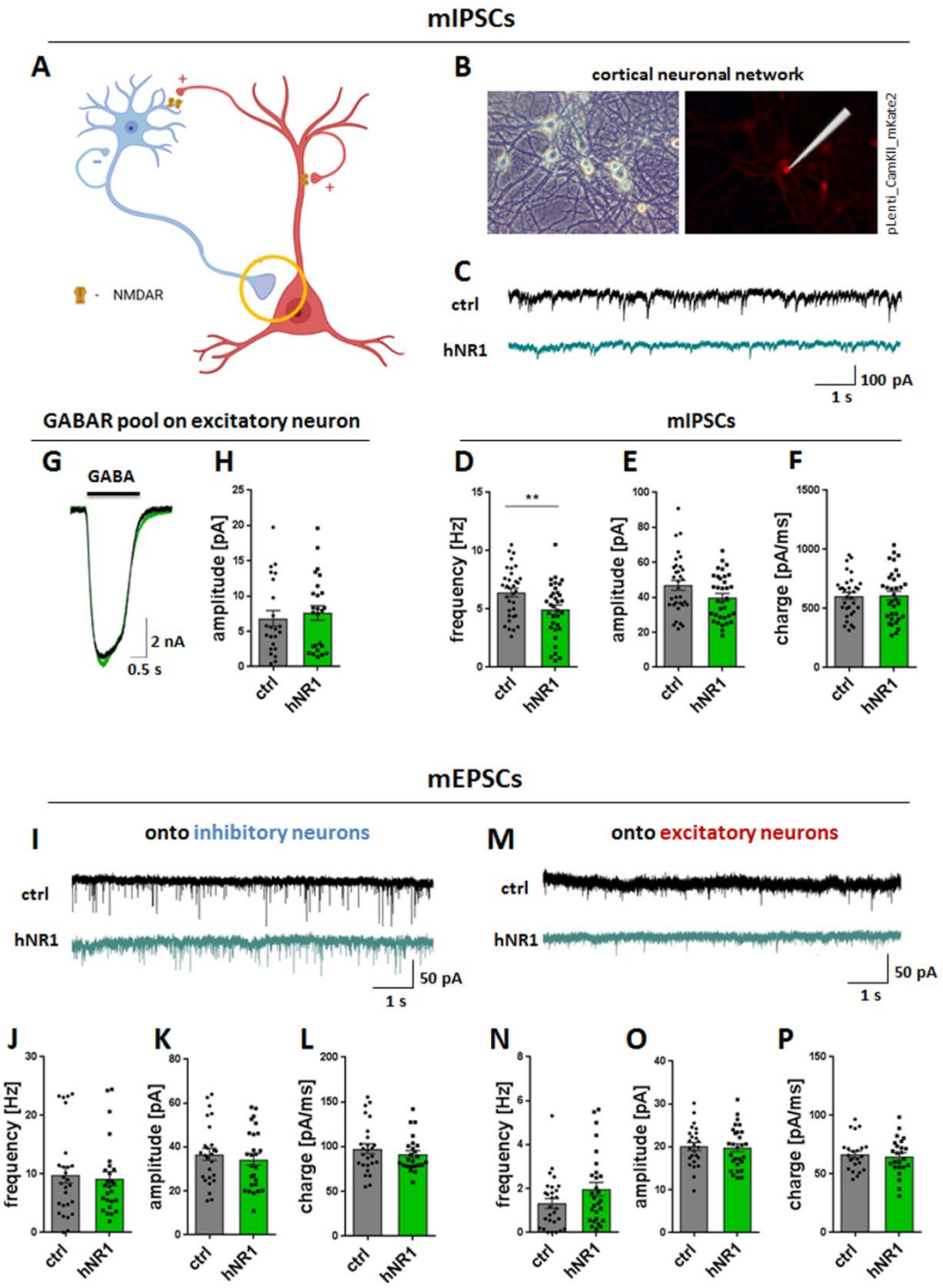

Figure 8. In cortical networks, hNR1 antibody treatment decreases inhibitory drive onto excitatory neurons, without affecting excitatory drive. (A) Inhibitory drive onto cortical excitatory neurons was determined by recording mIPSCs from excitatory neurons in cultured networks. **(B)** Representative images of cultured neurons (left) and excitatory neuron (right) identified by infecting cultures with a lentivirus expressing mKate2 driven by the CaMKII promoter. **(C-F)** hNR1 antibody treatment was observed to reduce mIPSCs frequency of excitatory neurons (D, unpaired t-test, p=0.009), without affecting mIPSCs amplitude or charge. **(I-P)** Excitatory drive onto excitatory (I-L) or inhibitory (M-P) cortical neurons is not affected by hNR1 antibody treatment. **(I, M)** representative traces of mIPSCs

recorded from inhibitory (I) or excitatory (M) neurons. Amplitude, frequency and charge of mEPSCs were not changed by hNR1 treatment on both inhibitory (J-L) and excitatory (N-P) neurons. Error bars indicate SEM. From Fig. 4 in Andrzejak et al., 2022.

4.4. hNR1 antibody affects cortical inhibitory synapses, specifically onto excitatory neurons

Thus far, we observed that the hNR1 antibody disinhibits cortical networks (Fig. 6, 7) by decreasing synaptic output of inhibitory neurons (Fig. 3, 8). To investigate how hNR1 antibody affects these inhibitory synapses in more detail, we designed a set of immunocytochemical experiments. Neurotransmitter release takes place from the pre-synaptic boutons. Two proteins crucial for inhibitory pre-synaptic function include the glutamate decarboxylase 65 (GAD65) which synthetizes GABA, and vesicular GABA transporter (VGAT) – required for loading GABA into synaptic vesicles. To investigate whether the hNR1 antibody affects levels of these pre-synaptic proteins, we quantified the intensities of GAD65 and VGAT puncta before and after treatment with the hNR1 antibody. Additionally, by employing GAD67-eGFP animals, we could distinguish between GAD65/VGAT puncta on dendrites of excitatory (GFP-negative) and inhibitory (GFP-positive) neurons (Fig. 9B-C). Remarkably, the intensity of VGAT puncta was reduced by a 24h treatment with the hNR1 antibody (Fig. 9D-E). Moreover, this decrease was selective for inhibitory synapses formed onto excitatory, but not inhibitory, neurons (Fig. 9D-F). Conversely, the 24h antibody treatment did not alter the intensity of GAD65 puncta (Fig. 9G-I). Intriguingly, when we additionally measured the intensity of GAD65 puncta 6h after hNR1 antibody treatment, a decrease in the GAD65 puncta intensity was observed due to this shorter hNR1 antibody treatment (Fig. 9G-I). Remarkably, this effect was again specific only to inhibitory synapses formed onto excitatory, and not those formed onto inhibitory, neurons (Fig. 9H-I).

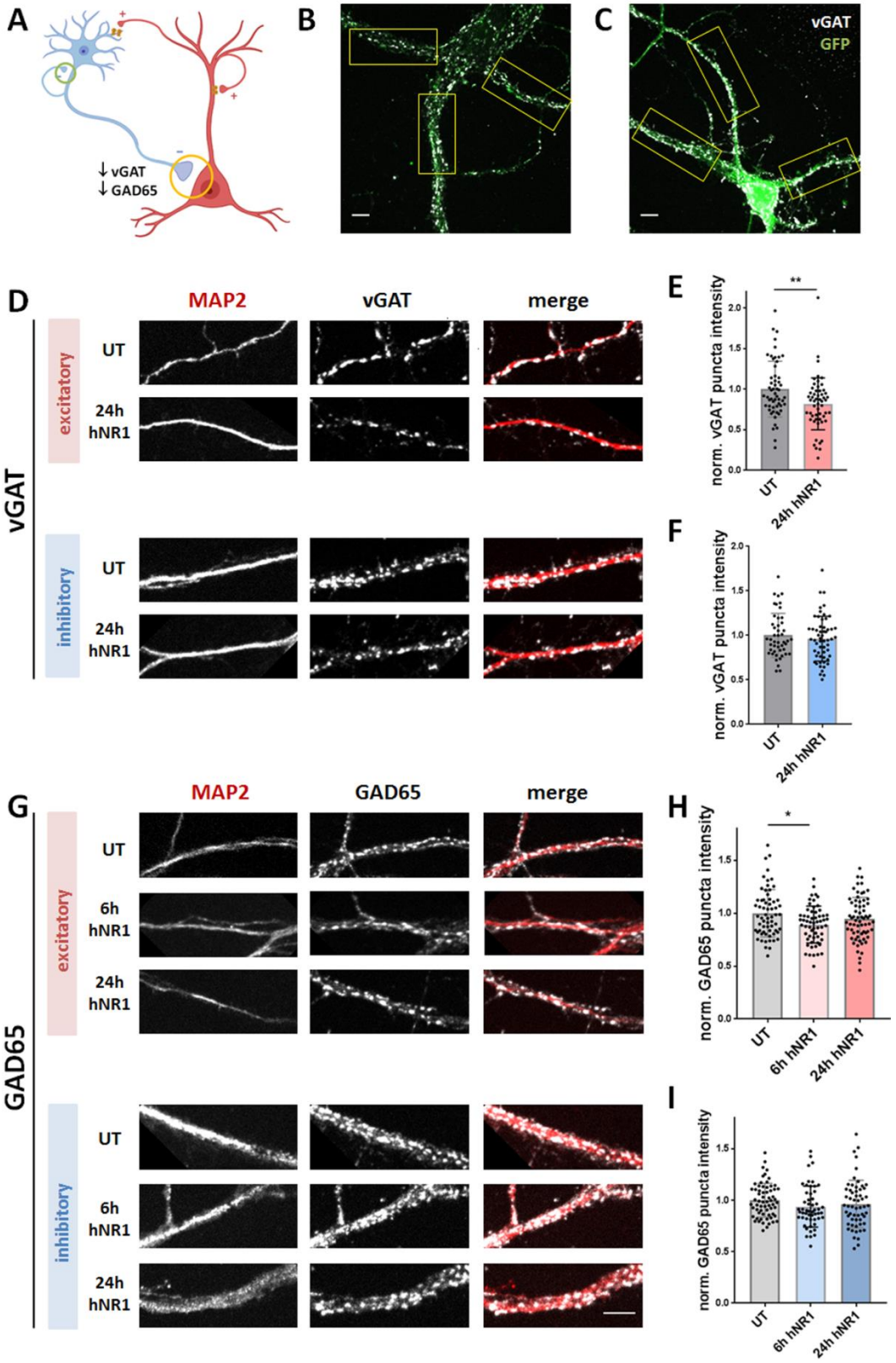

Figure 9. hNR1 antibody decreases levels of inhibitory proteins VGAT and GAD65 at synapses formed onto excitatory, but not inhibitory, neurons. (A) Schematic summarizing the finding of reduced VGAT and GAD65 levels at inhibitory synapses formed onto excitatory neurons. **(B-C)** Excitatory and inhibitory dendrites were identified based on GFP expression from GAD67-eGFP

animals. **(D-F)** Intensity of VGAT puncta onto excitatory (E, paired t-test, p=0.005) but not inhibitory (F) neurons was decreased by a 24h treatment with hNR1 antibody. **(G-I)** Intensity of GAD65 puncta on excitatory dendrites was reduced by 6h (H, ANOVA, p=0.01) but not 24h treatment with hNR1 antibody. **(I)** This effect was again specific to excitatory neurons, as intensity of GAD65 puncta onto inhibitory neurons was unchanged. Each data point represents a mean intensity value of all detected puncta per ROI (dendrite). Error bars indicate SEM. From Fig. 7 in Andrzejak et al., 2022.

Finally, we explored whether the impairment of inhibitory synapses in cortical neurons is associated with a specific hNR1 antibody binding pattern. Although we observed that hNR1 antibody partially co-localizes with the excitatory synaptic marker VGLUT1 (Fig. 5A-B), there was a large pool of hNR1 antibody puncta accumulating outside of excitatory synapses on both excitatory and inhibitory neurons. It is therefore conceivable that the hNR1 antibody also binds NMDARs within/in proximity to inhibitory synapses, where it could affect their function locally. To test this hypothesis, we live-labeled cortical cultures with hNR1 antibody, fixed and co-stained the neurons with gephryin, an inhibitory post-synaptic marker. Remarkably, our confocal microscopy and z-stack analysis revealed that up to 30% of inhibitory synapses formed onto excitatory neurons were also immuno-positive for the hNR1 antibody (Fig. 10A-D). Moreover, this phenomenon was much less frequent at inhibitory synapses formed onto inhibitory neurons, where the hNR1 antibody bound to only ¬10% of these gephyrin-positive puncta (Fig. 10C).

Together, these data illustrate that the hNR1 antibody interacts with NMDAR within a subset of cortical inhibitory synapses (Fig. 10) leading to a decrease in the inhibitory pre-synaptic proteins GAD65 and VGAT (Fig. 9), specifically at inhibitory-to-excitatory neuron synapses.

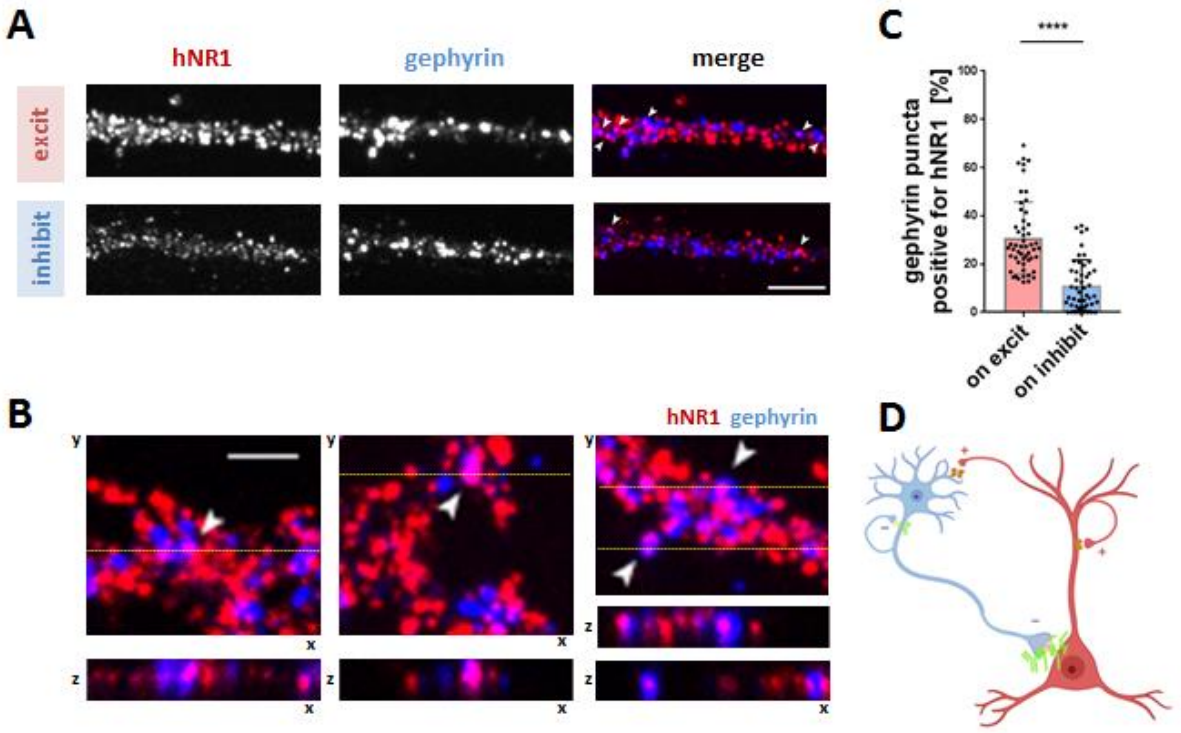

Figure 10. hNR1 antibody binds within inhibitory synapses, preferentially on excitatory neurons. (A) Acute antibody staining of cortical cultures reveals that hNR1 antibody accumulates in a subpopulation of gephyrin-positive puncta. **(B)** Z-stack (3D) analysis of confocal images shows overlap between individual hNR1 antibody and gephyrin puncta in both x-y (upper panel) and x-z (lower panel) planes. **(C)** Percentage of gephyrin puncta decorated with the hNR1 antibody is higher on excitatory than inhibitory dendrites (~30% vs 10%, respectively, unpaired t-test, $p<0.0001$). Each data point represents a percentage of hNR1-positive gephyrin puncta per ROI (dendrite). **(D)** Schematic illustrating the selective binding of hNR1 antibody (green) within inhibitory synapses with a preference to those onto excitatory neurons. Scale bar in A = 10 μm; in B = 5 μm. Error bars indicate SEM. Modified from Fig. 8 in Andrzejak et al., 2022.

5. Discussion

The present work aimed to understand the molecular and cellular effects of recently developed monoclonal NMDAR autoantibodies derived from patients with anti-NMDAR encephalitis and their potential contribution to disease pathology. We found that both affinity-matured and unmutated, germline-configured NMDAR autoantibodies can pose a pathogenic effect and reduce NMDA-specific currents in cultured rodent neurons. Moreover, we report that these autoantibodies show brain regional specificity, differently affecting hippocampal versus cortical neurons. While in hippocampal neuronal cultures the hNR1 antibody decreases NMDA currents of excitatory neurons, in cortical cultures it selectively affects synaptic transmission and NMDA currents of inhibitory, but not excitatory, neurons. Consequently, impaired inhibitory drive leads to disinhibition of cortical networks, leaving them in a hyper-excitable state. Interestingly, apart from targeting different NMDAR pools on cortical inhibitory vs excitatory neurons, the hNR1 antibody also bound within a subset of inhibitory synapses in cultured cortical neurons. This is associated with decreased protein levels of crucial components of inhibitory presynaptic boutons, such as VGAT and GAD65, specifically at synapses formed onto excitatory neurons.

5.1. Germline g-hNR1 antibody shows pathogenic potential

Interestingly, our initial analysis of a panel of monoclonal antibodies derived from individual encephalitis patients revealed that a subset of the NMDAR autoantibodies were unmutated (Kreye et al., 2016). This suggested that they were derived from naïve B cells of the natural B cell repertoire present in healthy individuals (Dahm et al., 2014). The function of such “naturally occurring” autoantibodies is not fully understood, yet they are thought to have a beneficial function in regulating immune responses, dampening inflammation and clearing apoptotic cells and debris (Lutz et al., 2009). Indeed, one study suggested that preexisting NMDAR antibodies were associated with a smaller progression of lesions in acute ischemic stroke (Zerche et al., 2015). However, little is known whether such naturally occurring NMDAR autoantibodies can also pose a pathogenic effect in context of autoimmune encephalitis. In our study, we observed that a germline antibody g-hNR1 indeed selectively reduced whole-cell and synaptic NMDA currents (Fig 2K-O), indicating its pathogenic potential. Of note, antibody concentration required to elicit reduction in NMDA currents

was 5-fold higher for the g-hNR1 antibody compared to the affinity-matured hNR1 antibody. This was not surprising given the g-hNR1 has a much lower affinity for NMDARs (Wenke et al., 2019). These data indicate that even naturally occurring NMDAR antibodies, which have not undergone affinity-maturation, have the potential to be pathologically-relevant after gaining access or being produced within the brain. This is of importance, as circulating peripheral NMDAR autoantibodies have been reported in up to 10% of healthy individuals (Dahm et al., 2014; Hammer et al., 2014), and therefore their pathogenic potential could readily rely on the integrity of the blood-brain barrier (Hammer et al., 2014). Notably, future studies will need to determine whether concentration/affinity of these naturally occurring antibodies is sufficient to elicit any pathogenic effects in the CNS of encephalitis patients.

5.2. hNR1 antibody acts with brain regional and neuronal-subtype specificity

Strikingly, our data indicate that NMDAR autoantibodies can exhibit differential effects between brain regions (Fig. 2 vs Fig. 3) and neuronal subpopulations (Fig. 3). A major novel finding of the current study is that in cortex the hNR1 antibody impairs the function of inhibitory neurons, yet it has no effect on excitatory neurons (Fig. 3). These data are in stark contrast to the earlier body of literature focusing on hippocampal neurons, where patient CSF/IgGs impaired the function of excitatory neurons (Kreye et al., 2016; Hughes et al., 2010) yet had no effect on mIPSCs (Moscato et al., 2014). This discrepancy of hNR1 antibody effects on excitatory neurons in cortex cannot be due to technical limitations of our assay, as we could reproduce these previous finding in our hippocampal recording, where the hNR1 antibody indeed impaired function of excitatory cells (Fig. 2).

At present, the mechanisms underlying these differential effects on cortical vs hippocampal neurons remain unclear. Importantly, NMDARs subcellular localization and subunit composition is brain area dependent (Sanz-Clemente et al., 2013) and could therefore contribute to antibody specificity. We addressed the former by analyzing the acute hNR1 antibody binding in cortical and hippocampal cultures. The synaptic vs extra-synaptic distribution of hNR1 antibody binding did not differ between cortical and hippocampal excitatory neurons (Fig. 4). This suggests that the subcellular distribution of NMDARs does not directly underlie the observed lack of effect of the hNR1 antibody on cortical excitatory neurons (Fig. 3) and other mechanisms must be at play. On the other hand, the subcellular

distribution of hNR1 antibody on inhibitory neurons was strikingly different in cortical vs hippocampal cultures (70% vs 20% synaptic, respectively, Fig. 5). Extensive characterization of hNR1 antibody effect on hippocampal inhibitory neurons was beyond the scope of current work, however these latter results imply that hNR1 antibody's effects on hippocampal inhibitory function, and therefore possibly network activity, might be different to what we observed in cortex (Fig 3, 6-8).

Regarding specificity to cortical inhibitory neurons, it could be achieved by autoantibodies binding to NMDARs with a specific subunit composition. Cortical interneurons have a fivefold higher ratio of NR2A/NR2B, the two most abundant NMDAR subunits apart from NR1, while compared to neighboring pyramidal neurons (Kinney et al., 2006; Xi et al., 2009). Although autoantibodies bind the obligatory NR1 subunit (Kreye et al., 2016), subunit-specific subcellular localization, scaffolding proteins or interaction partners (Paoletti et al., 2013; Petit-Pedrol & Groc, 2020; Planagumà et al., 2016) could affect an antibody's binding. In our assay, hNR1 antibody did not change the sensitivity of NMDA currents to the NR2B-specific blocker ifenprodil on neither cell type (Fig. 4), suggesting that hNR1 antibody does not drastically affect the NR2A/NR2B ratio. Nonetheless, cortical interneurons are also enriched for less commonly expressed NR2C and NR2D subunits (Monyer et al., 1994) and autoantibodies' interactions with these could account for more subtle changes in NMDAR subunit composition. Further yet, a recent RNA sequencing study revealed that cortical excitatory and inhibitory neurons express different splice variants of the obligatory NR1 subunit (Huntley et al., 2020), altering extracellular region in close proximity to the described antibody-binding site (Gleichman et al., 2012), which could also contribute to interneuron specificity. More detailed future studies will help answer these questions.

hNR1 antibody's regional specificity also raises an important question of validity of current pre-clinical models. To date, the majority of animal models have employed passive transfer approaches delivering patient CSF/antibodies into brain ventricles (Wright et al., 2015; Taraschenko et al., 2019; Planagumà et al., 2016) or the hippocampus (Kersten et al., 2019; Würdemann et al., 2016), providing antibodies with direct access to hippocampal structures, but they rarely reach cortical regions (Planagumà et al., 2015). While these approaches can be sufficient to test hippocampus-dependent behaviors such as spatial memory (Li et al., 2015), they might not be suitable for studying more complex behaviors requiring broader

cortical involvement. Indeed, studies assessing depressive-like behavior using tail-suspension test (Planagumà et al., 2015 vs Planagumà et al., 2016)), anxiety (Kersten et al., 2019) or locomotor activity (Taraschenko et al., 2019) produced conflicting results or failed to induce phenotypes observed in encephalitis patients. Thus, models that use active immunization, which are more prone to seizures (Wagnon et al., 2020; Jones et al., 2019), may be preferable for future investigations seeking to reach a more clinically-relevant antibody distribution in the brain, which would encompass their varying region-specific effects.

5.3. hNR1 antibody causes synaptic inhibitory dysfunction in cortex

The major finding of our study is that in cortical cultures the primarily effect of hNR1 antibody is the impairment of the synaptic output of inhibitory neurons. Initial cell-autonomous, autaptic recordings demonstrated this specificity, as hNR1 antibody significantly decreased NMDAR- and synaptic currents exclusively in inhibitory neurons (Fig. 3). How decreased NMDAR function leads to impaired synaptic inhibitory transmission remains unclear (see more below). However, the mechanisms involved do not necessarily depend on the activation of NMDARs, as our inhibitory autaptic neurons do not receive excitatory input. This implies that activity-independent, non-canonical functions of NMDARs or their numbers and/or distribution are important for the stability and effectiveness of inhibitory synaptic transmission in cortical circuits.

Moreover, our whole-cell mass culture recordings proved that antibody-induced inhibitory dysfunction is not exclusive to single-cell effects, but also translates into networks of neurons (Fig. 8). Consistently, the addition of hNR1 antibody decreased action potential-independent, tonic inhibitory drive onto excitatory neurons, determined by measuring mIPSCs frequency (Fig. 8A-F). Importantly, this effect was again specific to inhibitory neurons, as excitatory mEPSCs remained unchanged (Fig. 8I-P). A third line of evidence for synaptic inhibitory dysfunction comes from our immunocytochemical analysis, which revealed that hNR1 antibody decreased levels of VGAT and GAD65 (Fig. 9), two proteins crucial for the proper functionality of pre-synaptic inhibitory boutons. Importantly, this phenomenon was exclusive to inhibitory synapses formed onto excitatory, but not inhibitory, neurons (Fig. 9).

5.4. Disinhibition of cortical networks

In cortex, GABAergic interneurons are responsible for maintaining the delicate E/I balance by orchestrating the excitability of pyramidal neurons. Therefore, observed reduction in synaptic inhibitory transmission, especially onto excitatory cortical neurons, with constant excitatory drive (Fig. 8) suggest possible changes on global network activity levels. Remarkably, our calcium imaging and MEA recordings indeed demonstrated that a 24h treatment with the hNR1 antibody dramatically increased the spiking (Fig. 6) and somatic firing (Fig. 7) of cortical neuronal networks, leading them into a hyper-excitable state.

This very novel observation seems counterintuitive when considering the hNR1 antibody to act as a simple NMDAR antagonist. Cortical networks normally react to NMDAR antagonists such as ketamine or AP5 with a rapid shout-down of neuronal spiking (Teppola et al., 2018, 2019; Emnett et al., 2013), a phenomenon opposite to the one observed with the hNR1 antibody (Fig. 6). Although counterintuitive, our findings are consistent with previous clinical and several molecular studies reporting that seizures occur in ~80% of patients with NMDAR encephalitis and epileptiform dischargers are frequent in EEG recordings, especially early in disease progression (Irani et al., 2010). Patient CSF also increased susceptibility to seizures in mice (Wright et al., 2015). Consistently, patient CSF was found to increase cortical extracellular glutamate levels (Manto et al., 2010) and induced corticomotor hyper-excitability in rats (Manto et al., 2011).

Accordingly, several cues from our cortical network recordings suggest that NMDA hypofunction, leading to decreased inhibition, indeed underlies the observed increase in network spiking. Firstly, networks treated for 24h with the hNR1 antibody partially lose their responsiveness to application of AP5 (Fig 6B, F) and quickly recover to their elevated levels of activity thereafter (Fig. 6G), suggesting that their activity becomes largely NMDAR-independent. Secondly, antibody-induced increase in neuronal spiking is a gradual phenomenon, steadily developing over many hours (Fig. 6B). This suggests that hNR1 antibody does not act as an acute antagonist, but rather it reflects the slower rate of antibody-induced NMDAR internalization (Moscato et al., 2014). Moreover, we further verified if hNR1 antibody also impairs the inhibitory system with our network experiments. Adding bicuculline at the end of 24h antibody treatment failed to further increase somatic

calcium firing (Fig. 7C, G), suggesting that the network cannot be further disinhibited. Finally, analysis of bursting activity of MEA recordings revealed that antibody treated networks quickly increase 3-fold their bursting activity (Fig. 6I), a behavior characteristic of removal of inhibition (Chen et al., 2012). Together with evidence for synaptic inhibitory dysfunction from autaptic (Fig. 3) and mass culture (Fig. 8) recordings, these data strongly suggests that antibody-induced NMDAR hypofunction decreases inhibition and subsequently disinhibits cultured cortical networks.

5.5. hNR1 antibody binds distinct NMDAR pools and affects inhibitory synapses

A major still open question is how hypofunction of NMDARs on inhibitory neurons leads to the changes of their synaptic output and ultimately decreases inhibitory drive. One possibility is that autoantibodies disrupt NMDARs downstream signaling leading to gene expression changes which subsequently influence overall neuron function. Interestingly, synaptic and extra-synaptic NMDARs trigger distinct, often opposing functional pathways: activation of synaptic NDMARs induces expression of anti-apoptotic, pro-survival genes, whereas extra-synaptic NMDARs trigger pro-death pathways (Hardingham & Bading, 2010). Remarkably, in our analysis of acute hNR1 antibody binding, we observed that hNR1 antibodies bind predominantly to synaptic NMDARs on inhibitory neurons (~70% of all antibodies puncta, Fig. 5A-B). This binding preference could lead to the suppression of proliferatory pathways and domination of extra-synaptic NMDAR signaling, leading to interneuron hypofunction. However, more detailed gene expression studies are needed to explore these mechanisms.

An alternative and/or complementary mechanism could be that the hNR1 antibody locally disrupts the function of pre-synaptic NMDARs situated directly within inhibitory pre-synaptic boutons. Such pre-synaptic NMDARs have previously been reported to directly control presynaptic neurotransmitter release (Bouvier et al., 2015), a situation that could partially explain the observed decline in mIPSCs (Fig. 8). Accordingly, physiological studies showed that these receptors play a crucial role in controlling inhibitory drive onto pyramidal neurons in prefrontal cortex (Pafundo et al., 2018). Furthermore, they can regulate the size of pre-synaptic inhibitory boutons measured by intensity of GAD65 puncta (Fiszman et al., 2005). In our study, we observed that a population of hNR1 antibody indeed accumulated

within inhibitory synapses (Fig. 10). There, they could potentially dysregulate proteins of the presynaptic release machinery, as we also observed decreased levels of the pre-synaptic proteins VGAT and GAD65 after hNR1 antibody treatment (Fig. 9). Importantly, both hNR1 antibody binding to inhibitory synapses and the reduction in pre-synaptic proteins were specific to inhibitory synapses formed onto excitatory neurons (Fig. 9, 10), which could directly regulate excitability of cortical outputs. It is therefore conceivable that apart from the more general effects of autoantibodies on cortical inhibitory cells, they might also affect a sub-population of inhibitory synapses, altering cortical network excitability in patients suffering from NMDAR encephalitis.

At present, it is unclear whether hNR1 antibody binding to inhibitory synapses is pre- or post-synaptic. However, the antibody used in our study has recently been reported to bind to pre-NMDARs, albeit on excitatory synapses (#003-102, Wagner et al., 2020). Importantly, Wagner and colleagues described 2 groups of patient-derived antibodies with distinct binding pattern to brain tissue, which differ in binding to pre- or post-synaptic NDMARs. If a pre-synaptic-NMDAR-related mechanism is indeed partly involved in the observed disinhibition of cortical networks, it will certainly be exciting to see whether these 2 groups of antibodies are associated with distinct set of symptoms observed in patients. In this regard, one would predict that pre-synaptic NMDAR-binding pattern could infer more seizures and perhaps more pronounced psychotic episodes. If that was the case, it would allow for a quick diagnostic method and prediction of clinical progression and open avenues for more targeted and personalized treatment.

Importantly, the mechanisms described above are not mutually exclusive. In fact, it is likely that they act in a complementary manner to trigger regional changes in synaptic plasticity, subcellular localization-specific transcriptional changes as well as altered regulation of presynaptic inhibitory drive to produce complex cognitive and behavioral phenotypes. Taken together, our data demonstrates a new, cortex-specific mechanism wherein autoantibodies against NMDAR can cause inhibitory synaptic dysfunction and disinhibit cortical networks.

5.6. Implications for neuropsychiatry

Importantly, hypofunction of NMDARs present on cortical GABAergic interneurons has long been suggested as a mechanism underlying the disinhibition of cortical networks and core psychiatric symptoms observed in other psychiatric disorders (Nakazawa et al., 2012). In particular, data from schizophrenia research suggests that genetic ablation of NMDARs in mouse interneurons leads to schizophrenia-like phenotypes (Belforte et al., 2010), caused by increases in excitability of cortical pyramidal neurons and loss of E/I balance (Pafundo et al., 2021). Similarly, treatment with ketamine not only causes loss of inhibitory phenotype of cortical interneurons (Kinney et al., 2006), but it also decreases frequency and amplitude of mIPSCs, without altering mEPSCs, and increases pyramidal cell excitability in prefrontal cortical slices (Y. Zhang et al., 2008). These latter observations are in striking similarity to the effects of hNR1 antibody treatment observed in our study. (Fig. 6, 7, 8). Therefore, our results provide evidence that autoantibodies derived from NMDAR encephalitis patients can affect similar pathways, indicating a possible common mechanism underlying psychiatric symptoms across several neuropsychiatric disorders.

References

Andrzejak, E., Rabinovitch, E., Kreye, J., Prüss, H., Rosenmund, C., Ziv, N. E., Garner, C. C., & Ackermann, F. (2022). Patient-derived anti-NMDAR antibody disinhibits cortical neuronal networks through dysfunction of inhibitory neuron output. *Journal of Neuroscience*, *42*(15), 3253-3270.

Arancillo, M., Min, S.-W., Gerber, S., Münster-Wandowski, A., Wu, Y.-J., Herman, M., Trimbuch, T., Rah, J.-C., Ahnert-Hilger, G., Riedel, D., Südhof, T. C., & Rosenmund, C. (2013). Titration of Syntaxin1 in mammalian synapses reveals multiple roles in vesicle docking, priming, and release probability. *Journal of Neuroscience*, *33*(42), 16698–16714.

Banker, G., & Goslin, K. (1988). Developments in neuronal cell culture. *Nature*, *336*(6195), 185–186.

Belforte, J. E., Zsiros, V., Sklar, E. R., Jiang, Z., Yu, G., Li, Y., Quinlan, E. M., & Nakazawa, K. (2010). Postnatal NMDA receptor ablation in corticolimbic interneurons confers schizophrenia-like phenotypes. *Nature Neuroscience*, *13*(1), 76–83.

Bliss, T. V., & Collingridge, G. L. (1993). A synaptic model of memory: Long-term potentiation in the hippocampus. *Nature*, *361*(6407), 31–39.

Bouvier, G., Bidoret, C., Casado, M., & Paoletti, P. (2015). Presynaptic NMDA receptors: Roles and rules. *Neuroscience*, *311*, 322–340.

Carlén, M., Meletis, K., Siegle, J. H., Cardin, J. A., Futai, K., Vierling-Claassen, D., Rühlmann, C., Jones, S. R., Deisseroth, K., Sheng, M., Moore, C. I., & Tsai, L.-H. (2012). A critical role for NMDA receptors in parvalbumin interneurons for gamma rhythm induction and behavior. *Molecular Psychiatry*, *17*(5), 537–548. https://doi.org/10.1038/mp.2011.31

Catts, V. S., Lai, Y. L., Weickert, C. S., Weickert, T. W., & Catts, S. V. (2016). A quantitative review of the postmortem evidence for decreased cortical N-methyl-d-aspartate receptor expression levels in schizophrenia: How can we link molecular abnormalities to mismatch negativity deficits? *Biological Psychology*, *116*, 57–67.

Chang, C.-L., Trimbuch, T., Chao, H.-T., Jordan, J.-C., Herman, M. A., & Rosenmund, C. (2014). Investigation of synapse formation and function in a glutamatergic-GABAergic two-neuron microcircuit. *Journal of Neuroscience*, *34*(3), 855–868.

Chen, J.-Y., Chauvette, S., Skorheim, S., Timofeev, I., & Bazhenov, M. (2012). Interneuron-mediated inhibition synchronizes neuronal activity during slow oscillation. *The Journal of Physiology*, *590*(16), 3987–4010.

Dahm, L., Ott, C., Steiner, J., Stepniak, B., Teegen, B., Saschenbrecker, S., Hammer, C., Borowski, K., Begemann, M., Lemke, S., Rentzsch, K., Probst, C., Martens, H., Wienands, J., Spalletta, G., Weissenborn, K., Stöcker, W., & Ehrenreich, H. (2014). Seroprevalence of autoantibodies against brain antigens in health and disease. *Annals of Neurology*, *76*(1), 82–94.

Dalmau, J. (2016). NMDA receptor encephalitis and other antibody-mediated disorders of the synapse: The 2016 Cotzias Lecture. *Neurology*, *87*(23), 2471–2482. https://doi.org/10.1212/WNL.0000000000003414

Dalmau, J., Tüzün, E., Wu, H., Masjuan, J., Rossi, J. E., Voloschin, A., Baehring, J. M., Shimazaki, H., Koide, R., King, D., Mason, W., Sansing, L., Dichter, M. A., Rosenfeld, M. R., & Lynch, D. R. (2007). Paraneoplastic anti–N-methyl-D-aspartate receptor encephalitis associated with ovarian teratoma. *Annals of Neurology*, *61*(1), 25–36.

Dana, H., Mohar, B., Sun, Y., Narayan, S., Gordus, A., Hasseman, J. P., Tsegaye, G., Holt, G. T., Hu, A., Walpita, D., Patel, R., Macklin, J. J., Bargmann, C. I., Ahrens, M., Schreiter, E. R., Jayaraman, V., Looger, L. L., Svoboda, K., & Kim, D. S. (2016). Sensitive red protein calcium indicators for imaging neural activity. *Elife*, *5*, e12727.

Emnett, C. M., Eisenman, L. N., Taylor, A. M., Izumi, Y., Zorumski, C. F., & Mennerick, S. (2013). Indistinguishable synaptic pharmacodynamics of the N-methyl-D-aspartate receptor channel blockers memantine and ketamine. *Molecular Pharmacology*, *84*(6), 935–947.

Fiszman, M. L., Barberis, A., Lu, C., Fu, Z., Erdélyi, F., Szabó, G., & Vicini, S. (2005). NMDA receptors increase the size of GABAergic terminals and enhance GABA release. *Journal of Neuroscience*, *25*(8), 2024–2031.

Gleichman, A. J., Spruce, L. A., Dalmau, J., Seeholzer, S. H., & Lynch, D. R. (2012). Anti-NMDA receptor encephalitis antibody binding is dependent on amino acid identity of a small region within the GluN1 amino terminal domain. *Journal of Neuroscience*, *32*(32), 11082–11094.

Hammer, C., Stepniak, B., Schneider, A., Papiol, S., Tantra, M., Begemann, M., Sirén, A.-L., Pardo, L. A., Sperling, S., Mohd Jofrry, S., Gurvich, A., Jensen, N., Ostmeier, K., Lühder, F., Probst, C., Martens, H., Gillis, M., Saher, G., Assogna, F., Spalletta, G., Stöcker, W., Schulz, T. F., Nave, K. A., & Ehrenreich, H (2014). Neuropsychiatric disease relevance of circulating anti-NMDA receptor autoantibodies depends on blood–brain barrier integrity. *Molecular Psychiatry*, *19*(10), 1143–1149.

Hardingham, G. E., & Bading, H. (2010). Synaptic versus extrasynaptic NMDA receptor signalling: Implications for neurodegenerative disorders. *Nature Reviews Neuroscience*, *11*(10), 682–696.

Hazan, H., & Ziv, N. E. (2017). Closed Loop Experiment Manager (CLEM)—An open and inexpensive solution for multichannel electrophysiological recordings and closed loop experiments. *Frontiers in Neuroscience*, *11*, 579.

Hazan, L., & Ziv, N. E. (2020). Activity dependent and independent determinants of synaptic size diversity. *Journal of Neuroscience*, *40*(14), 2828–2848.

Homayoun, H., & Moghaddam, B. (2007). NMDA receptor hypofunction produces opposite effects on prefrontal cortex interneurons and pyramidal neurons. *Journal of Neuroscience*, *27*(43), 11496–11500.

Howes, O., McCutcheon, R., & Stone, J. (2015). Glutamate and dopamine in schizophrenia: An update for the 21st century. *Journal of Psychopharmacology*, *29*(2), 97–115.

Hughes, E. G., Peng, X., Gleichman, A. J., Lai, M., Zhou, L., Tsou, R., Parsons, T. D., Lynch, D. R., Dalmau, J., & Balice-Gordon, R. J. (2010). Cellular and synaptic mechanisms of anti-NMDA receptor encephalitis. *Journal of Neuroscience*, *30*(17), 5866–5875.

Huntley, M. A., Srinivasan, K., Friedman, B. A., Wang, T.-M., Yee, A. X., Wang, Y., Kaminker, J. S., Sheng, M., Hansen, D. V., & Hanson, J. E. (2020). Genome-wide analysis of differential gene expression and splicing in excitatory neurons and interneuron subtypes. *Journal of Neuroscience*, *40*(5), 958–973.

Irani, S. R., Bera, K., Waters, P., Zuliani, L., Maxwell, S., Zandi, M. S., Friese, M. A., Galea, I., Kullmann, D. M., Beeson, D., Lang, B., Bien, C. G., & Vincent, A. (2010). N-methyl-D-aspartate antibody encephalitis: Temporal progression of clinical and paraclinical observations in a predominantly non-paraneoplastic disorder of both sexes. *Brain*, *133*(6), 1655–1667.

Jentsch, J. D., & Roth, R. H. (1999). The neuropsychopharmacology of phencyclidine: From NMDA receptor hypofunction to the dopamine hypothesis of schizophrenia. *Neuropsychopharmacology*, *20*(3), 201–225.

Johnston, G. A. (2013). Advantages of an antagonist: Bicuculline and other GABA antagonists. *British Journal of Pharmacology*, *169*(2), 328–336. https://doi.org/10.1111/bph.12127

Jones, B. E., Tovar, K. R., Goehring, A., Jalali-Yazdi, F., Okada, N. J., Gouaux, E., & Westbrook, G. L. (2019). Autoimmune receptor encephalitis in mice induced by active immunization with conformationally stabilized holoreceptors. *Science Translational Medicine*, *11*(500).

Kersten, M., Rabbe, T., Blome, R., Porath, K., Sellmann, T., Bien, C. G., Köhling, R., & Kirschstein, T. (2019). Novel object recognition in rats with NMDAR dysfunction in CA1 after stereotactic injection of anti-NMDAR encephalitis cerebrospinal fluid. *Frontiers in Neurology*, *10*, 586.

Khawaled, R., Bruening-Wright, A., Adelman, J. P., & Maylie, J. (1999). Bicuculline block of small-conductance calcium-activated potassium channels. *Pflügers Archiv*, *438*(3), 314–321. https://doi.org/10.1007/s004240050915

Kinney, J. W., Davis, C. N., Tabarean, I., Conti, B., Bartfai, T., & Behrens, M. M. (2006). A specific role for NR2A-containing NMDA receptors in the maintenance of parvalbumin and GAD67 immunoreactivity in cultured interneurons. *Journal of Neuroscience*, *26*(5), 1604–1615.

Kreye, J., Wenke, N. K., Chayka, M., Leubner, J., Murugan, R., Maier, N., Jurek, B., Ly, L.-T., Brandl, D., Rost, B. R., Stumpf, A., Schulz, P., Radbruch, H., Hauser, A. E., Pache, F., Meisel, A., Harms, L., Paul, F., Dirnagl, U., Garner, C., Schmitz, D., Wardemann, H., & Prüss, H. (2016). Human cerebrospinal fluid monoclonal N-methyl-D-aspartate receptor autoantibodies are sufficient for encephalitis pathogenesis. *Brain*, *139*(10), 2641–2652.

Krystal, J. H., Karper, L. P., Seibyl, J. P., Freeman, G. K., Delaney, R., Bremner, J. D., Heninger, G. R., Bowers, M. B., & Charney, D. S. (1994). Subanesthetic effects of the

noncompetitive NMDA antagonist, ketamine, in humans: Psychotomimetic, perceptual, cognitive, and neuroendocrine responses. *Archives of General Psychiatry*, *51*(3), 199–214.

Ladépêche, L., Planagumà, J., Thakur, S., Suárez, I., Hara, M., Borbely, J. S., Sandoval, A., Laparra-Cuervo, L., Dalmau, J., & Lakadamyali, M. (2018). NMDA receptor autoantibodies in autoimmune encephalitis cause a subunit-specific nanoscale redistribution of NMDA receptors. *Cell Reports*, *23*(13), 3759–3768.

Lancaster, E., Martinez-Hernandez, E., & Dalmau, J. (2011). Encephalitis and antibodies to synaptic and neuronal cell surface proteins. *Neurology*, *77*(2), 179–189. https://doi.org/10.1212/WNL.0b013e318224afde

Lee, E.-J., Choi, S. Y., & Kim, E. (2015). NMDA receptor dysfunction in autism spectrum disorders. *Current Opinion in Pharmacology*, *20*, 8–13.

Li, Y., Tanaka, K., Wang, L., Ishigaki, Y., & Kato, N. (2015). Induction of memory deficit in mice with chronic exposure to cerebrospinal fluid from patients with anti-N-methyl-D-aspartate receptor encephalitis. *The Tohoku Journal of Experimental Medicine*, *237*(4), 329–338.

Lutz, H. U., Binder, C. J., & Kaveri, S. (2009). Naturally occurring auto-antibodies in homeostasis and disease. *Trends in Immunology*, *30*(1), 43–51.

Malviya, M., Barman, S., Golombeck, K. S., Planagumà, J., Mannara, F., Strutz-Seebohm, N., Wrzos, C., Demir, F., Baksmeier, C., Steckel, J., Falk, K. K., Gross, C. C., Kovac, S., Bönte, K., Johnen, A., Wandinger, K. P., Martin-Garcia, E., Becker, A. J., Elger, C. E., Klöcker, N., Wiendl, H., Meuth, S. G., Hartung, H. P., Seebohm, G., Leypold, F., Maldonado, R., Stadelmann, C., Dalmau, J., Melzer, N., & Goebels, N. (2017). NMDAR encephalitis: Passive transfer from man to mouse by a recombinant antibody. *Annals of Clinical and Translational Neurology*, *4*(11), 768–783.

Manto, M., Dalmau, J., Didelot, A., Rogemond, V., & Honnorat, J. (2010). In vivo effects of antibodies from patients with anti-NMDA receptor encephalitis: Further evidence of synaptic glutamatergic dysfunction. *Orphanet Journal of Rare Diseases*, *5*(1), 1–12.

Manto, M., Dalmau, J., Didelot, A., Rogemond, V., & Honnorat, J. (2011). Afferent facilitation of corticomotor responses is increased by IgGs of patients with NMDA-receptor antibodies. *Journal of Neurology*, *258*(1), 27–33.

Meberg, P. J., & Miller, M. W. (2003). Culturing hippocampal and cortical neurons. *Methods Cell Biol*, *71*(2), 111–127.

Mikasova, L., De Rossi, P., Bouchet, D., Georges, F., Rogemond, V., Didelot, A., Meissirel, C., Honnorat, J., & Groc, L. (2012). Disrupted surface cross-talk between NMDA and Ephrin-B2 receptors in anti-NMDA encephalitis. *Brain*, *135*(5), 1606–1621.

Minerbi, A., Kahana, R., Goldfeld, L., Kaufman, M., Marom, S., & Ziv, N. E. (2009). Long-term relationships between synaptic tenacity, synaptic remodeling, and network activity. *PLoS Biol*, *7*(6), e1000136.

Monyer, H., Burnashev, N., Laurie, D. J., Sakmann, B., & Seeburg, P. H. (1994). Developmental and regional expression in the rat brain and functional properties of four NMDA receptors. *Neuron*, *12*(3), 529–540.

Moscato, E. H., Peng, X., Jain, A., Parsons, T. D., Dalmau, J., & Balice-Gordon, R. J. (2014). Acute mechanisms underlying antibody effects in anti–N-methyl-D-aspartate receptor encephalitis. *Annals of Neurology*, *76*(1), 108–119.

Nakazawa, K., Zsiros, V., Jiang, Z., Nakao, K., Kolata, S., Zhang, S., & Belforte, J. E. (2012). GABAergic interneuron origin of schizophrenia pathophysiology. *Neuropharmacology*, *62*(3), 1574–1583.

Nicoll, R. A. (2017). A Brief History of Long-Term Potentiation. *Neuron*, *93*(2), 281–290. https://doi.org/10.1016/j.neuron.2016.12.015

Pafundo, D. E., Miyamae, T., Lewis, D. A., & Gonzalez-Burgos, G. (2018). Presynaptic effects of N-methyl-D-aspartate receptors enhance parvalbumin cell–mediated inhibition of pyramidal cells in mouse prefrontal cortex. *Biological Psychiatry*, *84*(6), 460–470.

Pafundo, D. E., Pretell Annan, C. A., Fulginiti, N. M., & Belforte, J. E. (2021). Early NMDA Receptor Ablation in Interneurons Causes an Activity-Dependent E/I Imbalance in vivo in Prefrontal Cortex Pyramidal Neurons of a Mouse Model Useful for the Study of Schizophrenia. *Schizophrenia Bulletin*.

Paoletti, P., Bellone, C., & Zhou, Q. (2013). NMDA receptor subunit diversity: Impact on receptor properties, synaptic plasticity and disease. *Nature Reviews Neuroscience*, *14*(6), 383–400.

Petit-Pedrol, M., & Groc, L. (2020). Regulation of membrane NMDA receptors by dynamics and protein interactions. *Journal of Cell Biology*, *220*(1).

Petrenko, A. B., Yamakura, T., Sakimura, K., & Baba, H. (2014). Defining the role of NMDA receptors in anesthesia: Are we there yet? *European Journal of Pharmacology*, *723*, 29–37.

Planagumà, J., Haselmann, H., Mannara, F., Petit-Pedrol, M., Grünewald, B., Aguilar, E., Röpke, L., Martín-García, E., Titulaer, M. J., Jercog, P., Graus, F., Maldonado, R., Geis, C., & Dalmau, J. (2016). Ephrin-B2 prevents N-methyl-D-aspartate receptor antibody effects on memory and neuroplasticity. *Annals of Neurology*, *80*(3), 388–400.

Planagumà, J., Leypoldt, F., Mannara, F., Gutiérrez-Cuesta, J., Martín-García, E., Aguilar, E., Titulaer, M. J., Petit-Pedrol, M., Jain, A., Balice-Gordon, R., Lakadamyali, M., Graus, F., Maldonado, R., & Dalmau, J. (2015). Human N-methyl D-aspartate receptor antibodies alter memory and behaviour in mice. *Brain*, *138*(1), 94–109. https://doi.org/10.1093/brain/awu310

Sanz-Clemente, A., Nicoll, R. A., & Roche, K. W. (2013). Diversity in NMDA receptor composition: Many regulators, many consequences. *The Neuroscientist*, *19*(1), 62–75.

Tamamaki, N., Yanagawa, Y., Tomioka, R., Miyazaki, J.-I., Obata, K., & Kaneko, T. (2003). Green fluorescent protein expression and colocalization with calretinin, parvalbumin,

and somatostatin in the GAD67-GFP knock-in mouse. *Journal of Comparative Neurology*, *467*(1), 60–79.

Taraschenko, O., Fox, H. S., Pittock, S. J., Zekeridou, A., Gafurova, M., Eldridge, E., Liu, J., Dravid, S. M., & Dingledine, R. (2019). A mouse model of seizures in anti–N-methyl-d-aspartate receptor encephalitis. *Epilepsia*, *60*(3), 452–463.

Teppola, H., Aćimović, J., & Linne, M.-L. (2019). Unique features of network bursts emerge from the complex interplay of excitatory and inhibitory receptors in rat neocortical networks. *Frontiers in Cellular Neuroscience*, *13*, 377.

Teppola, H., Okujeni, S., Linne, M.-L., & Egert, U. (2018). AMPA, NMDA and GABAA receptor mediated network burst dynamics in cortical cultures in vitro. *ArXiv Preprint ArXiv:1802.00217*.

Titulaer, M. J., McCracken, L., Gabilondo, I., Armangué, T., Glaser, C., Iizuka, T., Honig, L. S., Benseler, S. M., Kawachi, I., Martinez-Hernandez, E., Aguilar, E., Gresa-Arribas, N., Ryan-Florance, N., Torrents, A., Saiz, A., Rosenfeld, M. R., Balice-Gordon, R., Graus, F., & Dalmau, J. (2013). Treatment and prognostic factors for long-term outcome in patients with anti-NMDA receptor encephalitis: An observational cohort study. *The Lancet Neurology*, *12*(2), 157–165. https://doi.org/10.1016/S1474-4422(12)70310-1

Uhlhaas, P. J., & Singer, W. (2010). Abnormal neural oscillations and synchrony in schizophrenia. *Nature Reviews Neuroscience*, *11*(2), 100–113.

Wagner, F., Goertzen, A., Kiraly, O., Laube, G., Kreye, J., Witte, O. W., Prüss, H., & Veh, R. W. (2020). Detailed morphological analysis of rat hippocampi treated with CSF autoantibodies from patients with anti-NMDAR encephalitis discloses two distinct types of immunostaining patterns. *Brain Research*, *1747*, 147033.

Wagnon, I., Hélie, P., Bardou, I., Regnauld, C., Lesec, L., Leprince, J., Naveau, M., Delaunay, B., Toutirais, O., Lemauff, B., Etard, O., Vivien, D., Agin, V., Macrez, Richard., Maubert, E., & Docagne, F. (2020). Autoimmune encephalitis mediated by B-cell response against N-methyl-d-aspartate receptor. *Brain*, *143*(10), 2957–2972.

Wardemann, H., Yurasov, S., Schaefer, A., Young, J. W., Meffre, E., & Nussenzweig, M. C. (2003). Predominant autoantibody production by early human B cell precursors. *Science*, *301*(5638), 1374–1377.

Wenke, N. K., Kreye, J., Andrzejak, E., van Casteren, A., Leubner, J., Murgueitio, M. S., Reincke, S. M., Secker, C., Schmidl, L., Geis, C., Ackermann, F., Nikolaus, M., Garner, C. C., Wardemann, H., Wolber, G., & Prüss, H. (2019). N-methyl-D-aspartate receptor dysfunction by unmutated human antibodies against the NR1 subunit. *Annals of Neurology*, *85*(5), 771–776.

Wright, S., Hashemi, K., Stasiak, L., Bartram, J., Lang, B., Vincent, A., & Upton, A. L. (2015). Epileptogenic effects of NMDAR antibodies in a passive transfer mouse model. *Brain*, *138*(11), 3159–3167.

Würdemann, T., Kersten, M., Tokay, T., Guli, X., Kober, M., Rohde, M., Porath, K., Sellmann, T., Bien, C. G., Köhling, R., & Kirschstein, T. (2016). Stereotactic injection of

cerebrospinal fluid from anti-NMDA receptor encephalitis into rat dentate gyrus impairs NMDA receptor function. *Brain Research*, *1633*, 10–18.

Xi, D., Keeler, B., Zhang, W., Houle, J. D., & Gao, W.-J. (2009). NMDA receptor subunit expression in GABAergic interneurons in the prefrontal cortex: Application of laser microdissection technique. *Journal of Neuroscience Methods*, *176*(2), 172–181.

Zerche, M., Weissenborn, K., Ott, C., Dere, E., Asif, A. R., Worthmann, H., Hassouna, I., Rentzsch, K., Tryc, A. B., Dahm, L., Steiner, J., Binder, L., Wiltfang, J., Siren, A.. L., Stöcker, W., & Ehrenreich, H. (2015). Preexisting serum autoantibodies against the NMDAR subunit NR1 modulate evolution of lesion size in acute ischemic stroke. *Stroke*, *46*(5), 1180–1186.

Zhang, Q., Tanaka, K., Sun, P., Nakata, M., Yamamoto, R., Sakimura, K., Matsui, M., & Kato, N. (2012). Suppression of synaptic plasticity by cerebrospinal fluid from anti-NMDA receptor encephalitis patients. *Neurobiology of Disease*, *45*(1), 610–615.

Zhang, Y., Behrens, M. M., & Lisman, J. E. (2008a). Prolonged exposure to NMDAR antagonist suppresses inhibitory synaptic transmission in prefrontal cortex. *Journal of Neurophysiology*, *100*(2), 959–965.

Zhang, Y., Behrens, M. M., & Lisman, J. E. (2008b). Prolonged Exposure to NMDAR Antagonist Suppresses Inhibitory Synaptic Transmission in Prefrontal Cortex. *Journal of Neurophysiology*, *100*(2), 959–965. https://doi.org/10.1152/jn.00079.2008

Statutory Declaration

I, Ewa Andrzejak, by personally signing this document in lieu of an oath, hereby affirm that I prepared the submitted dissertation on the topic “Effects of patient-derived pathogenic anti-NMDAR antibodies on synaptic function and network activity” - “Effekte pathogener Anti-NMDAR-Antikörper auf die Funktionalität von Synapsen und neuronalen Netzwerken”, independently and without the support of third parties, and that I used no other sources and aids than those stated.

All parts which are based on the publications or presentations of other authors, either in letter or in spirit, are specified as such in accordance with the citing guidelines. The sections on methodology (in particular regarding practical work, laboratory regulations, statistical processing) and results (in particular regarding figures, charts and tables) are exclusively my responsibility.

Furthermore, I declare that I have correctly marked all of the data, the analyses, and the conclusions generated from data obtained in collaboration with other persons, and that I have correctly marked my own contribution and the contributions of other persons (cf. declaration of contribution). I have correctly marked all texts or parts of texts that were generated in collaboration with other persons.

My contributions to any publications to this dissertation correspond to those stated in the below joint declaration made together with the supervisor. All publications created within the scope of the dissertation comply with the guidelines of the ICMJE (International Committee of Medical Journal Editors; www.icmje.org) on authorship. In addition, I declare that I shall comply with the regulations of Charité – Universitätsmedizin Berlin on ensuring good scientific practice.

I declare that I have not yet submitted this dissertation in identical or similar form to another Faculty.

The significance of this statutory declaration and the consequences of a false statutory declaration under criminal law (Sections 156, 161 of the German Criminal Code) are known to me.

_____ _____

Date Signature

Detailed Declaration of Contribution

Ewa Andrzejak contributed the following to the below listed publication:

1. **Publication:** Andrzejak E, Rabinovitch E, Kreye J, Prüss H, Rosenmund C, Ziv NE, Garner CC, Ackermann F. Patient-derived anti-NMDAR antibody disinhibits cortical neuronal networks through dysfunction of inhibitory neuron output. *Journal of Neuroscience*, 2022.

Contribution in detail:

Planning of the experiments:

Ewa Andrzejak, Craig Garner, Frauke Ackermann, Noam Ziv, Christian Rosenmund

Execution of experiments:

Multi-electrode array recordings (Fig. 1): Ewa Andrzejak and Eshed Rabinovitch

Immunocytochemistry (Fig. 2, 7, 8): Ewa Andrzejak

Calcium imaging (Fig. 3): Ewa Andrzejak

Mass culture electrophysiological recordings (Fig. 4): Ewa Andrzejak

Autaptic electrophysiological recordings (Fig. 5, 6): Ewa Andrzejak

Data analysis:

Analysis of MEA recordings: Noam Ziv, Eshed Rabinovitch, Ewa Andrzejak

Analysis of electrophysiology data: Ewa Andrzejak

Analysis of calcium imaging data: Ewa Andrzejak, Noam Ziv

Analysis of imaging data: Ewa Andrzejak

Data visualization: Ewa Andrzejak

Writing and editing of the manuscript:

Initial draft by Ewa Andrzejak, editing by Craig Garner, Frauke Ackermann and Ewa Andrzejak with inputs from all the authors.

2. **Publication:** Wenke, N.K., Kreye, J., Andrzejak, E., van Casteren, A., Leubner, J., Murgueitio, M.S., Reincke, S.M., Secker, C., Schmidl, L., Geis, C., Ackermann, F., Nikolaus, M., Garner, C.C., Wardemann, H., Wolber, G. and Prüss, H. 2019. N-methyl-D-aspartate receptor dysfunction by unmutated human antibodies against the NR1 subunit. Annals of neurology, 85(5), pp.771-776.

Ewa Andrzejak contributed to the following parts of the manuscript:

Execution of experiments:

Autaptic electrophysiological recordings (Fig. 3) together with Adriana van Casteren

Data analysis and visualization:

Electrophysiological recordings (Fig. 3)

Writing and editing of the manuscript:

Results, methods and figure legend of the electrophysiology experiments (Fig. 3)

Signature, date and stamp of first doctoral supervisor	Signature of doctoral candidate

Excerpt from Journal Summary List (ISI Web of Knowledge) - 1

Journal Data Filtered By: **Selected JCR Year: 2020** Selected Editions: SCIE,SSCI
Selected Categories: "**NEUROSCIENCES**" Selected Category Scheme: WoS
Gesamtanzahl: 273 Journale

Rank	Full Journal Title	Total Cites	Journal Impact Factor	Eigenfactor Score
1	NATURE REVIEWS NEUROSCIENCE	49,897	34.870	0.048890
2	NATURE NEUROSCIENCE	73,709	24.884	0.128020
3	TRENDS IN COGNITIVE SCIENCES	33,482	20.229	0.036270
4	NEURON	111,115	17.173	0.175220
5	ACTA NEUROPATHOLOGICA	28,031	17.088	0.036970
6	MOLECULAR PSYCHIATRY	28,622	15.992	0.046220
7	Molecular Neurodegeneration	6,772	14.195	0.011650
8	TRENDS IN NEUROSCIENCES	22,858	13.837	0.019470
9	Nature Human Behaviour	5,549	13.663	0.023120
10	BRAIN	64,627	13.501	0.061550
11	BIOLOGICAL PSYCHIATRY	50,155	13.382	0.045540
12	JOURNAL OF PINEAL RESEARCH	12,492	13.007	0.008170
13	BEHAVIORAL AND BRAIN SCIENCES	11,610	12.579	0.007760
14	Annual Review of Neuroscience	14,699	12.449	0.010490
15	PROGRESS IN NEUROBIOLOGY	15,161	11.685	0.010300
16	SLEEP MEDICINE REVIEWS	11,218	11.609	0.014840
17	ANNALS OF NEUROLOGY	43,728	10.422	0.039960
18	NEUROSCIENCE AND BIOBEHAVIORAL REVIEWS	36,525	8.989	0.048970
19	Brain Stimulation	9,206	8.955	0.015960
20	npj Parkinsons Disease	1,093	8.651	0.003040
21	FRONTIERS IN NEUROENDOCRINOLOGY	5,338	8.606	0.005050

Rank	Full Journal Title	Total Cites	Journal Impact Factor	Eigenfactor Score
22	Neurology-Neuroimmunology & Neuroinflammation	3,863	8.485	0.008390
23	Journal of Neuroinflammation	19,657	8.322	0.027070
24	NEUROPATHOLOGY AND APPLIED NEUROBIOLOGY	4,791	8.090	0.004640
25	NEURAL NETWORKS	18,837	8.050	0.019420
26	Translational Neurodegeneration	1,759	8.014	0.003160
27	NEUROPSYCHOPHARMACOLOGY	30,856	7.853	0.034600
28	Acta Neuropathologica Communications	6,580	7.801	0.016320
29	Fluids and Barriers of the CNS	1,956	7.662	0.002170
30	Neurotherapeutics	6,764	7.620	0.009400
31	NEUROSCIENTIST	5,949	7.519	0.005010
32	Molecular Autism	3,579	7.509	0.007400
33	GLIA	17,858	7.452	0.016000
34	NEUROPSYCHOLOGY REVIEW	3,941	7.444	0.003460
35	Current Neuropharmacology	6,080	7.363	0.007730
36	JOURNAL OF HEADACHE AND PAIN	5,400	7.277	0.008140
37	BRAIN BEHAVIOR AND IMMUNITY	24,161	7.217	0.026930
38	Alzheimers Research & Therapy	5,593	6.982	0.011680
39	PAIN	45,325	6.961	0.031030
40	Translational Stroke Research	3,377	6.829	0.003920
41	BIPOLAR DISORDERS	6,185	6.744	0.007510
42	CURRENT OPINION IN NEUROBIOLOGY	17,009	6.627	0.025180
43	NEUROIMAGE	119,618	6.556	0.105820

Rank	Full Journal Title	Total Cites	Journal Impact Factor	Eigenfactor Score
44	BRAIN PATHOLOGY	6,559	6.508	0.006220
45	Developmental Cognitive Neuroscience	4,477	6.464	0.011160
46	Annual Review of Vision Science	935	6.422	0.004560
47	Multiple Sclerosis Journal	15,551	6.312	0.016680
48	CEPHALALGIA	12,756	6.292	0.011940
49	Biological Psychiatry-Cognitive Neuroscience and Neuroimaging	2,193	6.204	0.007120
50	JOURNAL OF CEREBRAL BLOOD FLOW AND METABOLISM	22,732	6.200	0.019640
51	JOURNAL OF PSYCHIATRY & NEUROSCIENCE	4,100	6.186	0.004200
52	JOURNAL OF NEUROSCIENCE	186,015	6.167	0.130970
53	EUROPEAN JOURNAL OF NEUROLOGY	14,490	6.089	0.016730
54	NEUROBIOLOGY OF DISEASE	21,360	5.996	0.020680
55	Dialogues in Clinical Neuroscience	5,272	5.986	0.005200
56	SLEEP	28,688	5.849	0.023920
57	JOURNAL OF PAIN	13,655	5.820	0.014690
58	Frontiers in Aging Neuroscience	13,654	5.750	0.025540
59	CURRENT OPINION IN NEUROLOGY	6,723	5.710	0.008480
60	Frontiers in Molecular Neuroscience	10,570	5.639	0.022450
61	MOLECULAR NEUROBIOLOGY	20,795	5.590	0.033020
62	Journal of Parkinsons Disease	3,562	5.568	0.006390
63	Frontiers in Cellular Neuroscience	17,299	5.505	0.033870
64	Neurobiology of Stress	1,628	5.441	0.004280
65	Cognitive Computation	2,407	5.418	0.002870

Publication 1

Andrzejak, E., Rabinovitch, E., Kreye, J., Prüss, H., Rosenmund, C., Ziv, N.E., Garner, C.C. and Ackermann, F., 2022. Patient-derived anti-NMDAR antibody disinhibits cortical neuronal networks through dysfunction of inhibitory neuron output. Journal of Neuroscience.

Neurobiology of Disease

Patient-Derived Anti-NMDAR Antibody Disinhibits Cortical Neuronal Networks through Dysfunction of Inhibitory Neuron Output

Ewa Andrzejak,[1] Eshed Rabinovitch,[2] Jakob Kreye,[1,3] Harald Prüss,[1,3] Christian Rosenmund,[4,5] Noam E. Ziv,[2] Craig C. Garner,[1,5] and Frauke Ackermann[1]

[1]German Center for Neurodegenerative Diseases, Berlin 10117, Germany, [2]Technion Faculty of Medicine, Rappaport Institute and Network Biology Research Laboratories, Fishbach Building, Technion City, Haifa 32000, Israel, [3]Department of Neurology and Experimental Neurology, Charité – Universitätsmedizin, Berlin 10117, Germany, [4]Institute of Neurophysiology, Charité – Universitätsmedizin, Berlin 10117, Germany, and [5]NeuroCure Cluster of Excellence, Charité – Universitätsmedizin, Berlin 10117, Germany

Anti-NMDA receptor (NMDAR) encephalitis is a severe neuropsychiatric disorder associated with autoantibodies against NMDARs, which cause a variety of symptoms from prominent psychiatric and cognitive manifestations to seizures and autonomic instability. Previous studies mainly focused on hippocampal effects of these autoantibodies, helping to explain mechanistic causes for cognitive impairment. However, antibodies' effects on higher cortical network function, where they could contribute to psychosis and/or seizures, have not been explored in detail until now. Here, we employed a patient-derived monoclonal antibody targeting the NR1 subunit of NMDAR and tested its effects on *in vitro* cultures of rodent cortical neurons, using imaging and electrophysiological techniques. We report that this hNR1 antibody drives cortical networks to a hyperexcitable state and disrupts mechanisms stabilizing network activity such as Npas4 signaling. Network hyperactivity is in part a result of a reduced synaptic output of inhibitory neurons, as indicated by a decreased inhibitory drive and levels of presynaptic inhibitory proteins, specifically in inhibitory-to-excitatory neuron synapses. Importantly, on a single-cell level hNR1 antibody selectively impairs NMDAR-mediated currents and synaptic transmission of cortical inhibitory neurons, yet has no effect on excitatory neurons, which contrasts with its effects on hippocampal neurons. Together, these findings provide a novel, cortex-specific mechanism of antibody-induced neuronal hyperexcitability, highlighting regional specificity underlying the pathology of autoimmune encephalitis.

Key words: **autoantibodies; autoimmune encephalitis; cortical interneurons; network excitability; NMDAR**

Significance Statement

It is increasingly appreciated that the inadvertent activation of the immune system within CNS can underlie pathogenesis of neuropsychiatric disorders. Although the exact mechanisms remain elusive, autoantibodies derived from patients with autoimmune encephalitis pose a unique tool to study pathogenesis of neuropsychiatric states. Our analysis reveals that autoantibody against the NMDA receptor (NMDAR) has a distinct mechanism of action in the cortex, where it impairs function of inhibitory neurons leading to increased cortical network excitability, in contrast to previously described hippocampal synaptic mechanisms of information encoding, highlighting brain regional specificity. Notably, similar mechanism of NMDAR-mediated inhibitory hypofunction leading to cortical disinhibition has been suggested to underlie pathology of schizophrenia, hence our data provide new evidence for common mechanisms underlying neuropsychiatric disorders.

Received Aug. 19, 2021; revised Dec. 22, 2021; accepted Feb. 8, 2022.

Author contributions: E.A., C.R., N.E.Z., C.C.G., and F.A. designed research; E.A. and E.R. performed research; J.K. and H.P. contributed unpublished reagents/analytic tools; E.A., E.R., and N.E.Z. analyzed data; E.A. wrote the first draft of the paper; E.A., J.K., H.P., C.R., N.E.Z., C.C.G., and F.A. edited the paper; E.A., C.C.G., and F.A. wrote the paper.

This work was supported by the German Center for Neurodegenerative Diseases; the Federal Government of Germany (Deutsche Forschungsgemeinschaft) Grants SFB958 (to C.C.G.), EXC-2049-390688087 for the Center of Excellence NeuroCure (to F.A. and C.C.G.), and PR1274/2-1, PR1274/3-1, and PR1274/5-1 (to H.P.); the Helmholtz Association Grant HIL-A03 (to H.P.); the German Federal Ministry of Education and Research Grant Connect-Generate 01GM1908D (to H.P.); the Israel Science Foundation Grant 1470/18 (to N.E.Z.); and the State of Lower-Saxony and the Volkswagen Foundation (N.E.Z.). We thank Thorsten Trimbuch and the Viral Core Facility of the Charité – Universitätsmedizin, Berlin for cloning and production of viral constructs; Marisa Brockmann for electrophysiological training; Aleksandra Ichkova for valuable comments on the manuscript; Anny Kretschmer, Christine Bruns, Bettina Brokowski, and Katja Poetschke for technical assistance; and the Advanced Medical Bioimaging Core Facility (AMBIO) of the Charité – Universitätsmedizin for support in acquisition of the imaging data.

The authors declare no competing financial interests.

Correspondence should be addressed to Frauke Ackermann at frauke.ackermann@dzne.de or Craig C. Garner at craig.garner@dzne.de.

https://doi.org/10.1523/JNEUROSCI.1689-21.2022

Copyright © 2022 Andrzejak et al.

This is an open-access article distributed under the terms of the Creative Commons Attribution 4.0 International license, which permits unrestricted use, distribution and reproduction in any medium provided that the original work is properly attributed.

Introduction

Over the last decade, a growing number of central nervous system disorders have been linked to autoantibodies, which have been detected in patients' cerebrospinal fluid (CSF). Many of these bind synaptic and neuronal cell-surface proteins, including a variety of neuro-transmitter receptors (Dalmau and Graus, 2018). One of the most prevalent forms of autoimmune encephalitis is associated with IgG antibodies that bind NMDA receptors (NMDARs), a disease that is characterized by a rapid clinical progression and a broad range of symptoms (Dalmau et al., 2007). Most patients present with prominent psychiatric manifestations, including psychosis, hallucinations, and behavioral changes, which further progress to severe memory loss, seizures, and autonomic instability. Often patients require prolonged treatment in intensive care units (Irani et al., 2010). Interestingly, most are responsive to immunotherapies and show marked recovery (Titulaer et al., 2013). A fundamental question is how these autoantibodies mechanistically trigger such a broad range of symptoms in patients.

With regard to NMDAR encephalitis, most studies have focused on how autoantibodies cause memory deficits, in particular within hippocampal circuits. A framework for such investigations is based on a long-history of research showing that NMDARs are ligand-gated ion channels responsible for synaptic integration and plasticity and underlie hippocampal learning and memory processes (Bliss and Collingridge, 1993; Nicoll, 2017). Studies with patients' CSF reveal that most NMDAR autoantibodies recognize epitopes within the extracellular domain of the obligatory NR1 subunit of NMDARs (Gleichman et al., 2012). Antibody binding primarily triggers the reversible internalization of NMDARs and thereby a net decrease in surface receptor clusters in hippocampal neurons (Hughes et al., 2010; Planagumà et al., 2015). Loss of receptors has been shown to decrease synaptic NMDAR-mediated currents (Hughes et al., 2010; Kreye et al., 2016) and to compromise synaptic plasticity (Mikasova et al., 2012; Zhang et al., 2012; Würdemann et al., 2016). These conditions are thought to contribute to memory deficits described in patients with NMDAR encephalitis and corresponding animal models (Planagumà et al., 2016; Malviya et al., 2017).

At present, how such antibodies could also trigger psychiatric symptoms and/or epileptic seizures is less clear, although actions at higher network levels, for instance within cortical circuits, seem likely. Intriguingly, seizures have been observed in ~60% of encephalitis patients (de Bruijn et al., 2019), suggesting an increased excitability within these circuits (Manto et al., 2010). Yet there are few clues of how NMDARs autoantibodies could drive this cortical hyperexcitability. On the other hand, it has long been suggested that NMDARs are involved in the pathology of psychosis ("glutamatergic hypothesis of schizophrenia"), wherein NMDAR antagonists such as ketamine and phencyclidine (PCP) have been found to induce psychotic symptoms, as well as exacerbate them in schizophrenic patients (Krystal et al., 1994; Jentsch and Roth, 1999). This has led to the hypothesis that NMDAR hypofunction, in particular on inhibitory interneurons (Belforte et al., 2010), could also cause excitation/inhibition imbalances and disinhibition of prefrontal cortical circuits (Homayoun and Moghaddam, 2007), similar to those observed in schizophrenic patients (Uhlhaas and Singer, 2010). It is currently unclear, whether anti-NMDAR auto antibodies could similarly affect cortical interneurons and thus alter cortical network properties in patients with NMDAR encephalitis.

In the present study, we have evaluated whether a patient-derived antibody against the NR1 subunit of NMDARs has direct effects on cortical neurons. Our detailed imaging and electrophysiological analysis of cultured rodent cortical neurons revealed that this antibody increases network spiking and bursting, driving cortical neurons into a hyperactive state. Surprisingly, this hyperactivity seems to be a result of selective hypofunction of inhibitory interneuron output, specifically in inhibitory-to-excitatory neuron synapses, leading to a decrease in inhibitory drive and hyperexcitability of these cortical neuronal networks.

Materials and Methods

Preparation of cultured cortical neurons

All procedures for experiments involving animals were approved by the animal welfare committee of Charité Medical University and the Berlin state government. To distinguish inhibitory and excitatory neurons in some experiments, we used GAD67-GFP (Δneo)/+ (GAD67-GFP) mice, in which inhibitory neurons expressing GAD67 are fluorescently labeled (Tamamaki et al., 2003). In comparison to WT neurons, no changes in the electrophysiological properties of these GFP-expressing neurons have been reported (Chang et al., 2014). To prepare primary cortical neuronal cultures for immunocytochemistry and mass culture patch-clamp experiments, mouse WT (C57BL/6J; RRID:IMSR_JAX:000664; license: T0036/14) or GAD67-GFP animals (license: T0220/09) of either sex were prepared and grown on glass coverslips using the Banker Protocol (Banker and Goslin, 1988; Meberg and Miller, 2003). In brief, astrocytes were prepared from mouse WT cortices on postnatal day (P)0–P2 and seeded on 6-well or 12-well plates at a density of 10,000/1 cm^2, 7–11 d before the addition of neurons. Cortical neurons were prepared from cortices dissected from mice P0–P2 brains in cold HBSS (Millipore), followed by a 45-min incubation in enzyme solution containing DMEM (Invitrogen, Thermo Fisher Scientific), cysteine (3.3 mM), $CaCl_2$ (2 mM), EDTA (1 mM), and papain (20 U/ml, Worthington) at 37°C. Next, the papain reaction was inhibited by incubating cortical tissue in a DMEM solution containing 10% fetal calf serum (Thermo Fisher Scientific), bovine serum albumin (38 mM, Sigma-Aldrich), and trypsin inhibitor (95 mM; Sigma-Aldrich) for 5 min. Afterwards, cells were triturated in Neurobasal-A medium (2% B-27, 1% Glutamax, 0.2% P/S; Thermo Fisher Scientific) by gentle pipetting up and down. Isolated neuronal cells were plated onto nitric acid washed and poly-L-lysine-coated glass coverslips with paraffin dots, at a density of 50,000–200,000 per 12-well coverslip. After 1.5 h, the coverslips were placed upside down onto a bed of astrocytes and co-cultured in Neurobasal-A medium at 37°C, 5% CO_2, for 14–18 days *in vitro* (DIV) before starting experiments.

To create autaptic cultures for single-cell electrophysiological recordings, cortical or hippocampal neurons were plated on microislands of astrocyte feeder layers, generated one week before the neuronal culture preparations, as described previously (Arancillo et al., 2013). Neurons were plated at a lower density (4000 cells per six-well coverslip) to obtain a single neuron on an astrocytic island.

For calcium imaging experiments, primary mouse cortical neurons were plated on top of a one-week-old astrocyte feeder layer, on round dishes containing a cell location grid at the bottom (μ-Dish 35 mm, high Grid-500, Ibidi), at the density of 250,000 cells per dish. The cells were cultured in medium containing minimal essential medium (MEM; Sigma-Aldrich), insulin (25 mg/l, Sigma-Aldrich), glucose (20 mM, Sigma-Aldrich), L-glutamine (2 mM, Sigma-Aldrich), Pen/Strep (0.2%, Sigma-Aldrich), and NuSerum (10%, Becton Dickinson Labware). Seven days after plating, one-half of the culture medium was replaced with feeding medium as above, but lacking NuSerum and containing 0.5 mM L-glutamine and 2% B-27 supplement (Invitrogen). Approximately one-half of the medium was then replaced with the feeding medium one or two times per week.

For multielectrode array (MEA) experiments, primary cultures of rat cortical neurons were prepared as described previously (Minerbi et al., 2009), using a protocol approved by the Technion committee for the supervision of animal experiments (IL-116-08-71). Briefly, cortices of newborn P1 Wistar rats (either sex; Charles River Laboratories) were dissected, dissociated by trypsin treatment followed by trituration using a siliconized Pasteur pipette. A total of $1–1.5 \times 10^6$ cells were then plated on thin-glass MEA dishes (Multi Channel Systems, MCS), precoated with polyethylenimine (Sigma-Aldrich) for better cell adhesion.

Subsequently, neurons were cultured at 37°C and 5% CO_2, and grown in medium containing MEM (Sigma-Aldrich), insulin (25 mg/l, Sigma-Aldrich), glucose (20 mM, Sigma-Aldrich), L-glutamine (2 mM, Sigma-Aldrich), gentamycin sulfate (5 mg/ml, Sigma-Aldrich), and 10% NuSerum (Becton Dickinson Labware). At 7 DIV, one-half of the culture medium was replaced with feeding medium lacking NuSerum and containing 0.5 mM L-glutamine and 2% B-27 supplement (Invitrogen), and then the cultures were fed in this way three to four times per week.

Lentivirus production

All lentiviral particles were provided by the Viral Core Facility of the Charite – Universitätsmedizin, Berlin (https://vcf.charite.de/en/) and were prepared as described previously (Lois et al., 2002). Briefly, HEK293T (RRID:CVCL_0063) cells were cotransfected with 10 µg of shuttle vector, 5 µg of helper plasmid pCMVdR8.9, and 5 µg of pVSV.G with X-tremeGENE 9 DNA transfection reagent (Roche Diagnostics). Virus-containing cell culture supernatant was collected after 72 h and filtered for purification. Aliquots were flash-frozen in liquid nitrogen and stored at −80°C. Neurons were infected with lentivirus at 2–4 DIV.

Production of monoclonal antibodies

The human monoclonal antibody #003-102 is reactive to the NR1 subunit of NMDARs and was isolated from CSF of a patient with acute NMDAR encephalitis (Kreye et al., 2016). Isotype-matched control antibody mGO53 was isolated from blood of a healthy donor (Wardemann et al., 2003). For the recombinant expression of these antibodies, the paired expression vectors encoding for the antibodies' heavy and light chain were transiently transfected in HEK293T cells and purified from cell culture supernatants, as previously described (Kreye et al., 2016). The antibody concentration was determined using an anti-human IgG ELISA following the manufacturer's instructions (3850-1AD-6, Mabtech).

Immunocytochemistry of cultured neurons

Npas4 experiment

To verify the effects of the hNR1 antibody on somatic Npas4 expression, cortical neurons 14–17 DIV were incubated with 1 µg/ml of hNR1 antibody for 2, 4, or 24 h. Alternatively, to induce expression of Npas4, neurons were treated with NMDA (2 µM, Tocris) for 2 h. Untreated cells were used as a control. To study the effect of hNR1 and NMDAR antagonist (2R)-amino-5-phosphonovaleric acid (AP5) on NMDA-induced Npas4 expression, NMDA treatment was preceded by 6 h or 24 h of hNR1 (1 µg/ml) or 3 h of AP5 (100 µM, Tocris) treatment. After treatment, cells were fixed with 4% paraformaldehyde (PFA) in PBS for 10 min and washed 3 × 5 min with PBS. Subsequently, cells were permeabilized and blocked with a solution containing 5% normal goat serum, 2% BSA, and 0.1% Triton in PBS, for 1 h. Neurons were then incubated with primary antibodies against Npas4 (1:1500, rabbit, Activity Signaling) and MAP2 (1:2000, chicken, Millipore, AB5543) in antibody solution containing 2% BSA in PBS for 2 h at room temperature (RT). Cells were then washed 3 × 5 min with PBS and incubated with the differently labeled secondary antibodies (1:1000 in antibody solution, Invitrogen, Thermo Fisher Scientific), for 2 h at RT and washed 3 × 5 min with PBS. Finally, coverslips were dipped in H_2O and mounted in Pro-Long Diamon Antifade Mountant (Thermo Fisher Scientific).

Synaptic/extrasynaptic hNR1 labeling

Cortical neurons of GAD67-GFP animals were subjected to live staining with hNR1 and anti-human secondary antibody. Briefly, neurons were incubated with 1 µg/ml of hNR1 in original culture NBA medium (see above) for 20 min at 10°C. Cells were then washed once with same medium and incubated with Alexa Fluor 568-conjugated anti-human secondary antibody (1:1000, Thermo Fisher Scientific) for 20 min at 10°C. Afterwards, neurons were again washed once with culture medium, fixed with 4% PFA, blocked, stained with antibodies against excitatory presynaptic vesicle protein VGLUT1 (1:4000, SySy 135304, Synaptic Systems) or the inhibitory postsynaptic scaffold protein gephyrin (1:500, SySy 147011, Synaptic Systems) and labeled with secondary antibodies and mounted as described earlier (see Npas4 experiment).

Inhibitory presynaptic proteins labeling

Cortical neurons from GAD67-GFP animals were incubated with 1 µg/ml of hNR1 antibody in original culture NBA medium for 0, 6, or 24 h at 37°C. Subsequently, cells were fixed with 4% PFA, blocked, stained with antibodies against MAP2 (1:2000, AB5543, Millipore), glutamate decarboxylase 65 (GAD65; 1:750, MAB5406, Millipore), or vesicular GABA transporter (VGAT; 1:4000, SySy 131003, Synaptic Systems) and labeled with secondary antibodies before mounting as described above.

Image acquisition and quantification

Immunocytochemical staining for Npas4 experiments was acquired on a Nikon Spinning Disk Confocal CSU-X microscope equipped with an air 20× Plan Apo objective lens (NA = 0.8), controlled via NIS-Elements software (Nikon). Images were then processed using ImageJ (RRID: SCR_003070). ROIs were manually drawn around cell somas. After background subtraction, the mean intensity values of the ROIs were measured and normalized to the untreated control.

hNR1 labeling and staining for inhibitory presynaptic markers were analyzed using a spinning disk confocal microscope (Carl Zeiss Axio Oberserver.Z1 with Andor spinning disk and cobalt, omricron, i-beam laser; Carl Zeiss, Andor) using a 63× (1.4 NA) or 100× (1.4 NA) Plan-Apochromat oil objectives and an iXon ultra (Andor) camera controlled by iQ software (RRID: SCR_014461; Andor). Only dendrites in proximity to the soma were imaged, and inhibitory and excitatory dendrites were distinguished based on GFP signal. Images were processed using ImageJ (RRID: SCR_003070) and OpenView software (written by Prof. Dr. Noam Ziv, Technion Institute, Haifa, Israel). In brief, for synaptic protein levels at GAD65 and VGAT puncta along dendrites were detected with set parameters: 6 × 6-pixel boxes were placed over puncta and the mean fluorescence intensities were measured, followed by subtraction of background values. For hNR1 labeling within excitatory synapses, hNR1-positive puncta were detected in a similar manner and then VGLUT1 intensities within hNR1-positive puncta were measured. A value above a threshold of 5× background intensity was considered VGLUT1-positive and thus synaptic. The remaining hNR1 puncta were considered extrasynaptic. In a similar manner, boxes around detected gephyrin puncta served to measure hNR1 intensity for localization of hNR1 puncta to inhibitory synapses. Z-plane images were analyzed using Volume Viewer plugin in ImageJ. Values of all puncta per region of interest (individual dendrites) were averaged and considered one data point.

MEAs

Neuronal network activity was recorded continuously from MEA electrodes (59 electrodes, 30 µm in diameter, arranged in an 8 × 8 array), as described previously (Hazan and Ziv, 2020). Briefly, cells grown on MEA dishes were continuously perfused with fresh feeding medium at a rate of 4 ml/d using an ultra-low-flow peristaltic pump (Instech Laboratories), and maintained at 37°C and 5% CO_2. After setting up the perfusion system, network activity was allowed to equilibrate for 1 h and then 15 h of baseline activity was recorded. Next, 1 µg/ml of hNR1 antibody, control antibody or 1 µM AP5 was manually pipetted into the MEA dish and added to the perfusion system. Cell spiking was recorded in the presence of the antibodies or 1 µM AP5 for 24 h. Finally, saturating concentrations of AP5 (50 µM) were added to the dish to block remaining NMDARs, and the activity of the culture was recorded for additional 6 h. Recordings from MEA dishes were performed using a commercial 60-channel headstage (inverted MEA-1060-BC, MCS) with a gain of 53× and frequency limits of 0.02–8500 Hz. This signal was further filtered with frequency limits of 150–3000 Hz and amplified (20×) using a filter/amplifier (FA60S-BC, MCS). Data acquisition was performed using custom software [Closed Loop Experiment Manager (CLEM); Hazan and Ziv, 2017]. Data were collected at 16,000 samples per second. Action potentials were identified as negative threshold-crossing events, with the threshold calculated as 5× root-mean-square of traces recorded at the beginning of each experiment. Data were imported, converted and analyzed for spiking and bursting activity using custom scripts in MATLAB

(MathWorks). Data from each MEA dish was normalized to the activity of last 3 h of baseline recordings. To test whether there is a significant increase in spiking/bursting rate because of 24-h treatment, for each network the average rate at the end of baseline (1 h) was compared with end of 24-h treatment (1 h) by paired *t* test. To quantify percentage increase in spiking/bursting rates at the beginning/end of respective treatments (24-h treatment with antibodies or 1 μM AP5, 50 μM AP5 or recovery at the end of experiment), the spike/burst rate of 10-min intervals was measured.

Patch-clamp electrophysiology

Whole-cell patch-clamp recordings were performed on mass or autaptic, cortical or hippocampal neurons at 14–18 DIV, after 24-h incubation with 1 µg/ml of hNR1 or control antibody (mGo53; Wardemann et al., 2003). Cortical neurons from GAD67-eGFP mouse line were used to distinguish inhibitory (GFP-positive) and excitatory (GFP-negative) cells. All recordings were obtained at ~25°C from neurons clamped at −70 mV with a Multiclamp 700B amplifier (Molecular Devices) under the control of Clampex 10.4 software (Molecular Devices). Data were sampled at 10 kHz and low-pass Bessel filtered at 3 kHz and series resistance was typically under 15 MΩ and compensated at 70%. During all recordings, except for chemically induced NMDA and evoked synaptic NMDA responses, neurons were immersed in standard extracellular solution consisting of 140 mM NaCl, 2.4 mM KCl, 10 mM HEPES, 10 mM glucose, 2 mM $CaCl_2$, and 4 mM $MgCl_2$. Chemically induced whole-cell NMDA responses were measured in extracellular solution containing 0 mM Mg^{2+}, 0.2 mM $CaCl_2$, and 10 μM glycine, whereas synaptically evoked NMDAR currents were measured in extracellular solution containing 0 mM Mg^{2+}, 2 mM $CaCl_2$, and 10 μM glycine. The borosilicate glass pipettes (3–8 MΩ) were pulled with a micropipette puller device (Sutter Instruments) and filled with the internal solution containing 136 mM KCl, 17.8 mM HEPES, 1 mM EGTA, 0.6 mM $MgCl_2$, 4 mM ATP-Mg, 0.3 mM GTP-Na, 12 mM phosphocreatine, and 50 U/ml phosphocreatine kinase. All solutions were adjusted to pH 7.4 and osmolarity of ~300 mOsm.

To selectively induce NMDA, GABA, and kainate currents, NMDA (10 μM, Tocris), GABA (5 μM, Tocris), or kainic acid (20 μM, Tocris), were acutely applied to the neurons for 1 s by use of a fast-flow system. For synaptic responses in autaptic cultures, EPSCs were evoked by brief somatic depolarization of neurons from −70 to 0 mV for 2 ms. Synaptic NMDAR currents were measured in the presence of AMPAR antagonist NBQX (10 μM, Tocris).

All mass culture recordings were performed in the presence of TTX (0.5 μM, Tocris) to block propagation of action potentials. To identify spontaneous miniature (m)EPSCs and mIPSCs, neurons were additionally immersed in AP5 (50 μM) and bicuculline (20 μM, Tocris), or AP5 (50 μM) and NBQX (10 μM), respectively. Traces were recorded at a holding potential of −70 mV and were filtered at 1 kHz, mEPSCs and mIPSCs were detected by a template algorithm in Axograph X (Axograph Scientific). False-positive events were excluded by subtracting events detected from traces in the presence of NBQX (10 μM) or bicuculline (20 μM) for mEPSCs and mIPSCs, respectively. To identify excitatory neurons for detection of mIPSCs in mass cultures, WT mouse neurons were infected with pLenti_CamKIIa_mKate2, a lentivirus expressing mKate2 under a CamKII promoter, at 3–4 DIV. For experiments detecting mEPSCs, GAD67-GFP line neurons were used.

Electrophysiological data were analyzed offline using Axograph X (RRID:SCR_014284; Axograph Scientific), Excel (Microsoft), and Prism (GraphPad).

Calcium imaging

Cortical cultures grown on grid-bottomed dishes were infected with f(syn)-NES-jRCamP1b-WPRE-w, a lentivirus expressing jRCamP1b under the Synapsin promoter (Viral Core Facility, Charité – Universitätsmedizin), at 4 DIV. Images were acquired at 37°C and a CO_2-controlled environment, using Nikon Spinning Disk Confocal CSU-X microscope with an air 20× Plan Apo objective lens (NA = 0.8), controlled via the NIS-Elements software (Nikon). Time-lapse images were collected at 5 Hz using an iXon3 DU-888 Ultra camera (Andor) and 561-nm excitation laser. In each dish, three fields of view with ~10–20 cells were selected, and 2 min of spontaneous activity was measured twice, with 5-min interval between the runs. To study bicuculline-induced changes is network activity, bicuculline (30 μM) was manually pipetted into the cell culture dish immediately after the end of the second baseline activity recording. After a 30-s waiting period, two 2-min imaging sessions were recorded, separated by a 5-min waiting interval.

Time-lapse image analysis and automatic time-series event detection were accomplished with a custom-written script in OpenView software (Prof. Dr. Noam Ziv, Technion, Israel). In brief, ROIs were manually selected by placing boxes of 27 × 27 pixels over visually identified neuronal cell somas. Only active cells were included in analysis. Time series fluorescence values were converted into ΔF/F by calculating the ratio between the change in fluorescence signal intensity (δ F) and baseline fluorescence (F0). The custom-written algorithm identified the timestamps of calcium transient onset, which were then averaged per min to obtain the frequency of events.

Experimental design and statistical analysis

GraphPad Prism was used to analyze and represent data. Schematic figures were created with BioRender.com. Statistical design, sample sizes, and tests for each experiment can be found in the figure legends. All figures represent data from at least three independent experiments (independent cultures). Unpaired and paired *t* tests and ANOVA Tukey's multiple comparison tests were used to evaluate statistical significance.

Results

hNR1 antibody increases spiking and bursting of cortical networks

Previous studies have shown that human anti-NMDAR antibodies affect NMDAR function in hippocampal neurons, helping to explain potential mechanistic causes for cognitive impairment in patients with autoimmune NMDAR encephalitis (Hughes et al., 2010; Mikasova et al., 2012; Würdemann et al., 2016). However, other symptoms centered in cortical circuits, such as psychiatric manifestations, catatonia, coma and epilepsy, have yet to be explored. We were thus interested in addressing the question of whether these antibodies can also affect cortical network function and if so, what is their functional impact? To explore these fundamental issues, we took advantage of a patient-derived monoclonal antibody #003-102 targeting the NR1 subunit of NMDAR (hNR1; Kreye et al., 2016) and tested its effect on primary cortical neuron cultures. We began with examining effects of hNR1 antibody on neuronal network activity by growing cortical neurons on multielectrode array (MEA) dishes for 11–14 d. This approach allows a continuous and simultaneous monitoring of activity from dozens of neurons recorded by 59 electrodes. Initially, baseline spiking activity of the neuronal network was recorded for 15 h, afterward 1 µg/ml of hNR1 or control antibody (ctrl; mGO53; Wardemann et al., 2003) were added and the spiking activity was traced for another 24 h (Fig. 1*A*,*I*). Remarkably, we observed a dramatic change in network spiking activity in the presence of hNR1 antibody that gradually increased over the period of 24 h of antibody treatment, reaching a highly active state (baseline = 1.12 ± 0.47, after 24-h hNR1 = 3.02 ± 0.47, paired *t* test, $p = 0.02$; Fig. 1*B*,*D*). The effect of the control antibody was more limited, eliciting a modest, but not significant, change in network spiking activity during this period (normalized baseline = 1.01 ± 0.01, after 24 h ctrl = 1.72 ± 0.27, 5, paired *t* test, $p = 0.07$; Fig. 1*B*,*C*).

The observed increase in spiking caused by the hNR1 antibody is both surprising and counterintuitive, as earlier studies demonstrated that active neuronal networks commonly respond to blockage of NMDARs, by NMDAR antagonists like AP5 or

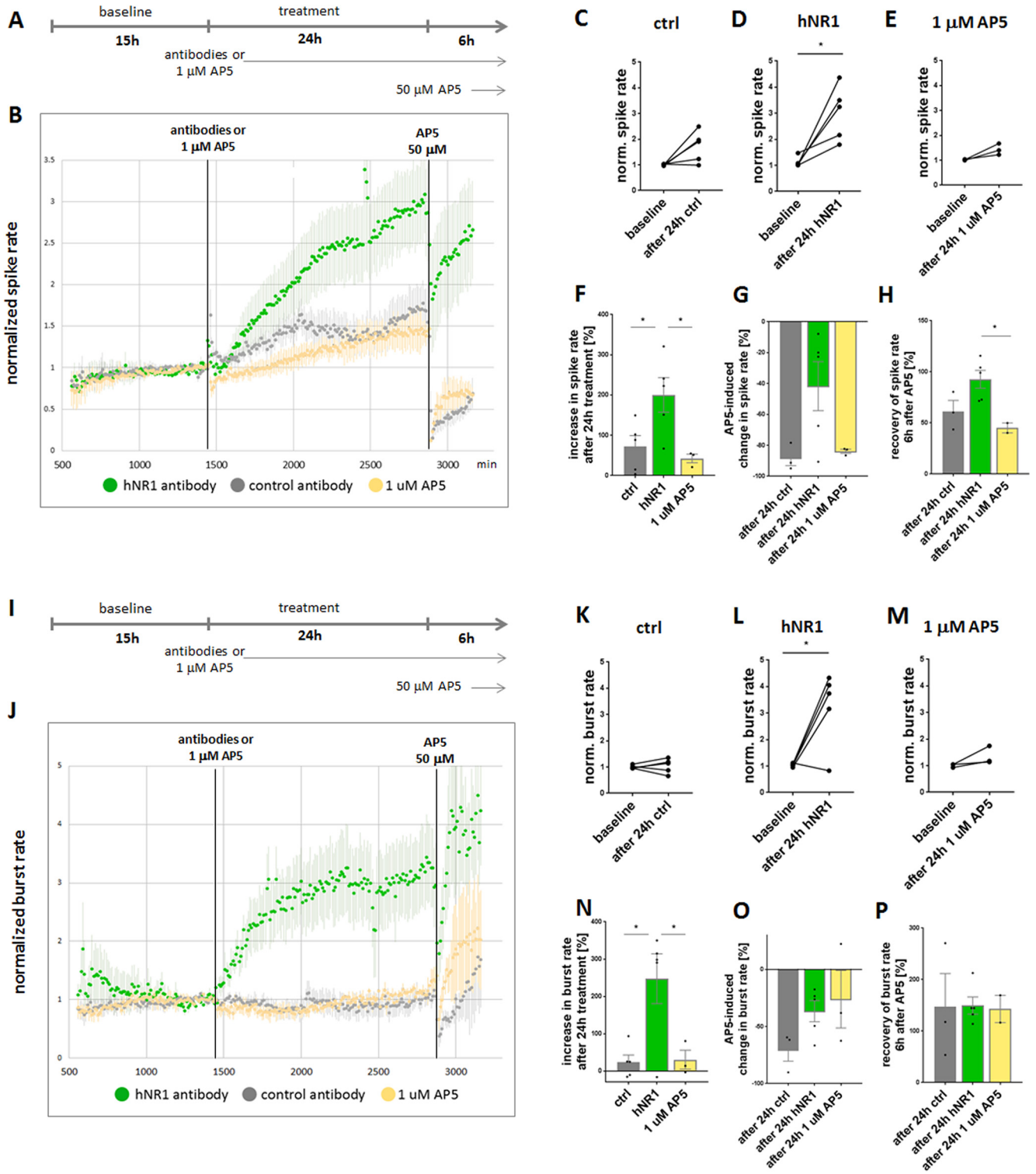

Figure 1. hNR1 antibody increases spiking and bursting activity of cortical cultures. ***A***, ***I***, Experimental design of MEA experiments. Baseline activity of cortical networks was recorded for 15 h, followed by addition of 1 μg/ml of hNR1 antibody, control (ctrl) antibody or 1 μM AP5 and 24-h recording of activity in the presence of antibodies/1 μM AP5. After 24 h of treatment, saturating concentration of AP5 (50 μM) was added to the network and another 6 h of activity were recorded. ***B***, Normalized spike rate of neuronal networks. Each data point represents a number of spikes recorded within a 10-min interval from all 59 electrodes and normalized to the last 3 h of baseline activity. Addition of hNR1 antibody (green data points), and to a much lesser degree control (ctrl, mGO53) antibody (gray data points) or AP5 at its IC_{50} concentration (1 μM; yellow data points), increase spiking of the network. hNR1 = 5 independent experiments, ctrl = 5 independent experiments, AP5 = 3 independent experiments. Error bars indicate SEM. ***C–E***, Within-dish comparison of normalized spike rate of the same network at the end of baseline recording (1 h) and after 24 h of treatment (1 h) tested by paired *t* test. ***C***, Baseline = 1.01 ± 0.01, after 24 h ctrl = 1.72 ± 0.27, 5, $p = 0.07$. ***D***, Baseline = 1,12 ± 0.47, after 24-h hNR1 = 3.02 ± 0.47, $p = 0.02$. ***E***, Baseline = 1.02 ± 0.01, after 24 h 1 μM AP5 = 1.43 ± 0.13, $p = 0.09$. ***F–H***, Percentage increase in normalized spike rate at the end (10 min) or beginning (10 min) of respective treatment. Each data point represents individual network (MEA dish). Percentage increase in spike rate: (***F***) at the end of baseline compared with end of antibody treatment, ctrl = 71.71 ± 27.46%; hNR1 = 200.5 ± 42.96%, 1 μM AP5 = 42.4 ± 10.76%, ctrl versus hNR1 $p = 0.045$, hNR1 versus 1 μM AP5 $p = 0.034$; (***G***) at the end of antibody treatment compared with beginning of 50 μM AP5, ctrl = −94.96 ± 5.03%; hNR1 = −41.69 ± 15.88%; 1 μM AP5 = −86.51 ± 1.33%, ctrl versus hNR1 $p = 0.085$; (***H***) at the end of antibody treatment compared with recovery 6 h after addition of 50 μM AP5, ctrl = 61.34 ± 10.65%; hNR1 = 92.65 ± 8.8%; 1 μM AP5 = 45.04 ± 4.88%, hNR1 versus 1 μM AP5 $p = 0.038$. ***J***, Normalized

ketamine, with a rapid decrease of their spiking activity (Emnett et al., 2013; Teppola et al., 2018, 2019), which slowly recovers over hours, because of various slow adaptive processes (Kaufman et al., 2014). Conceptually, this difference could be because of the fact that the hNR1 antibody only blocks ~50% of the whole-cell NMDAR currents in cultured hippocampal neurons (Hughes et al., 2010; Kreye et al., 2016), while saturating concentrations of AP5 and ketamine block all active NMDARs. We therefore hypothesized that the hNR1 antibody-induced increase in spiking activity could be an adaptive response of the network to an incomplete block of NMDARs. To test this hypothesis, we conducted similar experiments by adding 1 μM of the NMDAR antagonist AP5 (1 μM being the IC_{50} for NMDARs) instead of antibody, to block 50% of the surface NMDARs. Here, the presence of 1 μM AP5 was associated with a modest, yet nonsignificant, increase in spiking activity over 24 h (baseline = 1.02 ± 0.01, after 24 h 1 μM AP5 = 1.43 ± 0.13, paired *t* test, $p = 0.09$; Fig. 1*B*,*E*, yellow data points). As the magnitude of this change was just a fraction of that elicited by hNR1 antibody (~43% vs ~300%, respectively; Fig. 1*B*,*D-F*), it is possible that the underlying mechanism of the latter could be different, e.g., by affecting a subpopulation of receptors or cell types. Of note, AP5 is expected to act more quickly than the hNR1 antibody, yet as both conditions involved chronic multihour treatments, the observed outcomes are anticipated to be because of more slow adapting processes by both manipulations.

An interesting consequential question is whether networks treated with hNR1 antibody or AP5 are still responsive to pharmacological manipulations of NMDARs. This was examined by adding saturating concentrations of AP5 (50 μM) at the end of the 24-h treatment with hNR1, control antibody or 1 μM AP5 (Fig. 1*A*). Interestingly, networks treated with the control antibody or 1 μM AP5 remained responsive to high concentration of AP5, as their spiking rapidly decreased (95% and 87% reduction, respectively; Fig. 1*B*,*G*). Furthermore, spiking only partially recovered to ~60% of their initial value 6 h later (ctrl = 61%, AP5 = 45%; Fig. 1*F*). In contrast, the spiking activity of cortical cultures treated with hNR1 antibody only partially dropped because of AP5 treatment (42% reduction; Fig. 1*G*) and quickly recovered to 93% of the activity levels preceding AP5 treatment (Fig. 1*H*). These remained nearly fourfold higher than those observed in networks exposed to the control antibody or 1 μM AP5. Together, these data indicate that the addition of hNR1 antibody to cortical cultures renders the network largely insensitive to NMDAR blockage with AP5.

Subsequently, we asked whether other parameters crucial for behavior of neuronal network, such as bursting, number of spikes per burst and network synchrony, are also affected by hNR1 antibody treatment. While synchrony and number of spikes per burst were not different between the groups (data not shown), we observed a dramatic increase in network bursting activity because of hNR1 antibody treatment (baseline = 1.04 ± 0.03; after 24-h hNR1 = 3.22 ± 0.63, paired *t* test, $p = 0.027$; Fig. 1*J*,*L*). Burst rate of both control antibody (baseline = 1 ± 0.03; after 24 h ctrl = 1.05 ± 0.12, paired *t* test, $p = 0.72$) and 1 μM AP5 (baseline = 1 ± 0.04; after 24 h 1 μM AP5 = 1.36 ± 0.2, paired *t* test, $p = 0.2$) treated networks was not changed (Fig. 1*J*–*N*). Intriguingly, the hNR1 antibody-induced increase in burst rate seemed to have a more rapid onset than the increase in neuronal spiking (Fig. 1*B*,*J*), reaching a plateau after ~7 h of hNR1 antibody treatment (Fig. 1*J*). This phenomenon of elevated burst rates is a characteristic of networks in which inhibition has been removed (Chen et al., 2012). Interestingly, high concentrations of AP5 had a smaller effect on bursting activity than on spiking. Moreover, its immediate effects (Fig. 1*O*), or recovery of burst rate 6 h later (Fig. 1*P*), were not different between the treatments.

To summarize, these experiments reveal two unexpected effects of hNR1 antibody on cortical neurons: (1) substantial elevations in cortical network spiking and bursting activity and (2) a partial loss of responsiveness to NMDAR blockage by AP5, a situation that could conceivably both adversely affect network function and drive epileptic brain activity in patients.

hNR1 antibody impairs NMDA-mediated Npas4 expression in cortical cultures

Neuronal networks are complex systems whose function depends on the proper function of various neuronal cell types and regulatory mechanisms, allowing them to maintain their activity within a narrow range. Normally under increasing activity conditions, calcium influx through NMDARs signals to the cell nucleus and triggers an adaptive change in neuronal gene expression profiles, resulting in a homeostatic restoration of activity levels (Hardingham and Bading, 2003; Flavell and Greenberg, 2008). One such activity-dependent transcription factor, whose expression is partially triggered by calcium influx through NMDARs, is Neuronal PAS domain protein 4 (Npas4; Bloodgood et al., 2013; Spiegel et al., 2014). It was thus of interest to know whether this transcriptional program still operates following the addition of hNR1 antibody. Specifically, we asked whether the hNR1 antibody-induced increase in network activity (Fig. 1) was associated with a corresponding increase in Npas4 expression (Fig. 2). Surprisingly, treating cortical cultures with hNR1 antibody for 2, 4, or 24 h did not induce the expression of Npas4, as measured by changes in fluorescence intensity of somatic Npas4 in cortical cultured neurons (Fig. 2*A*–*D*). These data indicate that a Npas4-mediated homeostatic mechanism is not active and/or cannot be engaged in the presence of the hNR1 antibody. As a more direct test of the latter, we asked whether hNR1 antibody disrupts NMDA-mediated regulation of Npas4 expression. As expected under control conditions, the addition of NMDA to cortical cultures induced significant Npas4 expression (untreated UT = 1 ± 0.03, NMDA = 2.21 ± 0.17, $p < 0.0001$; Fig. 2*E*, first and second panels, *F*). However, the pretreatment with hNR1 antibody for 6 or 24 h blocked the increase in somatic Npas4 expression, similarly to

←

burst rate of neuronal networks. Each data point represents a number of bursts recorded within a 10-min interval, normalized to the last 3 h of baseline. Network bursting increases in the presence of hNR1 antibody, but not of control antibody nor 1 μM AP5. ***K–M***, Within-dish comparison of normalized burst rates of the same networks at the end of baseline recording (1 h) and after 24 h of treatment (1 h) tested by paired *t* test. ***K***, Baseline = 1 ± 0.03; after 24 h ctrl = 1.05 ± 0.12, $p = 0.72$. ***L***, Baseline = 1.04 ± 0.03; after 24-h hNR1 = 3.22 ± 0.63, $p = 0.027$. ***M***, Baseline = 1 ± 0.04; after 24 h 1 μM AP5 = 1.36 ± 0.2, $p = 0.2$. ***N–P***, Percentage increase in normalized burst rate at the end (10 min) or beginning (10 min) of respective treatments. Percentage increase in burst rate: (***N***) at the end of baseline compared with end of antibody treatment, ctrl = 23.31 ± 19.47%; hNR1 = 247.5 ± 66.75%; 1 μM AP5 = 30.14 ± 25.57%, ctrl versus hNR1 $p = 0.01$, hNR1 versus 1 μM AP5 $p = 0.03$; (***O***) end of antibody treatment compared with beginning of 50 μM AP5, ctrl = −70.46 ± 9.9%; hNR1 = −36.58 ± 25.24%; 1 μM AP5 = −26.05 ± 25.24%; (***P***) end of antibody treatment compared with recovery 6 h after addition of 50 μM AP5, ctrl = 147 ± 64.39%; hNR1 = 149.6 ± 16.73%; 1 μM AP5 = 143 ± 26.56%. Error bars indicate SEM. Paired *t* test (***C–E***, ***K–M***) or ANOVA Tukey's multiple comparison test (***F–H***, ***N–P***) were used to evaluate statistical significance. *$p < 0.05$.

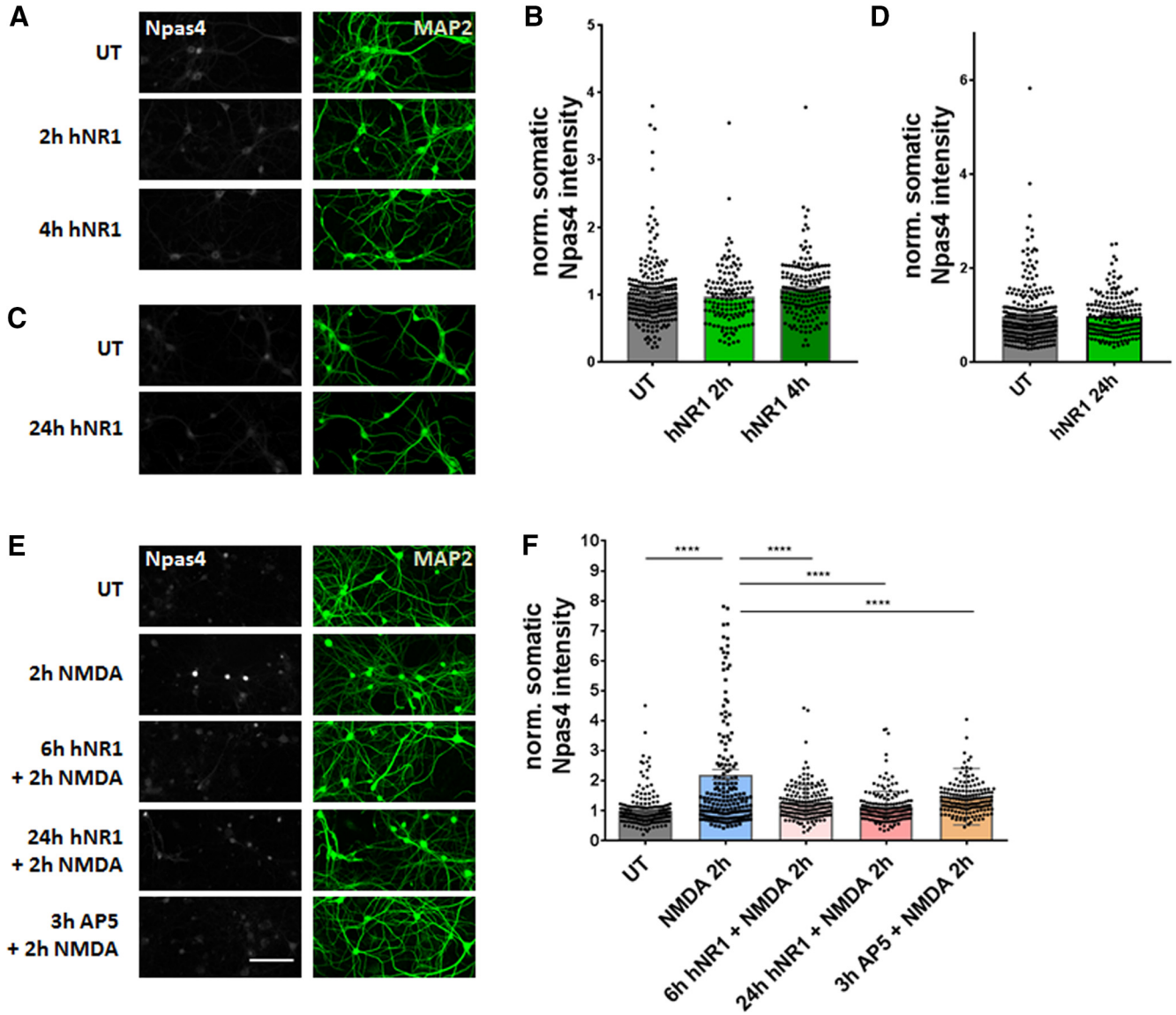

Figure 2. hNR1 antibody dysregulates NMDA-induced expression of Npas4, a transcription factor regulating network activity. ***A–D***, Cortical neuronal cultures 14–16 DIV were incubated with 1 μg/ml of hNR1 antibody for 2, 4, or 24 h, then fixed and stained with anti-Npas4 antibody to measure intensity of somatic Npas4 expression. Neither short-term (2, 4 h, ***A***) nor long-term (24 h, ***C***) treatment with hNR1 induced somatic Npas4 expression when compared to untreated (UT) condition. ***B***, ***D***, Normalized intensity of somatic Npas4 signal from three independent experiments: (***B***) UT = 1 ± 0.03, $n = 218$ neurons; 2-h hNR1 = 0.97 ± 0.04, $n = 133$ neurons; 4-h hNR1 = 1.08 ± 0.03, $n = 168$ neurons; (***D***) UT = 1 ± 0.04, $n = 280$ neurons; 24-h hNR1 = 0.98 ± 0.03, $n = 183$ neurons. ***E***, Stimulation of neurons with 2 μM NMDA for 2 h induces activity-driven increase of Npas4 expression compared with untreated (UT) condition. Six- or 24-h pretreatment with hNR1 antibody (1 μg/ml), as well as 3-h pretreatment with NMDAR antagonist AP5 (50 μM), blocks NMDA-induced expression of Npas4. ***F***, Normalized intensity of somatic Npas4 signal from three independent experiments: UT = 1 ± 0.03, $n = 235$ neurons; NMDA = 2.21 ± 0.17, $n = 197$ neurons; 6 h NR1 + NMDA = 1.28 ± 0.04, $n = 172$ neurons; 24-h hNR1 − NMDA = 1.13 ± 0.03, $n = 179$ neurons; 3 h AP5 + NMDA = 1.47 ± 0.07, $n = 166$ neurons. Error bars indicate SEM. Scale bar: 100 μm. ANOVA Tukey's multiple comparison test (***B***, ***F***) or paired *t* test (***D***) were used to evaluate statistical significance. ****$p < 0.0001$.

networks pretreated with AP5 (6 h NR1 + NMDA = 1.28 ± 0.04, 24-h hNR1 + NMDA = 1.13 ± 0.03, 3 h AP5 + NMDA = 1.47 ± 0.07, $p < 0.0001$; Fig. 2*E*,*F*). These data suggest that hNR1 antibody interferes with the capacity of cortical networks to decrease their activity through NMDA/Npas4 regulated gene expression, an observation that could help explain why the hNR1 antibody-induced hyperactivity is not downregulated to homeostatic levels over time. However, less clear is whether the dysregulation of NMDA/Npas4 regulated gene expression can explain why hNR1 antibody treatment increases network activity in the first place, or whether other mechanisms are at play that more directly regulate excitatory/inhibitory balance in these networks.

hNR1 antibody disinhibits cortical networks by specifically impairing output of inhibitory neurons

Proper function of cortical networks is determined by a fine balance between excitation and inhibition. Previous studies have shown that hypofunction of NMDARs can reduce inhibition and disinhibit cortical networks (Homayoun and Moghaddam, 2007; Zhang et al., 2008). It thus seemed feasible that the hNR1 antibody-induced hyperactivity is a result of network disinhibition. To test this hypothesis, we designed a set of calcium imaging and electrophysiological experiments. For calcium imaging, neurons were initially infected at 4 DIV with a lentivirus expressing RCaMP (Dana et al., 2016), a genetically encoded calcium indicator, and allowed to grow for 10 more days (14 DIV) before

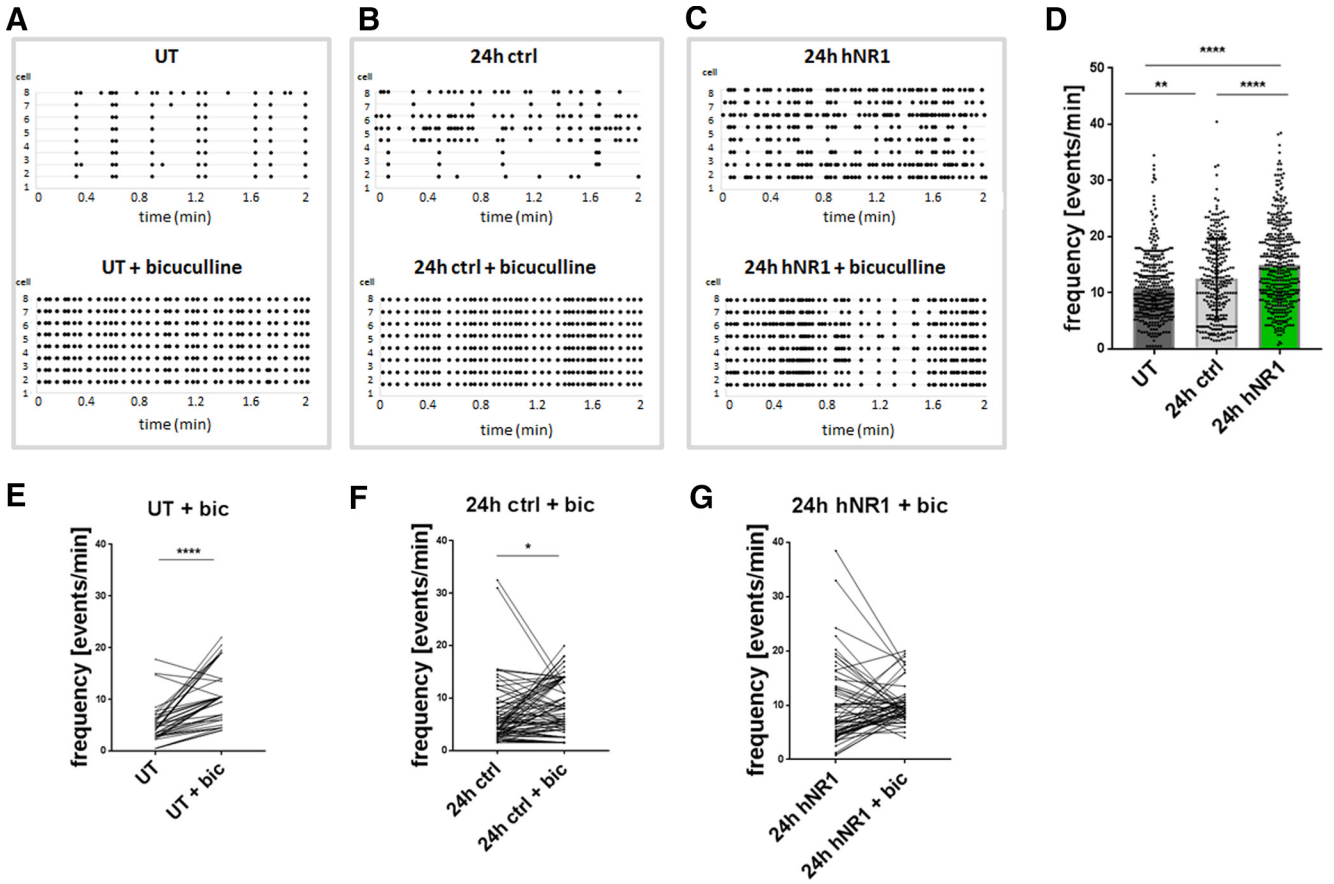

Figure 3. Calcium imaging reveals that networks treated with hNR1 antibody cannot be further disinhibited by bicuculline. ***A–C***, Representative raster plots of calcium events recorded from neuronal somas (neuron ID on the *y*-axis) expressing RCaMP in untreated condition (UT) (***A***, upper panel), after 24 h of control antibody (***B***, upper panel) or 24 h of hNR1 antibody (***C***, upper panel) treatment. ***A–C***, Lower panels: representative raster plots of calcium events of the same neurons as in upper panels following addition of bicuculline (bic, 30 μM) at the end of respective treatment. ***D***, Frequency of somatic calcium events in untreated condition, after 24 h of hNR1 or control antibodies treatment (***A–C***, upper panels); UT = 10.89 ± 0.31, $n = 366$ cells, ctrl = 12.55 ± 0.43, $n = 277$ cells, hNR1 = 14.99 ± 0.37, $n = 391$ cells, 6 independent experiments, $^{**}p = 0.007$, $^{****}p < 0.0001$. ***E–G***, Within-cell comparison of the frequency of calcium events in the same cells at the end of 24-h treatment and after addition of bicuculline, tested by paired *t* test from three independent experiments, reveals that bicuculline disinhibits the networks in untreated condition (***D***) and after control antibodies treatment (***E***) but not after hNR1 (***F***) treatment. Quantification of calcium events: (***E***) UT = 4.83 ± 0,51, UT + Bic = 10.87 ± 0,81, mean of difference = 6.05 ± 0.75, $n = 47$ neurons, $p < 0.0001$; (***F***) 24 h ctrl = 6.84 ± 0.0.74, 24 h ctrl + Bic = 8.61 ± 0,59, mean of difference = 1.76 ± 0.82, $n = 80$ neurons, $p = 0.035$; (***G***) 24-h hNR1 = 9.88 ± 0.88, 24-h hNR1 + Bic = 10.24 ± 0.45, mean of difference = 0.57 ± 0.9, $n = 62$ neurons, $p = 0.53$. Error bars indicate SEM. ANOVA Tukey's multiple comparison test (***D***) and paired *t* test (***E–G***) were used to evaluate statistical significance. $^{*}p < 0.05$, $^{**}p < 0.01$, $^{****}p < 0.0001$.

antibody treatment. Cortical networks of neurons were then subjected to live imaging 24 h after treatment with hNR1 or control antibodies. Subsequently, activity levels were measured by detecting somatic calcium transients of individual cells and compared with untreated cultures. Similar to MEA recordings (Fig. 1), in cortical cultures treated with the hNR1 antibody the frequency of somatic calcium events dramatically increased, as compared with both untreated networks and those treated with control antibody (UT = 10.89 ± 0.31, ctrl = 12.55 ± 0.43, hNR1 = 14.99 ± 0.37, $p < 0.0001$; Fig. 3*A–C*, upper panels, *D*). Interestingly, in this experimental setup the control antibody (ctrl) also increased the frequency of calcium events compared with untreated cultures ($p = 0.007$), although to a lesser extent than the hNR1 antibody (ctrl: 15%, hNR1: 38% increase; Fig. 3*D*). These latter data suggest that this antibody is not without its effects, although the mechanism and its antigen remain unknown.

Given the high spiking and bursting frequency of cortical cultures treated with hNR1 antibody, it was of interest to explore whether such cultures could be further disinhibited, perhaps by disengaging the GABAergic system. This was accomplished by adding bicuculline (30 μM), a $GABA_AR$ antagonist, at the end of 24-h treatment with antibodies and re-imaging activity of the same neurons for a within-cell comparison (Fig. 3*A–F*). As expected, in untreated and control antibody treated conditions, bicuculline increased the frequency of calcium events (paired *t* test, $p < 0.0001$, $p = 0.035$, respectively; Fig. 3*E*,*F*). Strikingly, bicuculline failed to further increase the frequency of calcium events in cultures treated with the hNR1 antibody (paired *t* test, $p = 0.53$; Fig. 3*G*). These data imply that critical features of the GABAergic system and/or Ca^{2+}-activated potassium channels, also known to be inhibited by bicuculline (Khawaled et al., 1999; Johnston, 2013), could contribute to antibody-induced hyperexcitability.

As the GABAergic system is a known key regulator of excitatory and inhibitory balance, we designed several experiments to further explore possible inhibitory dysfunction in the context of hNR1 antibody-disrupted NMDAR signaling. Interestingly, studies on the "glutamatergic hypothesis of schizophrenia" suggest that hypofunction of inhibitory drive onto excitatory pyramidal cells leads to disinhibition of cortical networks (Homayoun and Moghaddam, 2007), producing psychotic symptoms similar to those observed in patients with NMDAR encephalitis. We therefore asked whether the inhibitory drive onto excitatory neurons is also altered in cortical networks because of hNR1

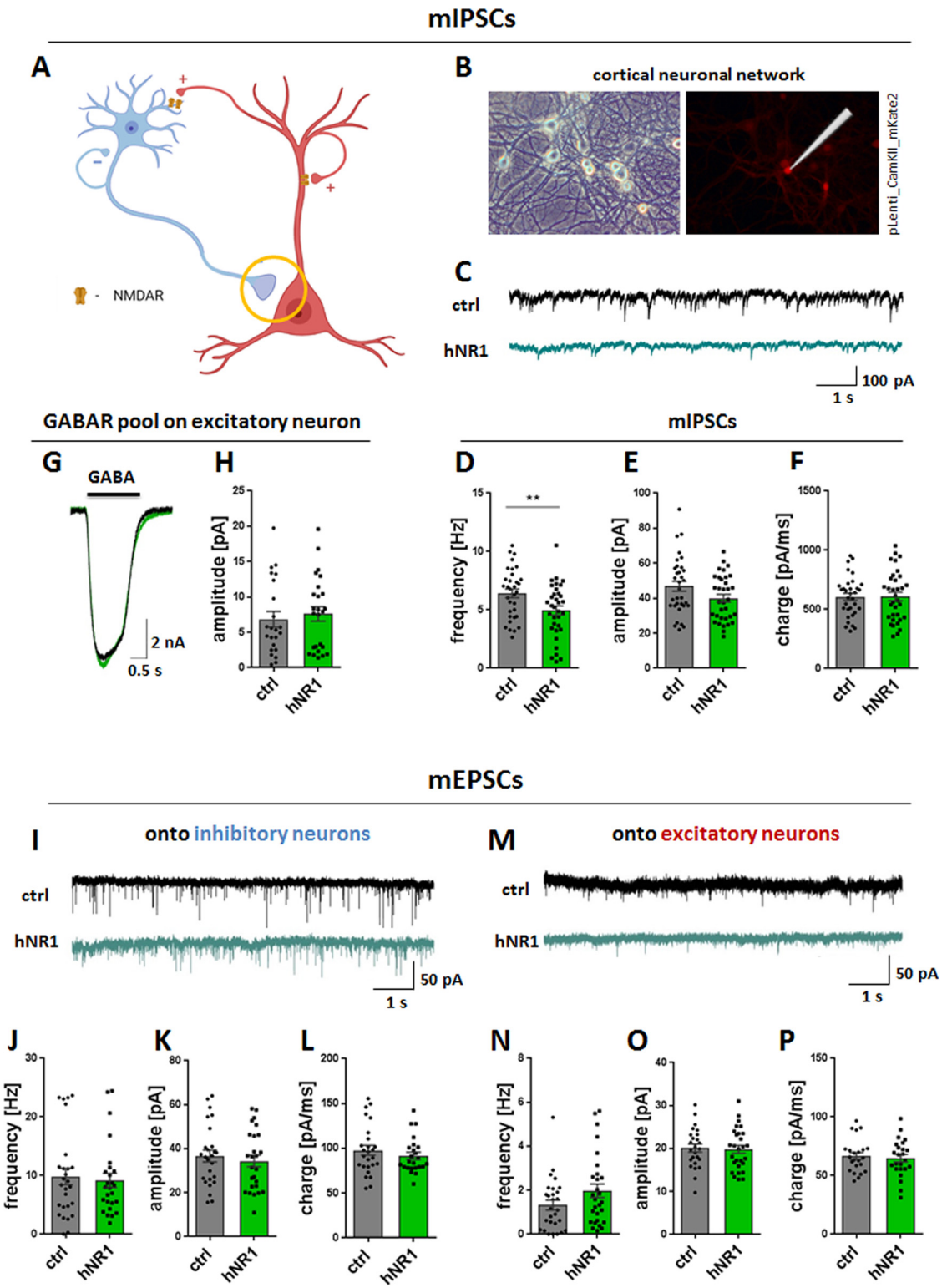

Figure 4. hNR1 antibody decreases inhibitory drive onto excitatory neurons in cortical circuits but does not affect excitatory drive. ***A–H***, Inhibitory drive onto excitatory neurons was measured by mIPSCs recorded from excitatory neurons in cortical neuronal networks. ***A***, Schematic model of a simplified neuronal network composed of excitatory pyramidal neurons (red) and inhibitory neurons (blue), forming different types of synapses onto each other. Inhibitory synapse onto excitatory neuron is marked with a circle as a synapse of interest measured in this experiment. ***B***, mIPSCs were recorded from excitatory neurons identified by expression of mKate2 expressed under excitatory neuron CamKII promoter. Left panel, BF image of representative cortical neuronal network. Right panel, Excitatory neuron identified by mKate2 fluorescent signal. ***C***, Representative traces of mIPSCs recorded in a whole-cell patch-clamp configuration from excitatory neurons after 24 h of treatment with control (ctrl, upper panel) or hNR1 (lower panel) antibodies. Treatment with hNR1 antibody decreases frequency of mIPSCs onto excitatory neurons (***D***) and has tendency to decrease their amplitude (***E***), without affecting their charge (***F***). ***D–F***, Quantification of mIPSCs parameters from three independent experiments, ctrl $n = 33$ neurons, hNR1 $n = 34$ neurons: (***D***) mIPSCs frequency: ctrl = 6.42 ± 0.37, hNR1 = 4.94 ± 0.4, $p = 0.009$; (***E***) mIPSCs amplitude: ctrl = 46.89 ± 2.89, hNR1 = 40.01 ± 2.25, $p = 0.06$; (***F***) mIPSCs charge: ctrl = 606.5 ± 29.72, hNR1 = 610 ± 36.37. ***G***, ***H***, hNR1 antibody treatment does not affect levels of GABA receptors on the postsynaptic excitatory neurons from which mIPSCs were recorded. ***G***, Representative traces of GABA currents recorded from excitatory neurons, evoked by 1-s pulse application of 5 μM GABA. ***H***, Quantification of GABA current amplitude presented in

antibody. Here, we performed a set of patch-clamp electrophysiology experiments to record miniature inhibitory post-synaptic currents (mIPSCs) from excitatory neurons in cortical cultures (Fig. 4*A*). Excitatory neurons were identified by infecting WT neurons with pLenti_CamKII_mKate2, a lentivirus expressing mKate2 under the glutamatergic specific CamKII promoter, at DIV2–DIV4 (Fig. 4*B*). At 15–18 DIV, we recorded mIPSCs from these neurons, after 24-h treatment with either hNR1 or control antibody. We observed that hNR1 antibody treatment significantly decreased mIPSCs frequency (ctrl = 6.42 ± 0.37, hNR1 = 4.94 ± 0.4, unpaired *t* test, $p = 0.009$) and had a tendency to decrease mIPSCs amplitude (ctrl = 46.89 ± 2.89, hNR1 = 40.01 ± 2.25, unpaired *t* test, $p = 0.06$) compared to treatment with control antibodies (Fig. 4*C–E*) without affecting charge (Fig. 4*F*). These data indicate that 24-h hNR1 antibody treatment indeed decreased inhibitory drive onto excitatory neurons. To test whether this is caused by an overall reduction of surface GABAR function on postsynaptic excitatory neurons, we measured currents induced by bath application of GABA (5 μM) using a fast-flow system. However, these GABA currents were similar between control and hNR1 antibody treated cultures (Fig. 4*G*,*H*), indicating that the total pools of $GABA_AR$ on excitatory neurons are not altered.

As network activity is sensitive to both excitation and inhibition, we next explored whether the excitatory drive in neuronal cultures was also altered by hNR1 antibody. This was accomplished by recording miniature excitatory post-synaptic currents (mEPSCs) in the presence of antibodies from both excitatory and inhibitory cortical neurons. Interestingly, the frequency, amplitude, and charge of mEPSCs onto either cell type were not affected by hNR1 antibody treatment (Fig. 4*I–P*). These data indicate that hNR1 antibody specifically reduces the inhibitory drive onto excitatory neurons in a cortical network, which could be causal for its overall disinhibition.

hNR1 antibody specifically impairs the function of inhibitory and not excitatory autapses

As we observed a decrease in overall inhibition and specific changes in inhibitory neuron output, we next examined the selective effects of the hNR1 antibody on inhibitory cortical neurons in more detail. Hence, we performed patch-clamp electrophysiological recordings in an autaptic system, where single neurons are grown on an astrocytic microislands, allowing the study of cell-autonomous effects on either inhibitory or excitatory neurons (Fig. 5*A*). To easily distinguish between these two neuronal populations, we employed GAD67-GFP mice, in which inhibitory neurons expressing GAD67 are fluorescently labeled (Tamamaki et al., 2003). Previous groups reported no changes in electrophysiological properties of these neurons when compared with WT neurons (Chang et al., 2014). In initial experiments, we examined whether the addition of hNR1 or control antibodies (24 h) affect the total surface expression of the 3 main groups of ionotropic receptors responsible for synaptic transmission, by acutely bath-applying NMDA (10 μM), GABA (5 μM), or kainate (20 μM) in 1-s pulses and comparing responses of inhibitory and excitatory cells. Intriguingly, we observed that in autaptic cultures of cortical neurons, hNR1 antibody treatment did not affect whole-cell NMDA currents on excitatory neurons (ctrl = 1 ± 0.08, hNR1 = 1.01 ± 0.11, unpaired *t* test, $p = 0.92$; Fig. 5*B*), yet it selectively decreased whole-cell NMDA currents on inhibitory neurons (ctrl = 1 ± 0.1, hNR1 = 0.71 ± 0.07, unpaired *t* test, $p = 0.018$; Fig. 5*E*). At the same time, total GABA-specific and kainate-specific currents in either cell type remained unchanged (Fig. 5*G*, data not shown). Next, we measured evoked synaptic responses by inducing an action potential in these cells, by a brief somatic depolarization of the neuron, and recording of the post-synaptic current that followed a few milliseconds afterward. Intriguingly, on inhibitory neurons, synaptic inhibitory transmission (IPSCs) was significantly reduced by ~41% (ctrl = 1 ± 0.12, hNR1 = 0.59 ± 0.11, $p = 0.01$; Fig. 5*F*), whereas synaptic excitatory transmission (EPSCs; ctrl = 1 ± 0.13, hNR1 = 1.31 ± 0.19, unpaired *t* test, $p = 0.19$; Fig. 5*C*) and pharmacologically isolated synaptic NMDA currents (ctrl = 1 ± 0.12, hNR1 = 1.38 ± 0.23, unpaired *t* test, $p = 0.13$; Fig. 5*D*) on excitatory neurons remained unchanged (Fig. 5*C*,*D*). What is more, on inhibitory neurons, the reduction of NMDA currents and the amplitude of IPSCs seemed to go hand in hand, as there was a significant correlation between these two parameters among inhibitory cells (linear regression, $R^2 = 0.132$, $p = 0.029$; Fig. 5*H*). These data suggest that in autaptic cortical neurons, hNR1 antibody treatment primarily affects the function of NMDARs on inhibitory neurons, which in turn reduces inhibitory synaptic output by these cells. To explore the mechanism further, we examined the impact of hNR1 antibody on the spontaneous release of GABA from inhibitory neurons by measuring mIPSCs in these autaptic cultures. Here, we observed a significant decrease in mIPSCs amplitude (Fig. 5*K*; ctrl = 43.87 ± 2.81, hNR1 = 30.72 ± 2.46, unpaired *t* test, $p = 0.0008$) and charge (Fig. 5*L*; ctrl = 789.7 ± 76.58, hNR1 = 551.9 ± 58.94, unpaired *t* test, $p = 0.016$). Similar to neuronal network experiments (Fig. 4*G*,*H*), we observed no differences in responses after bath application of GABA between autaptic neurons treated with control or hNR1 antibodies (Fig. 5*G*). Together, these data indicate that the hNR1 antibody specifically impairs NMDAR– and synaptic transmission of cortical inhibitory, but not excitatory neurons, in a cell-autonomous manner.

Importantly, as we observed a modest effect of the control antibody on neuronal network activity (Fig. 3), we evaluated whether it also exerts any significant effects in autaptic cultures. Here, no differences between untreated and control antibody treated cultures were observed in any of reported measures (whole-cell NMDA, GABA, and kainate currents, synaptic NMDA currents and EPSCs/IPSCs) in neither excitatory nor inhibitory neurons (data not shown). These data suggest that the control antibody generally has no direct effect on synaptic function in the autaptic system.

hNR1 antibody exerts different effects in cortical versus hippocampal neurons

The lack of effect of hNR1 antibody on NMDA currents in cortical excitatory neurons was surprising, as previous studies have robustly shown that patients' CSF/IgG reduce NMDA currents of hippocampal pyramidal cells (Moscato et al., 2014; Kreye et al., 2016). To verify that the lack of effect on cortical neurons

←

(***F***): ctrl = 6.84 ± 1.1, *n* = 23 neurons, hNR1 = 7.6 ± 1.04, *n* = 7.6 ± 1.04, *n* = 25 neurons. ***I–P***, hNR1 antibody does not affect excitatory miniature transmission (mEPSCs) onto neither inhibitory (***I–L***) nor excitatory (***M–P***) neurons. ***I***, ***M***, Representative traces of mEPSCs recorded from inhibitory (***I***) or excitatory (***M***) neurons. Quantification of mEPSCs parameters from three independent experiments: (***J***) mEPSCs frequency: ctrl = 9.83 ± 1.41, *n* = 27 neurons, hNR1 = 9.17 ± 1.2, *n* = 26 neurons; (***K***) mEPSCs amplitude: ctrl = 36.7 ± 2.71, *n* = 26 neurons, hNR1 = 34.41 ± 2.68, *n* = 26 neurons; (***L***) mEPSCs charge: 97.83 ± 5.47, *n* = 26 neurons, hNR1 = 91.52 ± 4.02, *n* = 24 neurons; (***N***) mEPSCs frequency: ctrl = 1.32 ± 0.23, *n* = 28 neurons, hNR1 = 1.98 ± 0.21, *n* = 28 neurons; (***O***) mEPSCs amplitude: ctrl = 20.09 ± 0.93, *n* = 25 neurons, hNR1 = 19.84 ± 0.92, *n* = 28 neurons; (***P***) mEPSCs charge: ctrl = 66.76 ± 2.96, *n* = 23 neurons, hNR1 = 64.86 ± 3.22, *n* = 24 neurons). Error bars indicate SEM. Unpaired *t* test was used to evaluate statistical significance. $^{**}p < 0.01$.

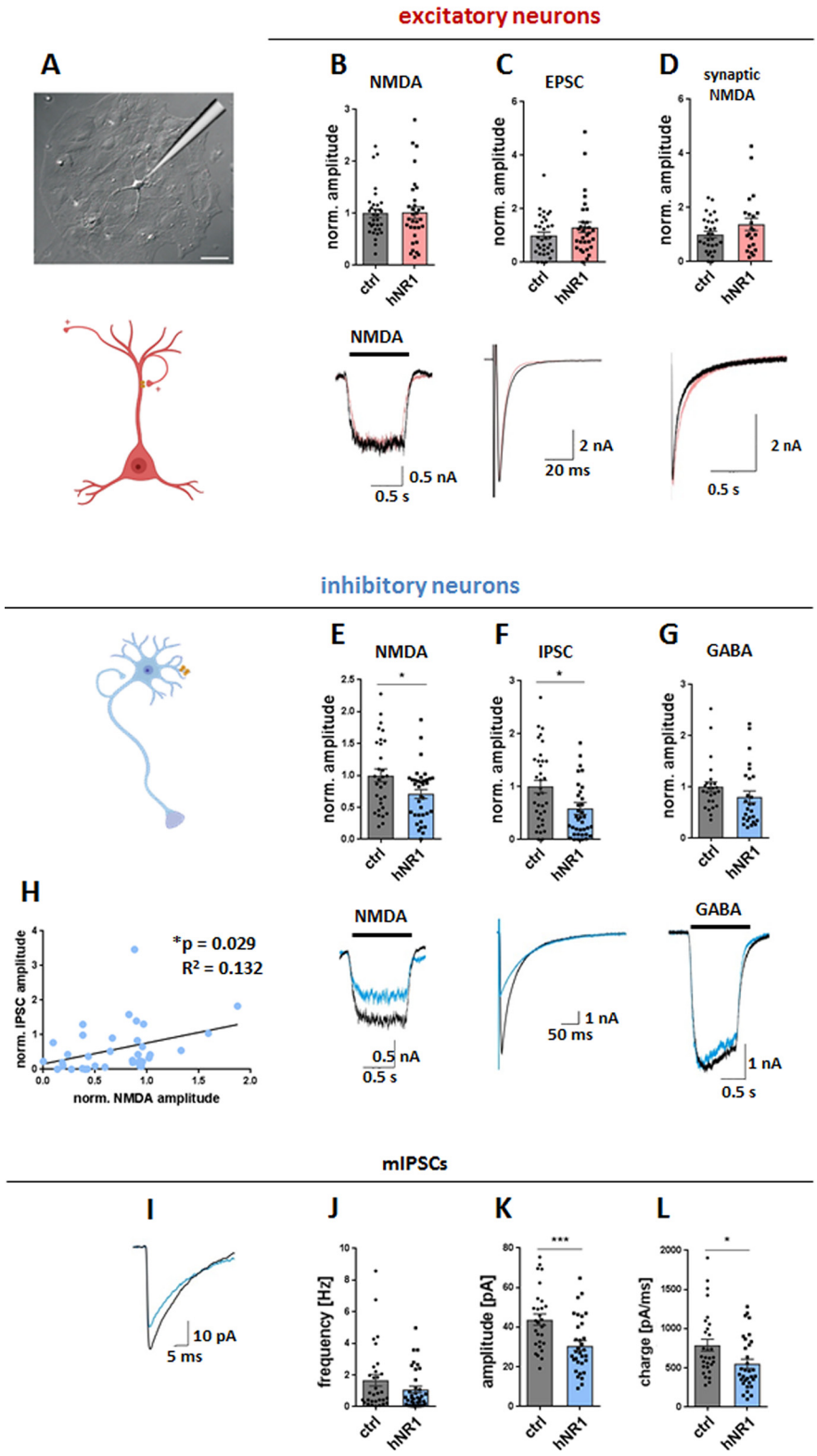

Figure 5. hNR1 antibody impairs function of cortical inhibitory, but not excitatory neurons, in a cell-autonomous manner. ***A***, Example image of a single cortical neuron grown on an astrocytic island in autaptic culture and a schematic representation of a patch pipette approaching the neuron. ***B–D***, Lower panels, representative traces of (***B***) whole-cell NMDA currents evoked by 1s bath application of NMDA (10 μM), (***C***) evoked EPSCs, (***D***) evoked synaptic NMDA currents in excitatory neurons after 24-h treatment with control (ctrl) or hNR1 antibodies. Upper panels, normalized current amplitudes from 4 independent experiments on excitatory neurons: (***B***) ctrl = 1 ± 0.08, n = 32 neurons, hNR1 = 1.01 ± 0.11, n = 32 neurons; (***C***) ctrl = 1 ± 0.13, n = 33 neurons, hNR1 = 1.31 ± 0.19, n = 31 neurons; and (***D***) ctrl = 1 ± 0.12, n = 29 neurons, hNR1 = 1.38 ± 0.23, n = 22 neurons. ***E–G***, Lower panels, representative traces of (***E***) whole-cell NMDA currents, (***F***) evoked IPSCs, (***G***) whole-cell GABA currents evoked by 1s bath application of GABA (5 μM) of inhibitory neurons after 24-h treatment with control or hNR1 antibodies. Upper panels, normalized current amplitudes from 4 independent experiments: (***E***) ctrl = 1 ± 0.1, n = 31 neurons, hNR1 = 0.71 ± 0.07, n = 36 neurons, p = 0.018; (***F***) ctrl = 1 ± 0.12, n = 35 neurons, hNR1 = 0.59 ± 0.11, n = 37 neurons, p = 0.014; (***G***) ctrl = 1 ± 0.1, n = 25 neurons, hNR1 = 0.81 ± 0.11, n = 26 neurons. ***H***, Correlation between normalized IPSC and NMDA current amplitudes of individual inhibitory neurons. Linear regression: R^2 = 0.132, p = 0.029. ***I–L***, Analysis of mIPSCs recorded from autaptic inhibitory neurons after 24 h of control or hNR1 antibodies treatment, 4 independent experiments. ***I***, Representative traces of mIPSCs. ***J***, mIPSCs frequency: ctrl = 1.66 ± 0.37, n = 31 neurons, hNR1 = 1.08 ± 0.21, n = 35 neurons. ***K***, mIPSCs amplitude: ctrl = 43.87 ± 2.81, n = 29 neurons, hNR1 = 30.72 ± 2.46, n = 32 neurons, p = 0.0008. ***L***, mIPSCs charge: ctrl = 789.7 ± 76.58, n = 29 neurons, hNR1 = 551.9 ± 58.94, n = 32 neurons, p = 0.016. Error bars indicate SEM. Unpaired t test (***B–D***, ***E–G***, ***J–L***) and linear regression (***H***) were used to evaluate statistical significance. *$p < 0.05$, ***$p < 0.001$.

is not because of technical limitations of our autaptic assays, we repeated the autaptic recordings on hippocampal excitatory neurons. As reported previously (Kreye et al., 2016), treatment with hNR1 antibody selectively reduced whole-cell NMDA currents (36% decrease, ctrl = 1 ± 0.08, hNR1 = 0.64 ± 0.06, unpaired t test, p = 0.0008; Fig. 6*A*) and synaptic NMDA currents (43% decrease, ctrl = 1 ± 0.15, hNR1 = 0.58 ± 0.12, unpaired t test, p = 0.039; Fig. 6*E*) in hippocampal excitatory neurons, without affecting EPSC (Fig. 6*D*), GABA (Fig. 6*B*), and kainate (Fig. 6*C*) currents. Importantly, these results demonstrate that hNR1 antibody shows tissue-specificity, and in cortical cultures selectively affect inhibitory, and not excitatory, neurons.

hNR1 antibody binds NMDARs within inhibitory synapses and reduce levels of inhibitory presynaptic proteins

The results from both neuronal networks (Fig. 4) and autaptic (Fig. 5) recordings suggest that hNR1 antibody causes a dysfunction of synaptic output of inhibitory neurons, represented by a reduced amplitude and/or frequency of IPSCs and mIPSCs. To explore possible presynaptic effects of the hNR1 antibody, we measured levels of proteins crucial for proper function of inhibitory presynapses before and after hNR1 antibody treatment by immunocytochemistry in cortical networks. Additionally, by employing GAD67-GFP mice, we distinguished between inhibitory synapses onto inhibitory (GFP-positive), and excitatory (GFP-negative) neurons (Fig. 7*B*,*C*). Two proteins are indispensable for proper neurotransmitter release within GABAergic presynapses: GAD65,

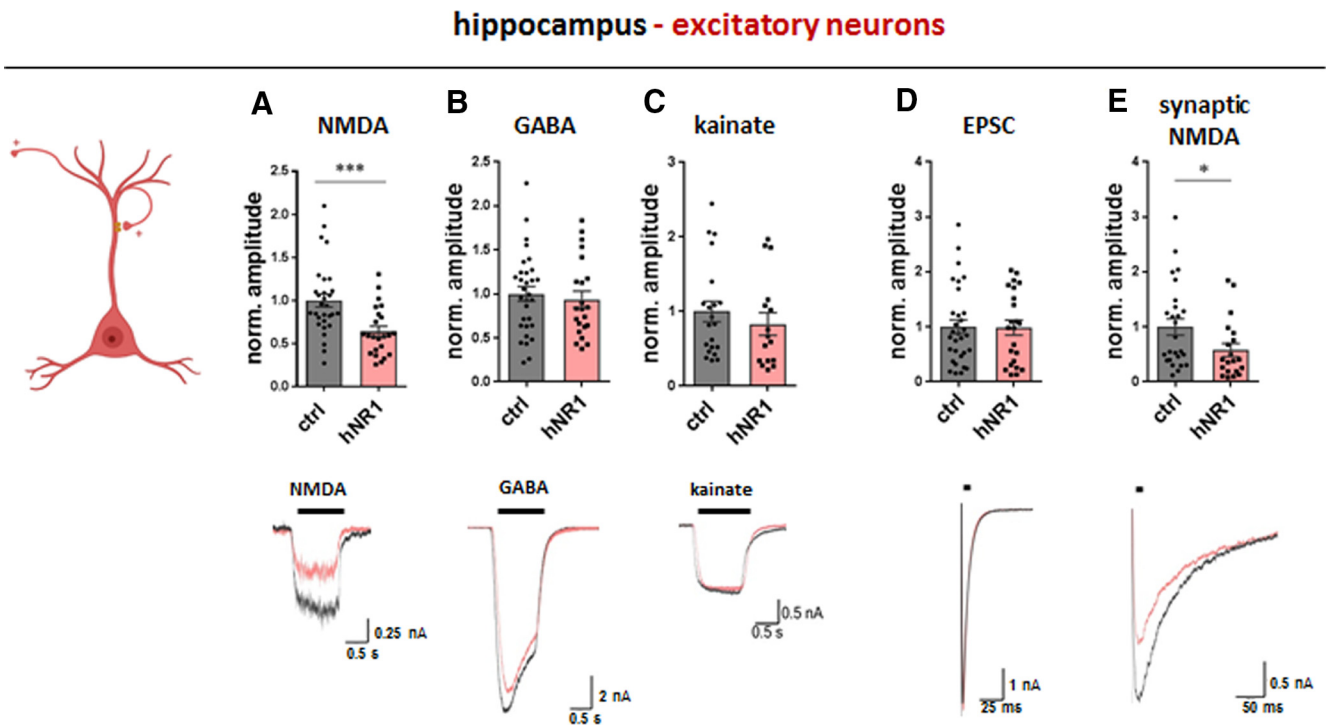

Figure 6. hNR1 antibody impairs NMDA currents of excitatory hippocampal neurons. In hippocampal autaptic cultures, 24-h treatment with hNR1 antibody (1 μg/ml) selectively decreases whole-cell (***A***) and synaptic (***E***) NMDA currents of excitatory neurons, when compared to treatment with control (ctrl) antibody. ***A–C***, Whole-cell receptor currents were evoked by 1s bath application of (***A***) NMDA (10 μM), (***B***) GABA (30 μM), or (***C***) kainate (20 μM). Quantification of normalized current amplitudes from three independent experiments: (***A***) NMDA currents: ctrl = 1 ± 0.08, $n = 30$ neurons, hNR1 = 0.64 ± 0.06, $n = 23$ neurons, $p = 0.0008$; (***B***) GABA currents: ctrl = 1 ± 0.08, $n = 31$ neurons, hNR1 = 0.94 ± 0.09, $n = 22$ neurons; (***C***) kainate currents: ctrl = 1 ± 0.14, $n = 21$ neurons, hNR1 = 0.83 ± 0.15, $n = 16$ neurons. ***D***, ***E***, Synaptic responses were evoked by a brief somatic depolarization of neurons from −70 to 0 mV for 2 ms, synaptic NMDA currents were recorded in the presence of 0 mM Mg^{2+}, 10 μM glycine, and 10 μM NBQX. Quantification of normalized current amplitudes from three independent experiments: (***D***) EPSCs: ctrl = 1 ± 0.13, $n = 31$ neurons, hNR1 = 0.99 ± 0.14, $n = 23$ neurons; (***E***) synaptic NMDA: ctrl = 1 ± 0.15, $n = 26$ neurons, hNR1 = 0.58 ± 0.12, $n = 20$ neurons, $p = 0.039$. Error bars indicate SEM. Unpaired *t* test was used to evaluate statistical significance. *$p < 0.05$, ***$p < 0.001$.

which synthetizes GABA from glutamate within presynaptic boutons, and the vesicular GABA transporter (VGAT/VIAAT), which subsequently loads GABA into synaptic vesicles. Using quantitative immunocytochemistry, we measured the intensities of fluorescently labeled VGAT and GAD65 puncta along dendrites, to quantify their expression levels. Remarkably, a 24-h treatment with hNR1 antibody significantly reduced intensities of VGAT puncta (UT = 1 ± 0.05, 24-h hNR1 = 0.82 ± 0.04, unpaired *t* test, $p = 0.005$; Fig. 7*D*,*E*). Moreover, this decrease was specific to inhibitory synapses onto excitatory neurons, and not onto inhibitory neurons (Fig. 7*D*,*F*). On the other hand, the intensities of GAD65 puncta were unchanged after 24 h of hNR1 antibody treatment (Fig. 7*G*–*I*). We then additionally measured GAD65 expression levels after 6 h of hNR1 antibody treatment. At this time point, we observed a significant decrease in GAD65 puncta intensity (UT = 1 ± 0.03, 6-h hNR1 = 0.89 ± 0.02, 24-h hNR1 = 0.95 ± 0.02, ANOVA Tukey's multiple comparison test, $p = 0.01$; Fig. 7*H*), which again was specific to inhibitory synapses onto excitatory, but not inhibitory, neurons (Fig. 7*G*–*I*). Together, these data demonstrate that the hNR1 antibody reduces levels of the presynaptic proteins VGAT and GAD65, specifically in inhibitory-to-excitatory neuron synapses.

Finally, we asked whether the observed specific effect of hNR1 antibody on inhibitory neurons can be explained by a distinct binding pattern of the antibody in cortical cultures. One possibility could be that the antibody binds specifically to inhibitory neurons. Alternatively, the hNR1 antibody could target different subcellular pools of NMDARs, or even bind directly to inhibitory synapses to affect their function locally. We explored these options by analyzing the acute binding patterns of hNR1 antibody in our cortical cultures. First, live neurons were incubated with hNR1 antibody for 20 min at 10°C, washed, and incubated with anti-human secondary antibody for 20 min at 10°C. Cells were then fixed and co-stained for the excitatory presynaptic marker VGLUT1 to verify whether hNR1 antibody binds to excitatory synapses, as expected. The degree of co-localization of the hNR1 antibody puncta with VGLUT1 signal was used as a measure of excitatory synaptic versus extrasynaptic antibody binding. Although the hNR1 antibody decorated all neurons present in the culture in a punctate pattern, there was a striking difference between the binding patterns on excitatory and inhibitory neurons. While on inhibitory neurons most of hNR1 antibody puncta (70%) co-localized with VGLUT1, on excitatory neurons only half of the hNR1 antibody puncta co-localized with VGLUT1 (excitatory = 47.28 ± 4.53%, inhibitory = 69.75 ± 4.19%, unpaired *t* test, $p = 0.006$; Fig. 8*A*,*B*), suggesting that on excitatory neurons a larger pool of hNR1 antibody binds to structures outside of VGLUT1-positive synapses. Next, we asked whether hNR1 antibody can also bind NMDARs associated with inhibitory synapses. Here, neurons were co-stained with the hNR1 antibody and the inhibitory postsynaptic marker gephyrin to assess the degree of co-localization. Using confocal microscopy and z-stack analysis, we observed that hNR1 antibody indeed binds to a subpopulation of inhibitory synapses in our cortical cultures (Fig. 8*C*,*D*). Remarkably, up to 30% of inhibitory synapses on excitatory neurons bound the hNR1 antibody, whereas this phenomenon was much less common for inhibitory synapses on inhibitory neurons (excitatory = 30.84 ± 2.05%,

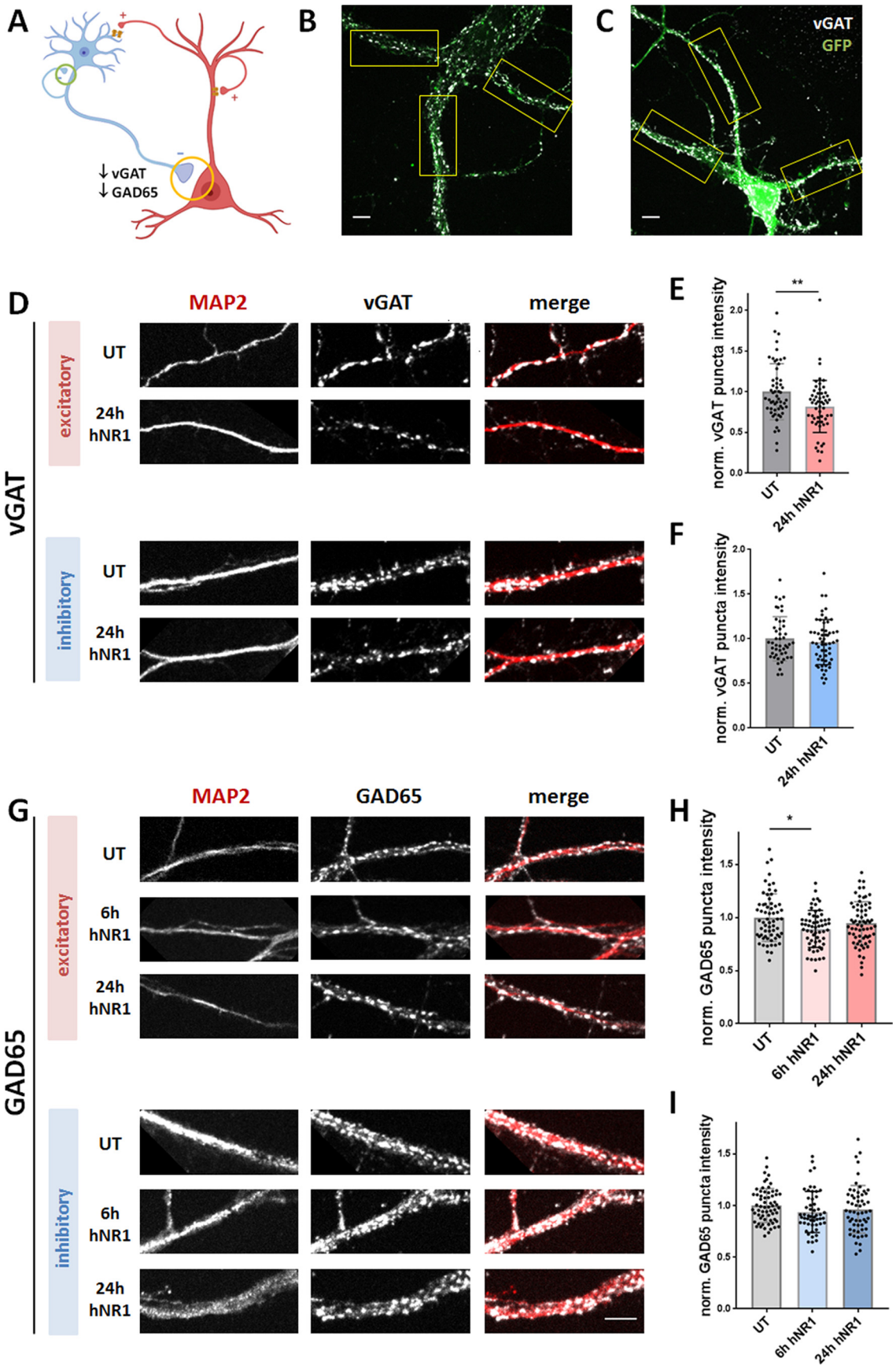

Figure 7. hNR1 antibody decreases levels of inhibitory presynaptic proteins VGAT and GAD65 in inhibitory-to-excitatory neuron synapses. ***A***, Schematic model showing investigated inhibitory synapses and summarizing the finding: decreased levels of GAD65 and VGAT at inhibitory synapses onto excitatory (yellow circle), but not inhibitory (green circle), neurons. ***B***, ***C***, Representative images of cortical excitatory (***B***) and inhibitory (***C***) neurons identified by staining with antibodies against GFP. Only proximal dendrites close to soma, which are easily identified as GFP-positive

inhibitory = 11.17 ± 1.52%, unpaired *t* test, $p < 0.0001$; Fig. 9*E*). This preference raises the possibility that the observed functional impact of the hNR1 antibody on inhibitory synapses may be because of the direct effects of this antibody on these synapses.

Discussion

Our study demonstrates that a patient-derived antibody targeting the NR1 subunit of NMDARs adversely affects the function of cortical neuronal networks, driving them into a hyperactive state (Figs. 1, 3). This increased excitability seems to be a result of reduced inhibitory neuron output onto excitatory neurons, as indicated by reduced amplitudes of IPSCs, lowered frequency of network mIPSCs and decreased levels of inhibitory presynaptic proteins (Fig. 9). This contrasts with the effects of this antibody on hippocampal neurons, where it primarily affects NMDAR function on excitatory neurons (Fig. 6; Kreye et al., 2016). Moreover, in cortical networks hNR1 antibody interferes with NMDAR-Npas4-mediated mechanisms of stabilizing network excitability (Fig. 2). These observations provide insights into how such autoantibodies can differentially affect hippocampal versus cortical circuits, giving rise to impaired memory function or psychiatric symptoms in patients with NMDAR encephalitis, respectively.

hNR1 antibody increases cortical network activity

Our primary observation is that hNR1 antibody causes a hyperexcitable state of cortical networks (Figs. 1, 3). Although counterintuitive, since NMDAR hypofunction should dampen glutamatergic transmission, our data are in line with clinical and molecular studies showing that seizures occur in ~60% of patients with NMDAR encephalitis (de Bruijn et al., 2019) and that seizure susceptibility is increased in mice exposed to patient CSF (Wright et al., 2015).

Intriguingly, in contrast to our findings (Fig. 1), two groups used MEAs to assess effects of patient CSF on cortical (Jantzen et al., 2013) or hippocampal (Koch et al., 2019) neuronal networks and reported a relative decrease in activity. Such differences could arise from varied approaches used. Both studies examined the acute effects of antibodies (10–15 min), using patient CSF containing a mixture of antibodies. In contrast, our 46-h recording revealed that the presence of the hNR1 antibody leads to a gradually increasing activity, however, over 24 h and not 15 min. Mechanistically, this occurs in a timeframe corresponding to the rate of antibody-induced receptor internalization both described previously (Moscato et al., 2014) and observed for hNR1 (data not shown). Thus, the increase in cortical network activity by the hNR1 antibody seems to be a relevant causal mechanism for both hyperexcitability and epilepsy in patients.

A fundamental question raised by our MEA analysis is how the hNR1 antibody leads to a steady increase in network spiking? One possibility is an adaptive response of the network to a partial block of NMDARs. Blocking half of surface NMDARs (1 μM AP5) lead to a modest but nonsignificant increase in network

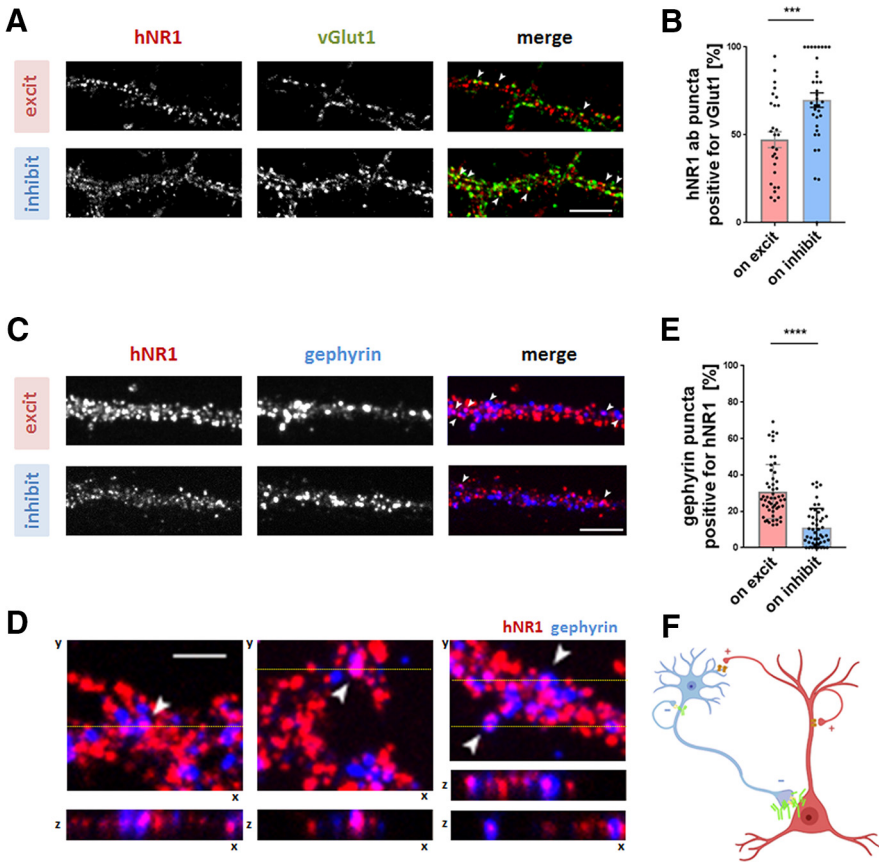

Figure 8. hNR1 antibody binds inhibitory synapses, preferentially on excitatory neurons. ***A***, Images of cortical neurons which were live stained with hNR1 antibody to detect acute binding pattern of the antibodies, and then fixed and co-stained for excitatory synaptic marker VGLUT1. Degree of colocalization of hNR1 antibody puncta and VGLUT1 puncta was used as a measure of excitatory synaptic or extrasynaptic staining. ***B***, Percentage of hNR1 antibody puncta positive for VGLUT1 (synaptic staining) per ROI: excitatory neurons = 47.28 ± 4.53, $n = 28$ ROIs, inhibitory neurons = 69.75 ± 4.19, $n = 35$ ROIs, 2 independent experiments, $p = 0.006$. ***C***, Images of cortical neurons live stained with hNR1 antibodies for acute hNR1 antibodies binding pattern, which were then fixed and co-stained with inhibitory synaptic marker gephyrin. Degree of colocalization between hNR1 antibody puncta and gephyrin puncta was used to assess inhibitory synaptic binding of the antibodies. Arrowheads indicate overlap between hNR1 and gephyrin. ***D***, Lower panel, 3D (z stack) volume images of individual inhibitory synapses from images in the upper panel at the level of yellow line, representing cross-section through 12 planes of z-stack. ***E***, Percentage of gephyrin puncta positive for hNR1 antibodies from three independent experiments: excitatory neurons = 30.84 ± 2.05, $n = 53$ ROIs, inhibitory neurons = 11.17 ± 1.52, $n = 48$ ROIs, $p < 0.0001$. ***F***, Schematic summarizing findings from these experiments: hNR1 antibody (green) binds within inhibitory synapses, preferentially onto excitatory neurons. Scale bar: 10 μm (***A***, ***C***) and 5 μm (***D***). Error bars indicate SEM. Unpaired *t* test was used to evaluate statistical significance. $^{*}p < 0.05$, $^{**}p < 0.01$, $^{****}p < 0.0001$.

←

or GFP-negative, were chosen for ROI selection (boxes). ***D***, ***G***, Images of ROIs of cortical excitatory and inhibitory neurons which were fixed and stained with antibodies against GFP, MAP2, and either VGAT (***D***) or GAD65 (***G***), in untreated condition (UT) or after 6 or 24 h of hNR1 antibodies treatment. ***E***, ***F***, Normalized intensity of VGAT puncta along dendrites from three independent experiments: (***E***) on excitatory neurons: UT = 1 ± 0.05, $n = 56$ ROIs, 24-h hNR1 = 0.82 ± 0.04, $n = 55$ ROIs, $p = 0.005$; (***F***) on inhibitory neurons: UT = 1 ± 0.04, $n = 47$ ROIs, 24-h hNR1 = 0.96 ± 0.03, $n = 57$ ROIs. ***H***, ***I***, Normalized intensity of GAD65 puncta along dendrites from three independent experiments: (***H***) on excitatory neurons: UT = 1 ± 0.03, $n = 64$ ROIs, 6-h hNR1 = 0.89 ± 0.02, $n = 59$ ROIs, 24-h hNR1 = 0.95 ± 0.02, $n = 67$ ROIs, $p = 0.01$; (***I***) on inhibitory neurons: UT = 1 ± 0.02, $n = 64$ ROIs, 6-h hNR1 = 0.94 ± 0.03, $n = 53$ ROIs, 24-h hNR1 = 0.96 ± 0.03, $n = 58$ ROIs. Error bars indicate SEM. Scale bar: 10 μm. Paired *t* test (***E***, ***F***) and ANOVA Tukey's multiple comparison test (***H***, ***I***) were used to evaluate statistical significance. $^{*}p < 0.05$, $^{**}p < 0.01$.

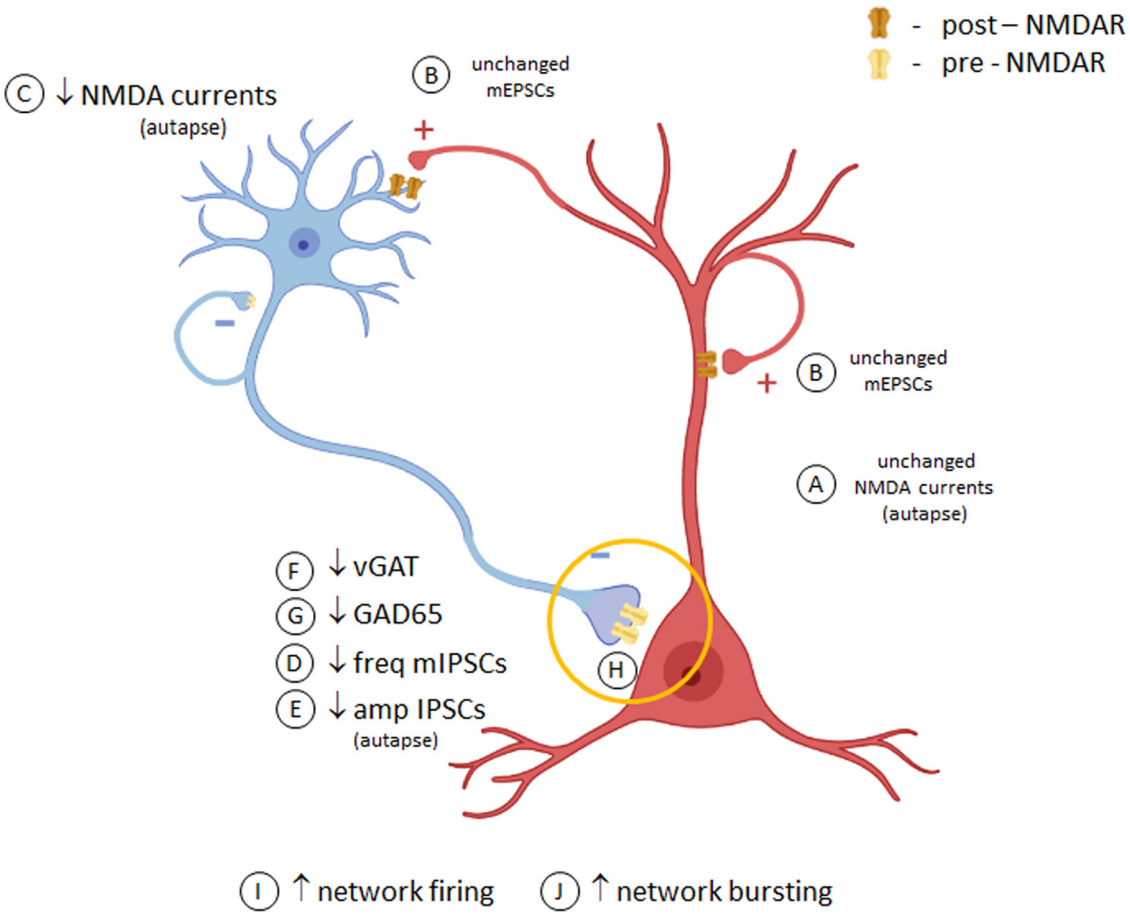

Figure 9. Speculative model of effects of hNR1 antibody on cortical inhibitory neuron and network function. In cortical neuronal cultures, hNR1 antibody does not affect NMDA currents (***A***) or synaptic transmission (***B***) of excitatory neurons, yet it selectively decreases NMDA currents on inhibitory cells (***C***). Antibody binding further impairs inhibitory synaptic transmission (***D***, ***E***) and decreases levels of GABA producing presynaptic proteins (***F***, ***G***), specifically in inhibitory-to-excitatory neuron synapses (yellow circle). Such reduced synaptic inhibitory output could result from altered transcriptional profiles of inhibitory neurons and/or local dysfunction of presynaptic NMDARs within these inhibitory synapses (***H***), mechanisms yet to be explored. This reduced inhibitory function disinhibits activity of excitatory neurons and the network as a whole (***I***, ***J***).

spiking, indicating that it is possible, yet unlikely, that a partial block of surface NMDARs contributes to the seen increase in network activity. Rather, these data suggest that hNR1 antibody might instead act through specific receptors/neuronal subtypes to disturb E/I balance. Indeed, in the presence of hNR1 antibody, cortical networks dramatically increase their bursting activity (Fig. 1*J*–*P*) and loose responsiveness to bicuculline (Fig. 3*A*–*F*), suggesting that the inhibitory system is likely affected.

A second puzzling question is why neuronal spiking continues to climb in the presence of hNR1 antibody, when one would expect mechanisms stabilizing network excitability, such as Npas4 signaling (Bloodgood et al., 2013), to counter a hyperactive state. Surprisingly, nuclear Npas4 levels did not increase in the presence of hNR1 antibody (Fig. 2*A*–*D*), suggesting that this mechanism became ineffective. Accordingly, normal NMDA-mediated increase in nuclear Npas4 was blocked by addition of hNR1 antibody (Fig. 2*E*,*F*). This could be because of a direct effect of hNR1 antibody on NMDARs, as AP5 also prevented the induction of Npas4 after NMDA application (Fig. 2*E*,*F*). Together, these data indicate that the hNR1 antibody can interfere with homeostatic mechanisms regulated by NMDAR/Npas4 signaling.

hNR1 antibody impairs the output of cortical inhibitory neurons

While the depression of NMDAR/Npas4 signaling may explain why hyperexcitability is not scaled down, it does not fully explain why the activity increases in the first place. One possibility is that hNR1 antibody acts on a subset of receptors, synapses or neurons. In the cortex, a correct E/I balance is maintained by GABAergic interneurons orchestrating excitability of pyramidal cells. Our data indicate that cortical GABAergic interneurons are indeed a primary target of hNR1 antibody, specifically altering the output of inhibitory synapses onto excitatory neurons. Consistently, hNR1 antibody treatment decreased action potential-independent, tonic inhibitory drive onto excitatory neurons, measured by frequency of mIPSCs (Fig. 4*A*–*F*). This was specific to inhibitory synapses, as mEPSCs frequency remained unchanged (Fig. 4*I*–*P*). This is further supported by a decrease in the levels of both VGAT and GAD65 in presynaptic inhibitory boutons formed onto excitatory neurons, but not inhibitory interneurons (Fig. 7).

Importantly, cell-autonomous autaptic recordings confirmed the specific impact of hNR1 antibody on inhibitory neuron function, where it significantly reduced NMDA– and evoked synaptic currents exclusively in inhibitory autaptic neurons (Fig. 5). Although reduced NMDA currents are likely because of receptor internalization, how loss of surface NMDARs translates into reduced inhibitory synaptic transmission remains elusive. Conceivably, reduced NMDAR-mediated Ca^{2+} influx could trigger changes in transcriptional profiles in these neurons, leading to decreased levels of presynaptic proteins (Fig. 7) and ultimately

synaptic output (Fig. 5), similarly to networks in which excitation has been removed (Lau and Murthy, 2012). However, given that we observed increased somatic calcium signals in all cortical neurons (Fig. 3), whether such mechanisms are involved remains unclear and further RNA sequencing studies are needed to elucidate possible cell type-specific transcriptional changes.

hNR1 antibody shows brain regional specificity

Remarkably, our data imply that autoantibodies can have different effects in varying brain regions. In cortex, we find that hNR1 specifically impairs cortical inhibitory, but not excitatory, neurons. This contrasts with studies in the hippocampus, showing that these autoantibodies primarily affect excitatory neuron function (Fig. 6; Hughes et al., 2010; Kreye et al., 2016). This regional specificity indicates that there are limitations with current preclinical models, which passively deliver patient CSF/antibodies into ventricles (Planagumà et al., 2016; Taraschenko et al., 2019) or hippocampus (Würdemann et al., 2016; Kersten et al., 2019). While this approach can provide direct antibody access to hippocampal structures, they rarely reach cortical regions (Planagumà et al., 2015). As such, active immunization models which more often report increased sensitivity to seizures (Jones et al., 2019; Wagnon et al., 2020) may provide for a more clinically-relevant distribution of antibodies and thus a better understanding of their region-specific effects.

hNR1 antibody binds specific pools of NMDARs and affects inhibitory synapses

At present, it is unclear which mechanisms lead to brain regional and/or neuronal type specificity of hNR1 antibody. One possibility could be that the hNR1 antibody binds variably on excitatory versus inhibitory neurons. Acute antibody binding studies supports this idea, as hNR1 antibody differentially binds synaptic and extrasynaptic NMDARs on inhibitory versus excitatory cortical neurons (Fig. 8*A*,*B*). This is relevant as synaptic and extrasynaptic NMDARs trigger distinct downstream signaling pathways and could therefore contribute to differential effects on each cell type.

An intriguing complementary mechanism could involve local effects of hNR1 antibody on presynaptic NMDARs. Although controversial and debated in the field, presynaptic NMDARs within inhibitory synapses have been shown to control neurotransmitter release (Bouvier et al., 2015) and regulate inhibitory drive onto pyramidal neuron in prefrontal cortex (Mathew and Hablitz, 2011; Pafundo et al., 2018). Thus, their hypofunction because of hNR1 binding could partially explain the observed decrease in mIPSCs (Fig. 4). Accordingly, we observed that the hNR1 antibody indeed decorates inhibitory synapses (Fig. 8). While it is unclear whether this binding is presynaptic or postsynaptic, a recent immuno-EM study found that the hNR1 antibody could indeed decorate presynaptic-NMDARs (Wagner et al., 2020). Importantly, studies by Fiszman et al. (2005) reported that reducing presynaptic-NMDAR signaling decreases the size of presynaptic inhibitory boutons, as measured by GAD65 puncta intensity, similar to our observations (Fig. 7). Thus, in addition to more general effects of the hNR1 antibodies on inhibitory interneurons, there is an emerging framework for how these antibodies could also have more selective actions on subsets of inhibitory synapses, which ultimately alter the excitability of cortical networks in patients with NMDAR encephalitis.

Relevance for neuropsychiatric disorders

Remarkably, NMDAR hypofunction on cortical interneurons has long been implicated to underlie cortical disinhibition and core psychiatric symptoms in schizophrenia (Nakazawa et al., 2012). Genetic deletion of NMDARs in interneurons *in vivo* produces schizophrenia-like behaviors (Belforte et al., 2010), impairs E/I balance and increases excitability of cortical pyramidal cells (Pafundo et al., 2021). Similarly, ketamine impairs mIPSCs, without affecting mEPSCs, and leads to increased pyramidal excitability in prefrontal cortical slices (Zhang et al., 2008), which is strikingly similar to our effects after hNR1 antibody treatment (Figs. 1, 3, 4). Our data thus provides evidence that patient-derived autoantibodies can disturb similar pathways and suggest a possible common mechanism across neuropsychiatric disorders.

Importantly, the proposed mechanisms of antibody action are not mutually exclusive and may act in a complementary manner to exert regional changes in synaptic plasticity, subunit-specific transcriptional changes and presynaptic regulation of inhibitory drive to produce complex behavioral and cognitive phenotypes. Together, our data reveal a novel, region-specific mechanism of anti-NMDAR antibodies in cortical neurons causing inhibitory dysfunction and network disinhibition.

References

Arancillo M, Min SW, Gerber S, Münster-Wandowski A, Wu YJ, Herman M, Trimbuch T, Rah JC, Ahnert-Hilger G, Riedel D, Südhof TC, Rosenmund C (2013) Titration of syntaxin1 in mammalian synapses reveals multiple roles in vesicle docking, priming, and release probability. J Neurosci 33:16698–16714.

Banker G, Goslin K (1988) Developments in neuronal cell culture. Nature 336:185–186.

Belforte JE, Zsiros V, Sklar ER, Jiang Z, Yu G, Li Y, Quinlan EM, Nakazawa K (2010) Postnatal NMDA receptor ablation in corticolimbic interneurons confers schizophrenia-like phenotypes. Nat Neurosci 13:76–83.

Bliss TV, Collingridge GL (1993) A synaptic model of memory: long-term potentiation in the hippocampus. Nature 361:31–39.

Bloodgood BL, Sharma N, Browne HA, Trepman AZ, Greenberg ME (2013) The activity-dependent transcription factor NPAS4 regulates domain-specific inhibition. Nature 503:121–125.

Bouvier G, Bidoret C, Casado M, Paoletti P (2015) Presynaptic NMDA receptors: roles and rules. Neuroscience 311:322–340.

Chang CL, Trimbuch T, Chao HT, Jordan JC, Herman MA, Rosenmund C (2014) Investigation of synapse formation and function in a glutamatergic-GABAergic two-neuron microcircuit. J Neurosci 34:855–868.

Chen JY, Chauvette S, Skorheim S, Timofeev I, Bazhenov M (2012) Interneuron-mediated inhibition synchronizes neuronal activity during slow oscillation. J Physiol 590:3987–4010.

Dalmau J, Graus F (2018) Antibody-mediated encephalitis. N Engl J Med 378:840–851.

Dalmau J, Tüzün E, Wu H-y, Masjuan J, Rossi JE, Voloschin A, Baehring JM, Shimazaki H, Koide R, King D, Mason W, Sansing LH, Dichter MA, Rosenfeld MR, Lynch DR (2007) Paraneoplastic anti-*N*-methyl-D-aspartate receptor encephalitis associated with ovarian teratoma. Ann Neurol 61:25–36.

Dana H, Mohar B, Sun Y, Narayan S, Gordus A, Hasseman JP, Tsegaye G, Holt GT, Hu A, Walpita D, Patel R, Macklin JJ, Bargmann CI, Ahrens MB, Schreiter ER, Jayaraman V, Looger LL, Svoboda K, Kim DS (2016) Sensitive red protein calcium indicators for imaging neural activity. Elife 5:e12727.

de Bruijn MAAM, van Sonderen A, van Coevorden-Hameete MH, Bastiaansen AEM, Schreurs MWJ, Rouhl RPW, van Donselaar CA, Majoie MHJM, Neuteboom RF, Sillevis Smitt PAE, Thijs RD, Titulaer MJ (2019) Evaluation of seizure treatment in anti-LGI1, anti-NMDAR, and anti-$GABA_B$R encephalitis. Neurology 92:e2185–e2196.

Emnett CM, Eisenman LN, Taylor AM, Izumi Y, Zorumski CF, Mennerick S (2013) Indistinguishable synaptic pharmacodynamics of the *N*-methyl-D-aspartate receptor channel blockers memantine and ketamine. Mol Pharmacol 84:935–947.

Fiszman ML, Barberis A, Lu C, Fu Z, Erdélyi F, Szabó G, Vicini S (2005) NMDA receptors increase the size of GABAergic terminals and enhance GABA release. J Neurosci 25:2024–2031.

Flavell SW, Greenberg ME (2008) Signaling mechanisms linking neuronal activity to gene expression and plasticity of the nervous system. Annu Rev Neurosci 31:563–590.

Gleichman AJ, Spruce LA, Dalmau J, Seeholzer SH, Lynch DR (2012) Anti-NMDA receptor encephalitis antibody binding is dependent on amino acid identity of a small region within the GluN1 amino terminal domain. J Neurosci 32:11082–11094.

Hardingham GE, Bading H (2003) The yin and yang of NMDA receptor signalling. Trends Neurosci 26:81–89.

Hazan H, Ziv NE (2017) Closed loop experiment manager (CLEM)—an open and inexpensive solution for multichannel electrophysiological recordings and closed loop experiments. Front Neurosci 11:579.

Hazan L, Ziv NE (2020) Activity dependent and independent determinants of synaptic size diversity. J Neurosci 40:2828–2848.

Homayoun H, Moghaddam B (2007) NMDA receptor hypofunction produces opposite effects on prefrontal cortex interneurons and pyramidal neurons. J Neurosci 27:11496–11500.

Hughes EG, Peng X, Gleichman AJ, Lai M, Zhou L, Tsou R, Parsons TD, Lynch DR, Dalmau J, Balice-Gordon RJ (2010) Cellular and synaptic mechanisms of anti-NMDA receptor encephalitis. J Neurosci 30:5866–5875.

Irani SR, Bera K, Waters P, Zuliani L, Maxwell S, Zandi MS, Friese MA, Galea I, Kullmann DM, Beeson D, Lang B, Bien CG, Vincent A (2010) *N*-methyl-D-aspartate antibody encephalitis: temporal progression of clinical and paraclinical observations in a predominantly non-paraneoplastic disorder of both sexes. Brain 133:1655–1667.

Jantzen SU, Ferrea S, Wach C, Quasthoff K, Illes S, Scherfeld D, Hartung HP, Seitz RJ, Dihné M (2013) In vitro neuronal network activity in NMDA receptor encephalitis. BMC Neurosci 14:17.

Jentsch JD, Roth RH (1999) The neuropsychopharmacology of phencyclidine: from NMDA receptor hypofunction to the dopamine hypothesis of schizophrenia. Neuropsychopharmacology 20:201–225.

Johnston GA (2013) Advantages of an antagonist: bicuculline and other GABA antagonists. Br J Pharmacol 169:328–336.

Jones BE, Tovar KR, Goehring A, Jalali-Yazdi F, Okada NJ, Gouaux E, Westbrook GL (2019) Autoimmune receptor encephalitis in mice induced by active immunization with conformationally stabilized holoreceptors. Sci Transl Med 11:eaaw0044.

Kaufman M, Reinartz S, Ziv NE (2014) Adaptation to prolonged neuromodulation in cortical cultures: an invariable return to network synchrony. BMC Biol 12:83.

Kersten M, Rabbe T, Blome R, Porath K, Sellmann T, Bien CG, Köhling R, Kirschstein T (2019) Novel object recognition in rats with NMDAR dysfunction in CA1 after stereotactic injection of anti-NMDAR encephalitis cerebrospinal fluid. Front Neurol 10:586.

Khawaled R, Bruening-Wright A, Adelman JP, Maylie J (1999) Bicuculline block of small-conductance calcium-activated potassium channels. Pflugers Arch 438:314–321.

Koch H, Niturad CE, Theiss S, Bien CG, Elger C, Wandinger KP, Vincent A, Malter M, Körtvelyessy P, Lerche H, Dihné M (2019) In vitro neuronal network activity as a new functional diagnostic system to detect effects of cerebrospinal fluid from autoimmune encephalitis patients. Sci Rep 9:5591.

Kreye J, Wenke NK, Chayka M, Leubner J, Murugan R, Maier N, Jurek B, Ly LT, Brandl D, Rost BR, Stumpf A, Schulz P, Radbruch H, Hauser AE, Pache F, Meisel A, Harms L, Paul F, Dirnagl U, Garner C, et al. (2016) Human cerebrospinal fluid monoclonal *N*-methyl-D-aspartate receptor autoantibodies are sufficient for encephalitis pathogenesis. Brain 139:2641–2652.

Krystal JH, Karper LP, Seibyl JP, Freeman GK, Delaney R, Bremner JD, Heninger GR, Bowers MB, Charney DS (1994) Subanesthetic effects of the noncompetitive NMDA antagonist, ketamine, in humans: psychotomimetic, perceptual, cognitive, and neuroendocrine responses. Arch Gen Psychiatry 51:199–214.

Lau CG, Murthy VN (2012) Activity-dependent regulation of inhibition via GAD67. J Neurosci 32:8521–8531.

Lois C, Hong EJ, Pease S, Brown EJ, Baltimore D (2002) Germline transmission and tissue-specific expression of transgenes delivered by lentiviral vectors. Science 295:868–872.

Malviya M, Barman S, Golombeck KS, Planagumà J, Mannara F, Strutz-Seebohm N, Wrzos C, Demir F, Baksmeier C, Steckel J, Falk KK, Gross CC, Kovac S, Bönte K, Johnen A, Wandinger KP, Martín-García E, Becker AJ, Elger CE, Klöcker N, et al. (2017) NMDAR encephalitis: passive transfer from man to mouse by a recombinant antibody. Ann Clin Transl Neurol 4:768–783.

Manto M, Dalmau J, Didelot A, Rogemond V, Honnorat J (2010) In vivo effects of antibodies from patients with anti-NMDA receptor encephalitis: further evidence of synaptic glutamatergic dysfunction. Orphanet J Rare Dis 5:31.

Mathew SS, Hablitz JJ (2011) Presynaptic NMDA receptors mediate IPSC potentiation at GABAergic synapses in developing rat neocortex. PLoS One 6:e17311.

Meberg JP ,Miller MW (2003) Culturing hippocampal and cortical neurons. Methods Cell Biol 71:111–127.

Mikasova L, De Rossi P, Bouchet D, Georges F, Rogemond V, Didelot A, Meissirel C, Honnorat J, Groc L (2012) Disrupted surface cross-talk between NMDA and ephrin-B2 receptors in anti-NMDA encephalitis. Brain 135:1606–1621.

Minerbi A, Kahana R, Goldfeld L, Kaufman M, Marom S, Ziv NE (2009) Long-term relationships between synaptic tenacity, synaptic remodeling, and network activity. PLoS Biol 7:e1000136.

Moscato EH, Peng X, Jain A, Parsons TD, Dalmau J, Balice-Gordon RJ (2014) Acute mechanisms underlying antibody effects in anti-*N*-methyl-D-aspartate receptor encephalitis. Ann Neurol 76:108–119.

Nakazawa K, Zsiros V, Jiang Z, Nakao K, Kolata S, Zhang S, Belforte JE (2012) GABAergic interneuron origin of schizophrenia pathophysiology. Neuropharmacology 62:1574–1583.

Nicoll RA (2017) A brief history of long-term potentiation. Neuron 93:281–290.

Pafundo DE, Miyamae T, Lewis DA, Gonzalez-Burgos G (2018) Presynaptic effects of *N*-methyl-D-aspartate receptors enhance parvalbumin cell–mediated inhibition of pyramidal cells in mouse prefrontal cortex. Biol Psychiatry 84:460–470.

Pafundo DE, Pretell Annan CA, Fulginiti NM, Belforte JE (2021) Early NMDA receptor ablation in interneurons causes an activity-dependent E/I imbalance in vivo in prefrontal cortex pyramidal neurons of a mouse model useful for the study of schizophrenia. Schizophr Bull 47:1300–1309.

Planagumà J, Leypoldt F, Mannara F, Gutiérrez-Cuesta J, Martín-García E, Aguilar E, Titulaer MJ, Petit-Pedrol M, Jain A, Balice-Gordon R, Lakadamyali M, Graus F, Maldonado R, Dalmau J (2015) Human *N*-methyl-D-aspartate receptor antibodies alter memory and behaviour in mice. Brain 138:94–109.

Planagumà J, Haselmann H, Mannara F, Petit-Pedrol M, Grünewald B, Aguilar E, Röpke L, Martín-García E, Titulaer MJ, Jercog P, Graus F, Maldonado R, Geis C, Dalmau J (2016) Ephrin-B2 prevents *N*-methyl-D-aspartate receptor antibody effects on memory and neuroplasticity. Ann Neurol 80:388–400.

Spiegel I, Mardinly AR, Gabel HW, Bazinet JE, Couch CH, Tzeng CP, Harmin DA, Greenberg ME (2014) Npas4 regulates excitatory-inhibitory balance within neural circuits through cell-type-specific gene programs. Cell 157:1216–1229.

Tamamaki N, Yanagawa Y, Tomioka R, Miyazaki J-I, Obata K, Kaneko T (2003) Green fluorescent protein expression and colocalization with calretinin, parvalbumin, and somatostatin in the GAD67-GFP knock-in mouse. J Comp Neurol 467:60–79.

Taraschenko O, Fox HS, Pittock SJ, Zekeridou A, Gafurova M, Eldridge E, Liu J, Dravid SM, Dingledine R (2019) A mouse model of seizures in anti-*N*-methyl-D-aspartate receptor encephalitis. Epilepsia 60:452–463.

Teppola H, Okujeni S, Linne ML, Egert U (2018) AMPA, NMDA and GABAA receptor mediated network burst dynamics in cortical cultures in vitro. arXiv:1802.00217.

Teppola H, Aćimović J, Linne ML (2019) Unique features of network bursts emerge from the complex interplay of excitatory and inhibitory receptors in rat neocortical networks. Front Cell Neurosci 13:377.

Titulaer MJ, McCracken L, Gabilondo I, Armangué T, Glaser C, Iizuka T, Honig LS, Benseler SM, Kawachi I, Martinez-Hernandez E, Aguilar E, Gresa-Arribas N, Ryan-Florance N, Torrents A, Saiz A, Rosenfeld MR, Balice-Gordon R, Graus F, Dalmau J (2013) Treatment and prognostic

factors for long-term outcome in patients with anti-NMDA receptor encephalitis: an observational cohort study. Lancet Neurol 12:157–165.

Uhlhaas PJ, Singer W (2010) Abnormal neural oscillations and synchrony in schizophrenia. Nat Rev Neurosci 11:100–113.

Wagner F, Goertzen A, Kiraly O, Laube G, Kreye J, Witte OW, Prüss H, Veh RW (2020) Detailed morphological analysis of rat hippocampi treated with CSF autoantibodies from patients with anti-NMDAR encephalitis discloses two distinct types of immunostaining patterns. Brain Res 1747:147033.

Wagnon I, Hélie P, Bardou I, Regnauld C, Lesec L, Leprince J, Naveau M, Delaunay B, Toutirais O, Lemauff B, Etard O, Vivien D, Agin V, Macrez R, Maubert E, Docagne F (2020) Autoimmune encephalitis mediated by B-cell response against *N*-methyl-D-aspartate receptor. Brain 143:2957–2972.

Wardemann H, Yurasov S, Schaefer A, Young JW, Meffre E, Nussenzweig MC (2003) Predominant autoantibody production by early human B cell precursors. Science 301:1374–1377.

Wright S, Hashemi K, Stasiak L, Bartram J, Lang B, Vincent A, Upton AL (2015) Epileptogenic effects of NMDAR antibodies in a passive transfer mouse model. Brain 138:3159–3167.

Würdemann T, Kersten M, Tokay T, Guli X, Kober M, Rohde M, Porath K, Sellmann T, Bien CG, Köhling R, Kirschstein T (2016) Stereotactic injection of cerebrospinal fluid from anti-NMDA receptor encephalitis into rat dentate gyrus impairs NMDA receptor function. Brain Res 1633:10–18.

Zhang Q, Tanaka K, Sun P, Nakata M, Yamamoto R, Sakimura K, Matsui M, Kato N (2012) Suppression of synaptic plasticity by cerebrospinal fluid from anti-NMDA receptor encephalitis patients. Neurobiol Dis 45:610–615.

Zhang YMM, Behrens JE Lisman (2008) Prolonged exposure to NMDAR antagonist suppresses inhibitory synaptic transmission in prefrontal cortex. J Neurophysiol 100:959–965.

Excerpt from Journal Summary List (ISI Web of Knowledge) - 2

Journal Data Filtered By: **Selected JCR Year: 2016** Selected Editions: SCIE,SSCI
Selected Categories: **"NEUROSCIENCES"** Selected Category Scheme: WoS
Gesamtanzahl: 258 Journale

Rank	Full Journal Title	Total Cites	Journal Impact Factor	Eigenfactor Score
1	NATURE REVIEWS NEUROSCIENCE	36,952	28.880	0.071380
2	NATURE NEUROSCIENCE	54,399	17.839	0.160740
3	Annual Review of Neuroscience	13,211	15.630	0.020660
4	TRENDS IN COGNITIVE SCIENCES	23,273	15.402	0.046360
5	BEHAVIORAL AND BRAIN SCIENCES	8,195	14.200	0.010940
6	NEURON	82,253	14.024	0.227070
7	PROGRESS IN NEUROBIOLOGY	12,163	13.217	0.018020
8	MOLECULAR PSYCHIATRY	17,452	13.204	0.049670
9	ACTA NEUROPATHOLOGICA	16,462	12.213	0.037060
10	BIOLOGICAL PSYCHIATRY	41,859	11.412	0.067400
11	TRENDS IN NEUROSCIENCES	19,178	11.124	0.029690
12	JOURNAL OF PINEAL RESEARCH	7,278	10.391	0.008040
13	BRAIN	48,061	10.292	0.077590
14	ANNALS OF NEUROLOGY	34,215	9.890	0.057310
15	FRONTIERS IN NEUROENDOCRINOLOGY	3,516	9.425	0.006600
16	SLEEP MEDICINE REVIEWS	4,980	8.958	0.009730
17	NEUROSCIENCE AND BIOBEHAVIORAL REVIEWS	20,452	8.299	0.047230
18	NEUROSCIENTIST	4,325	7.391	0.009890
19	Molecular Neurodegeneration	2,946	6.780	0.009540
20	CEREBRAL CORTEX	27,496	6.559	0.063240
21	NEUROPSYCHOPHARMACOLOGY	23,920	6.403	0.046670
22	NEUROPSYCHOLOGY REVIEW	2,478	6.352	0.004650
23	GLIA	12,781	6.200	0.021920
24	Alzheimers Research & Therapy	1,699	6.196	0.007180
25	MOLECULAR NEUROBIOLOGY	7,338	6.190	0.017440
26	NEUROSIGNALS	653	6.143	0.000670
27	CURRENT OPINION IN NEUROBIOLOGY	13,188	6.133	0.036730
28	Brain Stimulation	3,905	6.078	0.013020
29	JOURNAL OF NEUROSCIENCE	171,800	5.988	0.319910
30	BRAIN BEHAVIOR AND IMMUNITY	10,719	5.964	0.026460
31	NEUROIMAGE	85,630	5.835	0.173210
32	PAIN	35,333	5.445	0.044460
33	NEUROPATHOLOGY AND APPLIED NEUROBIOLOGY	3,413	5.347	0.006400
34	NEURAL NETWORKS	8,741	5.287	0.010250
35	BRAIN PATHOLOGY	4,580	5.272	0.008450
36	JOURNAL OF NEUROTRAUMA	12,787	5.190	0.021640
37	Neurotherapeutics	3,451	5.166	0.008220
38	JOURNAL OF PSYCHIATRY & NEUROSCIENCE	2,759	5.165	0.004970
39	NEUROBIOLOGY OF AGING	20,010	5.117	0.046250

Publication 2

Wenke, N.K., Kreye, J., **Andrzejak, E.**, van Casteren, A., Leubner, J., Murgueitio, M.S., Reincke, S.M., Secker, C., Schmidl, L., Geis, C., Ackermann, F., Nikolaus, M., Garner, C.C., Wardemann, H., Wolber, G. and Prüss, H., 2019. N-methyl-D-aspartate receptor dysfunction by unmutated human antibodies against the NR1 subunit. Annals of neurology, 85(5), pp.771-776.

Check for updates

N-Methyl-D-Aspartate Receptor Dysfunction by Unmutated Human Antibodies Against the NR1 Subunit

Nina Kerstin Wenke,[1,2]* Jakob Kreye,[1,2]* Ewa Andrzejak,[1] Adriana van Casteren,[1] Jonas Leubner,[1,2] Manuela S. Murgueitio,[3] S. Momsen Reincke,[1,2] Christopher Secker,[1,2] Lars Schmidl,[4] Christian Geis,[4] Frauke Ackermann,[1] Marc Nikolaus,[5] Craig C. Garner,[1] Hedda Wardemann,[6] Gerhard Wolber,[3] and Harald Prüss, MD[1,2]

Anti–N-methyl-D-aspartate receptor (NMDAR) encephalitis is the most common autoimmune encephalitis related to autoantibody-mediated synaptic dysfunction. Cerebrospinal fluid–derived human monoclonal NR1 autoantibodies showed low numbers of somatic hypermutations or were unmutated. These unexpected germline-configured antibodies showed weaker binding to the NMDAR than matured antibodies from the same patient. In primary hippocampal neurons, germline NR1 autoantibodies strongly and specifically reduced total and synaptic NMDAR currents in a dose- and time-dependent manner. The findings suggest that functional NMDAR antibodies are part of the human naïve B cell repertoire. Given their effects on synaptic function, they might contribute to a broad spectrum of neuropsychiatric symptoms.

ANN NEUROL 2019;85:771–776

Autoantibodies against the aminoterminal domain (ATD) of the NR1 subunit of the N-methyl-D-aspartate (NMDA) receptor (NMDAR) are the hallmark of NMDAR encephalitis, the most common autoimmune encephalitis presenting with psychosis, epileptic seizures, amnesia, and autonomic instability.[1] The disease can be triggered by NMDAR-expressing teratomas[2] and occur secondarily to viral encephalitis;[3,4] however, in most cases, the initiating events remain unclear. Intracerebroventricular injection of cerebrospinal fluid (CSF), as well as a single recombinant monoclonal NR1 immunoglobulin G1 (IgG1) antibody obtained from clonally expanded intrathecal plasma cells of a patient with NMDAR encephalitis into mice, led to transient behavioral changes compatible with human disease symptoms.[5,6]

We could recently generate a panel of human monoclonal NMDAR autoantibodies from antibody-secreting cells in CSF of patients with NMDAR encephalitis.[7] Unexpectedly, several NR1-reactive autoantibodies from different patients were unmutated, suggesting that they had not been selected for high affinity during germinal center reactions and instead were derived from activated naïve B cells. We therefore determined whether these germline NR1 antibodies showed functional effects similar to affinity-matured NR1 autoantibodies leading to synaptic dysfunction.

Materials and Methods

Recombinant Monoclonal NMDAR Antibodies

Recombinant monoclonal human NR1 IgG autoantibodies were generated as described.[7,8] The study was approved by the Charité University hospital Review Board, and informed consent was obtained from each subject. The control antibody (mGo53) is a nonreactive isotype-matched human antibody.[9] Immunostaining, using primary hippocampal neurons, unfixed mouse brain sections, HEK cell-expressed NR1 N368Q mutants, and brain sections after intravenous antibody injection, followed our established protocols.[7] We generated germline counterpart versions from maturated monoclonal NR1 antibodies with best matching variable V(D)J genes and elimination of somatic hypermutations.[10] Relative affinity curves were calculated based on concentration-dependent antibody binding to hippocampal sections, adapted from previous work using HEK cells transfected with the NR1 subunit.[11] For bilateral intracerebroventricular injection, 200 μg of antibodies were infused over 14 days using osmotic minipumps.[12]

Super-Resolution Imaging

Direct stochastic reconstruction microscopy (dSTORM) was performed in primary hippocampal neurons (DIV 14) as described.[12]

From the [1]German Center for Neurodegenerative Diseases (DZNE) Berlin, Germany; [2]Department of Neurology and Experimental Neurology, Charité–Universitätsmedizin Berlin, Berlin, Germany; [3]Freie Universität Berlin, Institute of Pharmacy, Berlin, Germany; [4]Hans-Berger Department of Neurology, University Hospital Jena, Jena, Germany; [5]Department of Pediatric Neurology, Charité–Universitätsmedizin Berlin, Berlin, Germany; and [6]German Cancer Research Center, B Cell Immunology, Heidelberg, Germany

Address correspondence to Dr Harald Prüss, German Center for Neurodegenerative Diseases (DZNE) Berlin, Charité–Universitätsmedizin Berlin, CharitéCrossOver (CCO), R 4-334, Charitéplatz 1, 10117 Berlin, Germany. E-mail: harald.pruess@charite.de

Received Apr 11, 2018, and in revised form Feb 26, 2019. Accepted for publication Mar 3, 2019.

View this article online at wileyonlinelibrary.com. DOI: 10.1002/ana.25460.

*These authors contributed equally to the work.

© 2019 The Authors. *Annals of Neurology* published by Wiley Periodicals, Inc. on behalf of American Neurological Association.
This is an open access article under the terms of the Creative Commons Attribution-NonCommercial License, which permits use, distribution and reproduction in any medium, provided the original work is properly cited and is not used for commercial purposes.

Human NR1 autoantibody (clone #003-109; 4 μg/ml) and polyclonal guinea pig anti-Homer-1 (1:300; Synaptic Systems GmbH, Goettingen, Germany) were used as primary antibodies followed by AlexaFluor-647 goat/anti-human (1:200; Life Technologies, Carlsbad, CA) and CF-568 donkey/anti–guinea pig (1:200; Biotium, Fremont, CA) as secondary antibodies.

Electrophysiological Recordings

Autaptic murine hippocampal neurons (DIV 14-17) were incubated with 1 or 5 μg/ml human NR1 (#003-109) or control antibody at 37°C for 3 or 24 hours. Data were acquired as described.[13] Cells were recorded in standard intra- and extracellular solutions, except for chemically induced NMDA responses, measured in extracellular solution containing 0 mM of Mg^{2+}, 0.2 mM of $CaCl_2$, and 10 μM of glycine, and evoked NMDA responses, measured in extracellular solution containing 0 mM of Mg^{2+}, 2 mM of $CaCl_2$, 10 μM of glycine, and 10 μM of NBQX (Tocris Bioscience, Bristol, UK). For kinetics of synaptic NMDA responses, non-silent traces from each cell were averaged and rise time and decay time constant (τ) measured from 10% to 90% or 90% to 10% of the peak, respectively. Decays were fitted with a double exponential and decay time constants for each of the fits converted to a weighted decay.

Homology Modeling

The homology model of the ATD of the human NMDA receptor was generated using the crystal structure of the rat NMDA receptor subunit, zeta-1. The homology modeling application of MOE 2014.09 ("Molecular Operating Environment [MOE], 2014.09", 2015) was used with 10 main chain models, each with one side chain. Samples were built using the amber12 force field.[14]

Results

Germline NR1 Autoantibodies Target the NMDAR in vitro and in vivo

The CSF autoantibody repertoire in NMDAR encephalitis contains NR1-binding and non-NR1-binding antibodies.[7] Across all 8 patients, NR1-binding antibodies had significantly lower numbers of somatic hypermutations (SHM) in the Ig heavy (5.1 ± 4.0 versus 11.9 ± 8.3) and corresponding Ig light chains (3.9 ± 4.8 versus 7.2 ± 5.4)

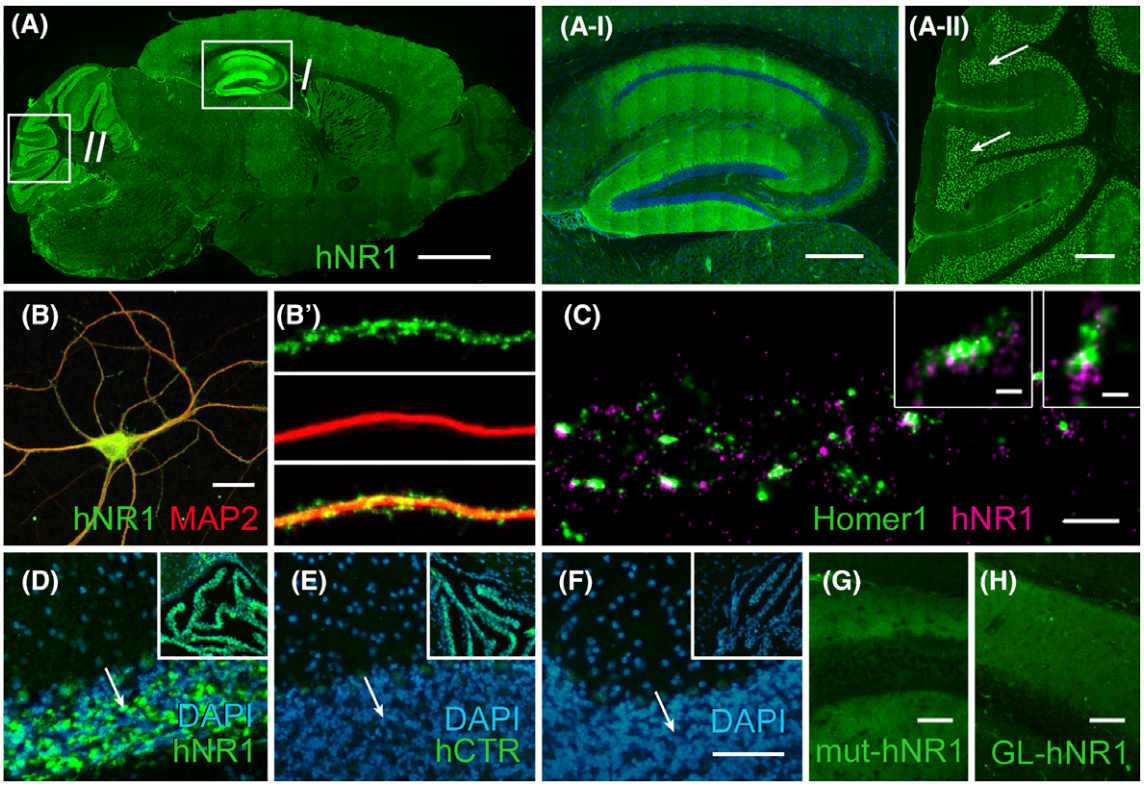

FIGURE 1: Target specificity of the germline NR1 autoantibody #003-109. Immunofluorescence staining showed the characteristic NR1 pattern in the brain (A), in particular of hippocampal neuropil (A-I) and cerebellar granule cells (A-II, arrows). NMDAR-expressing synaptic clusters were specifically labeled on primary hippocampal neurons (B; green: NR1, red: MAP2). dSTORM imaging confirmed NR1 expression in the synapse (C; purple: NR1, green: Homer1). Germline NR1 antibodies (D), but not isotype control antibodies (E), bound to cerebellar granule cells (arrows) 24 hours after intravenous injection together with lipopolysaccharide. Antibodies were present in the circulation as confirmed with stainings of the choroid plexus (D,E, inserts), in contrast to control brains of untreated mice (F). Intracerebroventricular injection of maturated (G) and germline (H) NR1 antibodies showed similar neuropil binding in the hippocampus. Scale bars: A = 2 mm; A-I/A-II = 500 μm; B = 20 μm; C = 1 μm (inserts: 200 nm); F = 100 μm (for D–F); G,H = 100 μm. DAPI = 4′,6-diamidino-2-phenylindole; MAP2, microtubule-associated protein 2; NMDAR = N-methyl-D-aspartate receptor.

15318249, 2019, 5, Downloaded from https://onlinelibrary.wiley.com/doi/10.1002/ana.25460 by Charité - Universitaetsmedizin, Wiley Online Library on [13/09/2023]. See the Terms and Conditions (https://onlinelibrary.wiley.com/terms-and-conditions) on Wiley Online Library for rules of use; OA articles are governed by the applicable Creative Commons License

than non-NR1-binding antibodies (total, 9.0 ± 7.9 versus 19.1 ± 12.6 mean ± SD; p = 0.018, unpaired t test). Individual NR1 antibodies were even completely unmutated (#003-109) or contained only silent SHM (#007-142, #007-169).[7]

The germline antibody, #003-109, accounted for 1 of 41 (2.4%) of antibody-secreting cells analyzed of this patient and showed the characteristic NR1 pattern on unfixed mouse brain sections (Fig 1A) and the NMDAR cluster distribution on primary hippocampal mouse neurons previously observed for mutated NR1 antibodies[7] (Fig 1B). dSTORM of hippocampal neurons demonstrated NMDAR distribution at synapses, opposed to Homer1-positive postsynaptic densities (Fig C). Intravenous injection of #003-109 resulted in binding to cerebellar granule cells *in vivo* (Fig 1D), which was not detectable with the isotype control (Fig 1E). Intracerebroventricular injection of maturated (Fig 1G) and germline (Fig 1H) NR1 antibodies showed similar neuropil binding in the hippocampus.

Binding of Mutated, Germline, and Reverted Antibodies to NR1

Binding of #003-109 was prevented by the single-amino-acid mutation, N368Q, in the ATD of NR1 (Fig 2A,B).[7] To model the possible antibody/ATD interaction *in silico*, protein-protein docking was performed against ATD using ClusPro (Fig 2C). ATD residues N368 and G369 are

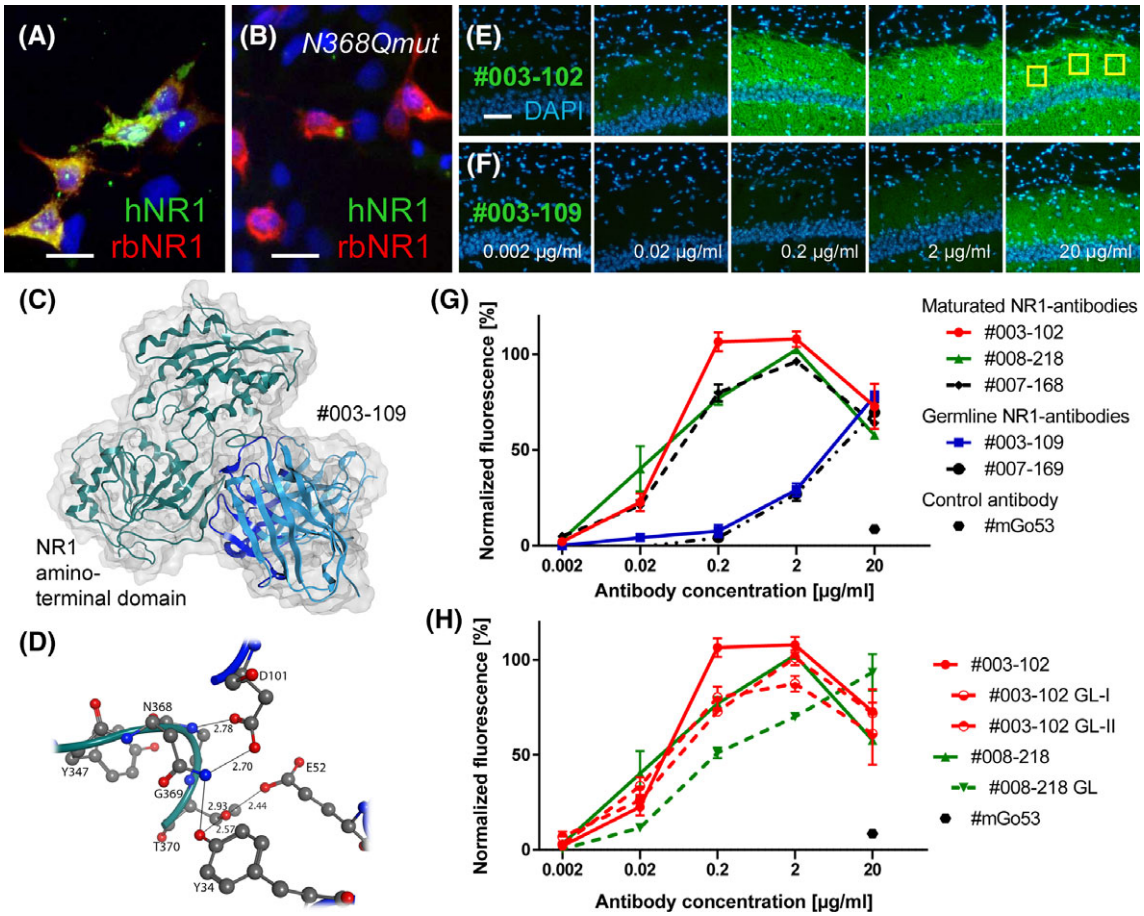

FIGURE 2: Interactions between germline antibodies and the NMDAR. Germline antibodies strongly bound to NR1 protein in transiently transfected HEK cells (A). In contrast, NR1 N368Q mutation completely omitted human antibody binding (B). Predicted binding pose of antibody #003-109 (blue, with complementarity determining regions in dark blue) to the ATD (green), the 3D model of the antibody, was generated by the antibody modeling tool of MOE2014.09 (C). Interaction of the key residues N368 and G369 in the H-bond network is illustrated in ball and stick mode; interactions are shown as black lines with the molecule distance in Å (D). Binding strengths with increasing concentrations of NR1 antibodies were determined by fluorescence intensities of hippocampal brain sections, exemplarily shown for a mutated (E) and germline antibody (F). Plotting these binding strengths against antibody concentrations showed the range of relative affinity curves of monoclonal patient-derived NR1 autoantibodies with weaker binding of the germline antibodies (G). "Back-mutation" of the high-affinity NR1 antibodies to germline configuration (*GL* = germline; two possible germline antibodies for #003-102) showed only minimal reduction of the binding strengths (H). Data are mean ± SEM, n = 3 independent stainings (G,H) each representing the mean of three hippocampal areas (yellow rectangles in E) per antibody/concentration. Scale bars: A,B = 20 µm; E = 100 µm (for E,F). DAPI = 4′,6-diamidino-2-phenylindole; hNR1/rbNR1 = human/rabbit NR1 antibody; NMDAR = N-methyl-D-aspartate receptor.

15318249, 2019, 5, Downloaded from https://onlinelibrary.wiley.com/doi/10.1002/ana.25460 by Charité - Universitaetsmedizin, Wiley Online Library on [13/09/2023]. See the Terms and Conditions (https://onlinelibrary.wiley.com/terms-and-conditions) on Wiley Online Library for rules of use; OA articles are governed by the applicable Creative Commons License

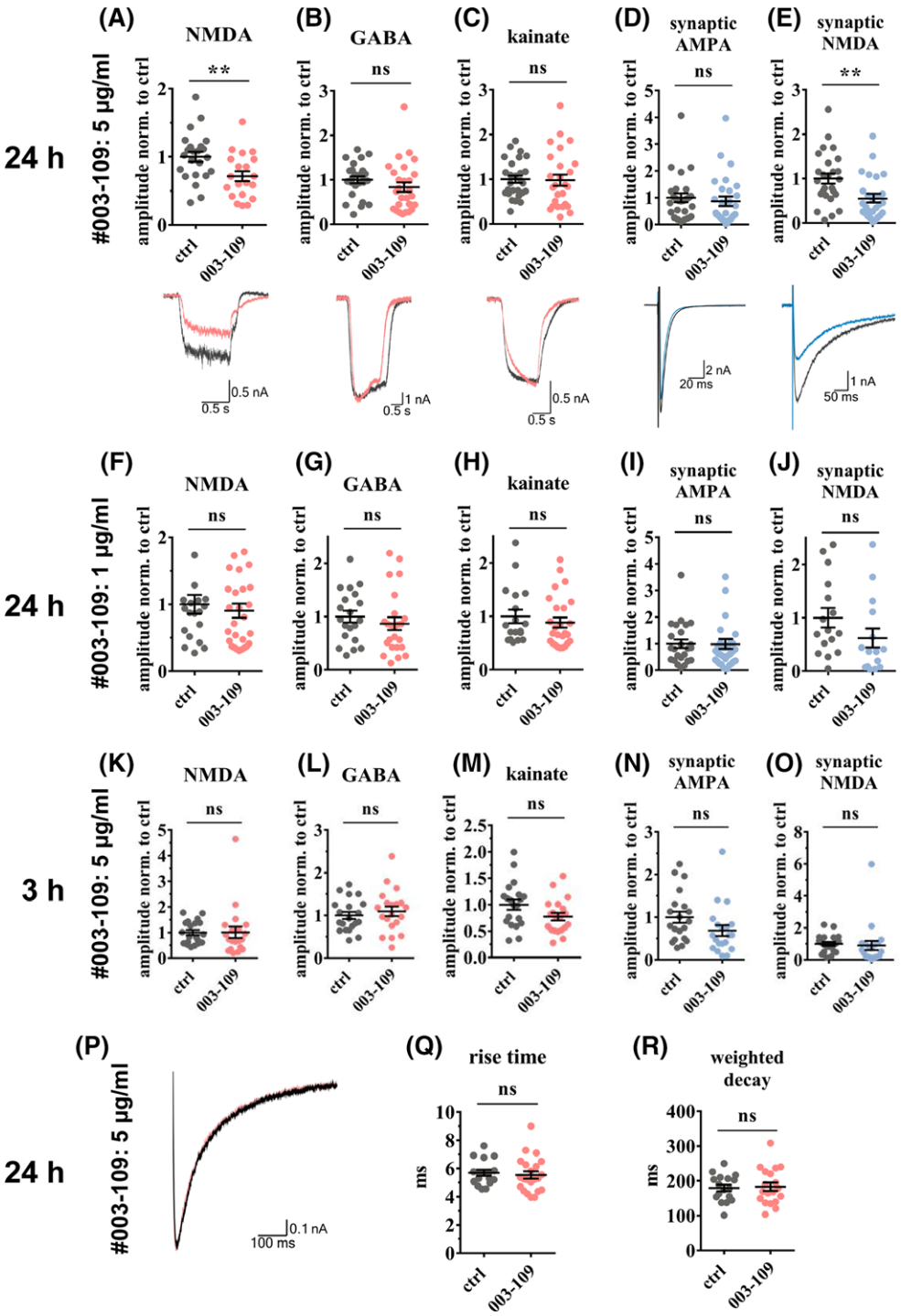

FIGURE 3: Germline antibody #003-109 reduced total and synaptic NMDA currents. Patch clamp whole-cell recordings of autaptic murine neuronal cultures showed that 24 hours of incubation with antibody #003-109 (5 µg/ml) selectively reduced total NMDA currents by 30% (A, $p = 0.009$), but not GABA or kainate currents (B,C), which were evoked by a 1-second bath application of 10 µM of NMDA (A), 5 µM of GABA (B), or 20 µM of kainate (C), respectively. Synaptic NMDA currents, evoked in the presence of 10 µM of glycine, 10 µM of NBQX, and $0Mg^{2+}$, showed 45% reduction (E, $p = 0.003$) whereas synaptic AMPA currents remained unchanged (D). The selective effect on NMDA currents was abolished at lower concentrations of antibody #003-109 (1 µg/ml; F–J). Total GABA and kainate and synaptic AMPA currents were not affected (G–I), while a trend toward reduced synaptic NMDA currents persisted at this antibody concentration (J, $p = 0.152$). Established concentrations of antibody #003-109 (5 µg/ml), but shorter incubation of 3 hours, were not sufficient to cause reduced NMDA currents (K–O). Averaged traces of exemplary cells incubated for 24 hours with germline and control antibodies (5 µg/ml) were scaled to 1 nA for easier comparison (P) and showed equal rise time (Q) and weighted decay (R) of synaptic NMDA currents. Data are mean ± SEM, Student's *t* test, n = 20 to 28 (A–E), n = 15 to 32 (F–J), or n = 20 (K–O) cells per group from four independent experiments. AMPA = alpha-amino propionic acid; ctrl = control; GABA = gamma-aminobutyric acid; NMDA = N-methyl-D-aspartate; ns = not significant.

15318249, 2019, 5, Downloaded from https://onlinelibrary.wiley.com/doi/10.1002/ana.25460 by Charité - Universitaetsmedizin, Wiley Online Library on [13/09/2023]. See the Terms and Conditions (https://onlinelibrary.wiley.com/terms-and-conditions) on Wiley Online Library for rules of use; OA articles are governed by the applicable Creative Commons License

embedded in the protein-protein interface forming a network of H-bonds with the antibody residues (Fig 2D). N368 is the only amino acid on the receptor side that stabilizes the binding to both, the antibody heavy and the light chains (Fig 2D). Binding curves of patient-derived germline NR1 antibodies showed generally lower relative affinity to hippocampal sections than mutated antibodies (Fig 2E–G). However, reverting mutated patient antibodies to germline changed the binding strengths only minimally, suggesting a similar functional role already of the naïve antibodies (Fig 2H).

Unmutated NR1 Antibodies Selectively Reduced Total and Synaptic NMDAR Currents

We expected smaller electrophysiological changes induced by antibody #003-109 compared to mutated NR1 antibodies, given the lower binding to murine brain (Fig 2E,F). Indeed, incubation of autaptic mouse hippocampal neurons with 5 μg/ml of germline antibody #003-109 for 24 hours resulted in ~30% reduction of the total NMDA currents compared to the isotype control antibody (Fig 3A). The antibody effect was specific, given that the total gamma-aminobutyric acid (GABA)- and kainate-mediated currents remained unaffected after application of 5 μM of GABA or 20 μM of kainate, respectively (Fig 3B,C). Measuring synaptic responses in the presence of 10 μM of glycine,10 μM of NBQX, and 0 mM of Mg^{2+}, NR1 antibody treatment also reduced synaptic NMDA currents by ~45%, while synaptic alpha-amino propionic acid (AMPA) currents did not differ from controls (Fig 3D,E). In contrast to higher-affinity mutated NR1 antibodies,[7] the effects were not detectable with lower antibody concentrations (1 μg/ml of #003-109; Fig 3F–J). In addition, shorter incubation for 3 hours with germline antibody was not sufficient to reduce synaptic or whole-cell NMDA currents (Fig 3K–O). The kinetics of synaptic NMDA responses were not altered by NR1 antibody treatment (Fig 3P–R).

Discussion

The present study followed the unexpected observation that human NR1 autoantibodies have low numbers of somatic hypermutations and that even germline-encoded, unmutated NR1 autoantibodies are found in patients with NMDAR encephalitis. Patient-derived germline antibodies had lower binding compared to mutated NR1 antibodies, but were also functional in selectively reducing synaptic NMDAR currents in a dose- and time-dependent manner. They should be present in the patient's CSF as clone #003-109 derived from a CSF plasma cell, which is believed to continuously produce several thousand IgG molecules per second.[15,16]

The finding of germline-configured functional NMDAR autoantibodies in the human repertoire might explain the mysterious observation of the high frequency of serum NMDAR antibodies in different diseases and blood donors.[17] Generally, B cells carrying high-affinity autoreactive antibodies undergo negative selection, while low-affinity antibodies might remain in the repertoire.[18] Thus, the here identified NR1 autoantibodies likely did not see their antigen during B cell development, or were of sufficiently low affinity to remain part of the naïve B cell repertoire,[19] and might therefore be present in every individual. The important role of naïve B cells in NMDAR encephalitis was recently suggested, although the experimental approach did not allow information on antibody mutations.[20] Likewise, autoreactive naïve B cells were recently observed in a related antibody-mediated disease, neuromyelitis optica.[21] It is still an open question how NMDAR-expressing tumors that might contain germinal center-like structures,[2,20,22,23] viral brain infections,[3,4] or additional factors lead to the maturation and expansion of NR1 antibody-producing cells in relatively rare cases, ultimately resulting in NMDAR encephalitis. In ovarian teratomas, tumor-intrinsic abnormalities, such as organized dysplastic neurons, may facilitate the development of NMDAR autoimmunity.[22] No clear distinction between the here examined germline and mutated antibodies was noted in patients without a tumor (#007, #008) compared to a patient with an ovarian carcinoma (#003).

Distinct unmutated ("naturally occurring") autoantibodies are innate-like components of the immune system that facilitate the clearance of invading pathogens, induce apoptosis in cancer cells, promote remyelination, or delay disease progression in murine models of inflammation and neurodegeneration.[24–26] May unmutated NMDAR autoantibodies have been similarly selected because of evolutionary importance (eg, for neutralization of released NMDAR protein), thereby preventing dysfunctional immune stimulation? Indeed, preexisting NMDAR antibodies were associated with smaller lesion size after stroke in one study, possibly related to reduction of glutamate-mediated excitotoxicity.[27] Also, there are examples of other germline antibodies that are reactive to commensal bacteria at mucosal barriers, but at the expense of pathogenic reactivity to self-proteins.[28]

Future studies should examine antibody effects beyond receptor internalization[29] and clarify under which conditions NR1 (and potentially further) autoantibody-producing cells escape negative selection and expand to cause encephalitis. They should also address whether and at which concentrations functional NMDAR autoantibodies are part of the healthy human naïve B cell repertoire and

15318249, 2019, 5, Downloaded from https://onlinelibrary.wiley.com/doi/10.1002/ana.25460 by Charité - Universitaetsmedizin, Wiley Online Library on [13/09/2023]. See the Terms and Conditions (https://onlinelibrary.wiley.com/terms-and-conditions) on Wiley Online Library for rules of use; OA articles are governed by the applicable Creative Commons License

may thus contribute to a broader spectrum of neuropsychiatric symptoms than previously assumed.

Acknowledgment

This study has been supported by grants from the German Research Foundation (DFG; to H.P.: PR 1274; 2-1, to C.G.: CRC/TRR166, TP B02), Focus Area DynAge (Freie Universität Berlin and Charité–Universitätsmedizin Berlin, to H.P. and G.W.).

Author Contributions

N.K.W., J.K., H.W., G.W., and H.P. contributed to the conception and design of the study. N.K.W., J.K., E.A., A.v.C., J.L., M.S.M., S.M.R., C.S., L.S., C.G., F.A., M.N., C.C.G., H.W., G.W., and H.P. contributed to the acquisition and analysis of data. N.K.W., J.K., E.A., A.v.C., M.S.M., S.M.R., L.S., C.G., H.W., G.W., and H.P. contributed to drafting the text and preparing the figures.

Potential Conflicts of Interest

Nothing to report.

References

1. Dalmau J, Gleichman, AJ, Hughes EG, et al. Anti-NMDA-receptor encephalitis: case series and analysis of the effects of antibodies. Lancet Neurol 2008;7:1091–1098.
2. Titulaer MJ, McCracken L, Gabilondo I, et al. Treatment and prognostic factors for long-term outcome in patients with anti-NMDA receptor encephalitis: an observational cohort study. Lancet Neurol 2013;12:157–165.
3. Armangue T, Leypoldt F, Malaga I, et al. Herpes simplex virus encephalitis is a trigger of brain autoimmunity. Ann Neurol 2014;75: 317–323.
4. Prüss H, Finke C, Höltje M, et al. N-methyl-D-aspartate receptor antibodies in herpes simplex encephalitis. Ann Neurol 2012;72:902–911.
5. Malviya M, Barman S, Golombeck KS, et al. NMDAR encephalitis: passive transfer from man to mouse by a recombinant antibody. Ann Clin Transl Neurol 2017;4:768–783.
6. Planaguma J, Leypoldt F, Mannara F, et al. Human N-methyl D-aspartate receptor antibodies alter memory and behaviour in mice. Brain 2015;138:94–109.
7. Kreye J, Wenke NK, Chayka M, et al. Human cerebrospinal fluid monoclonal N-methyl-D-aspartate receptor autoantibodies are sufficient for encephalitis pathogenesis. Brain 2016;139:2641–2652.
8. Tiller T, Meffre E, Yurasov S, et al. Efficient generation of monoclonal antibodies from single human B cells by single cell RT-PCR and expression vector cloning. J Immunol Methods 2008;329:112–124.
9. Wardemann H, Yurasov S, Schaefer A, et al. Predominant autoantibody production by early human B cell precursors. Science 2003; 301:1374–1377.
10. Murugan R, Buchauer L, Triller G, et al. Clonal selection drives protective memory B cell responses in controlled human malaria infection. Sci Immunol 2018;3:eaap8029.
11. Ly LT, Kreye J, Jurek B, et al. Affinities of human NMDA receptor autoantibodies: implications for disease mechanisms and clinical diagnostics. J Neurol 2018;265:2625–2632.
12. Werner C, Pauli M, Doose S, et al. Human autoantibodies to amphiphysin induce defective presynaptic vesicle dynamics and composition. Brain 2016;139:365–379.
13. Zimmermann J, Herman MA, Rosenmund C. Co-release of glutamate and GABA from single vesicles in GABAergic neurons exogenously expressing VGLUT3. Front Synaptic Neurosci 2015;7:16.
14. Case DA, Darden TA, Cheatham TE, et al. *AMBER 12*. San Francisco, CA: University of California; 2012.
15. Helmreich E, Kern M, Eisen HN. The secretion of antibody by isolated lymph node cells. J Biol Chem 1961;236:464–473.
16. Hibi T, Dosch HM. Limiting dilution analysis of the B cell compartment in human bone marrow. Eur J Immunol 1986;16:139–145.
17. Dahm L, Ott C, Steiner J, et al. Seroprevalence of autoantibodies against brain antigens in health and disease. Ann Neurol 2014;76: 82–94.
18. Melchers F. Checkpoints that control B cell development. J Clin Invest 2015;125:2203–2210.
19. Meffre E, Wardemann H. B-cell tolerance checkpoints in health and autoimmunity. Curr Opin Immunol 2008;20:632–638.
20. Makuch M, Wilson R, Al-Diwani A, et al. N-methyl-D-aspartate receptor antibody production from germinal center reactions: therapeutic implications. Ann Neurol 2018;83:553–561.
21. Wilson R, Makuch M, Kienzler AK, et al. Condition-dependent generation of aquaporin-4 antibodies from circulating B cells in neuromyelitis optica. Brain 2018;141:1063–1074.
22. Day GS, Laiq S, Tang-Wai DF, Munoz DG. Abnormal neurons in teratomas in NMDAR encephalitis. JAMA Neurol 2014;71:717–724.
23. Dabner M, McCluggage WG, Bundell C, et al. Ovarian teratoma associated with anti-N-methyl D-aspartate receptor encephalitis: a report of 5 cases documenting prominent intratumoral lymphoid infiltrates. Int J Gynecol Pathol 2012;31:429–437.
24. Xu X, Denic A, Jordan LR, et al. A natural human IgM that binds to gangliosides is therapeutic in murine models of amyotrophic lateral sclerosis. Dis Model Mech 2015;8:831–842.
25. Wootla B, Watzlawik JO, Warrington AE, et al. Naturally occurring monoclonal antibodies and their therapeutic potential for neurologic diseases. JAMA Neurol 2015;72:1346–1353.
26. Rodriguez M, Lennon VA, Benveniste EN, Merrill JE. Remyelination by oligodendrocytes stimulated by antiserum to spinal cord. J Neuropathol Exp Neurol 1987;46:84–95.
27. Zerche M, Weissenborn K, Ott C, et al. Preexisting serum autoantibodies against the NMDAR subunit NR1 modulate evolution of lesion size in acute ischemic stroke. Stroke 2015;46:1180–1186.
28. Schickel JN, Glauzy S, Ng YS, et al. Self-reactive VH4-34-expressing IgG B cells recognize commensal bacteria. J Exp Med 2017;214: 1991–2003.
29. Gleichman AJ, Spruce LA, Dalmau J, et al. Anti-NMDA receptor encephalitis antibody binding is dependent on amino acid identity of a small region within the GluN1 amino terminal domain. J Neurosci 2012;32:11082–11094.

15318249, 2019, 5, Downloaded from https://onlinelibrary.wiley.com/doi/10.1002/ana.25460 by Charité - Universitaetsmedizin, Wiley Online Library on [13/09/2023]. See the Terms and Conditions (https://onlinelibrary.wiley.com/terms-and-conditions) on Wiley Online Library for rules of use; OA articles are governed by the applicable Creative Commons License

Curriculum vitae

My curriculum vitae does not appear in the electronic version of my paper
for the reasons of data protection

My curriculum vitae does not appear in the electronic version of my paper
for the reasons of data protection

My curriculum vitae does not appear in the electronic version of my paper
for the reasons of data protection

Publication List

Andrzejak, E., Rabinovitch, E., Kreye, J., Prüss, H., Rosenmund, C., Ziv, N.E., Garner, C.C. and Ackermann, F., 2022. Patient-derived anti-NMDAR antibody disinhibits cortical neuronal networks through dysfunction of inhibitory neuron output. Journal of Neuroscience, 42(15), 3253-3270. Impact factor: 6.167 (2022)

Wenke, N.K., Kreye, J., **Andrzejak, E.**, van Casteren, A., Leubner, J., Murgueitio, M.S., Reincke, S.M., Secker, C., Schmidl, L., Geis, C., Ackermann, F., Nikolaus, M., Garner, C.C., Wardemann, H., Wolber, G. and Prüss, H., 2019. N-methyl-D-aspartate receptor dysfunction by unmutated human antibodies against the NR1 subunit. Annals of neurology, 85(5), pp.771-776. Impact factor: 9.037 (2019)

Hoffmann, S., Orlando, M., **Andrzejak, E.**, Bruns, C., Trimbuch, T., Rosenmund, C., Garner, C.C. and Ackermann, F., 2019. Light-activated ROS production induces synaptic autophagy. Journal of Neuroscience, 39(12), pp.2163-2183. Impact factor: 6.074 (2019)

Rahman, K. A., Orlando, M., Boulos, A**., Andrzejak, E.**, Schmitz, D., Ziv, N. E., ... & Ichkova, A. (2023). Microglia actively remove NR1 autoantibody-bound NMDA receptors and associated post-synaptic proteins in neuron microglia co-cultures. Glia. Impact factor: 8.073 (2023)

van Casteren, A.C., Ackermann, F., Rahman, K.A., **Andrzejak, E.**, Rosenmund, C., Kreye, J., Prüss, H., Garner, C.C. and Ichkova, A., 2022. Differential modes of action of α1-and α1γ2-autoantibodies derived from patients with GABAAR encephalitis. Eneuro. Impact factor: 4.36 (2022)

Acknowledgements

First and foremost, I would like to express my sincere gratitude to my doctoral supervisor Craig Garner, for his guidance, support and true mentorship throughout my PhD, especially for giving me the scientific creative freedom to shape my project and encouraging me to follow my interests. I feel truly grateful for having had such an inspiring role model, mentor and a friend guiding me through this process and shaping me as a scientist.

I would like to thank all my collaborators, especially Noam Ziv for welcoming me in his lab in Israel, great working dynamics with stimulating conversations about science and beyond and for making my stay there so memorable. I would also like to thank Christian Rosenmund, Harald Prüss, Eshed Rabinovitch and Jakob Kreye for conceptual and experimental insights in my project.

A special thank you goes to Frauke Ackermann who co-supervised my PhD thesis, for her patience and support during all these years and always being there to answer my questions, co-write the manuscripts and for bringing the voice of reason to our discussions.

I would also like to thank all of my colleagues and friends in Garner lab for their support and useful input during lab meetings. Big thanks go also to our technicians Anny Kretschmer and Christine Bruns for all the technical assistance. I am especially grateful to Jo for sharing this PhD journey with me from day 1 and her wonderful friendship and inspiration inside and outside of the lab.

I feel incredibly grateful for all my wonderful friends who continuously supported me, made my time in Berlin joyful and became my family: Jo, Aleks, Alex, Lee, Loic, Özge, CJ and the Pirates. A special thank you goes to my dearest friend Aleks who was there for me from afar and close, always believing in me and giving advice. Thank you for being such a wonderful friend.

Finally, I would like to thank my whole family for supporting and believing in me through these years and especially my mom and my late Grandmother Marta, who had been my home and love and harbor I could always return to.